# INTERACTION OF SECRETORY PROTEIN SecA WITH ITS BINDING PARTNERS: LIPIDS AND SecB

A Dissertation

presented to

the Faculty of the Graduate School

at the University of Missouri-Columbia

In Partial Fulfillment

of the Requirements for the Degree

Doctor of Philosophy

by

Bahar Tuba Findik

Dr. Linda Randall, Dissertation Supervisor

DECEMBER 2016

The undersigned, appointed by the dean of the Graduate School, have examined the dissertation entitled

INTERACTION OF SECRETORY PROTEIN SECA
WITH ITS BINDING PARTNERS: LIPIDS AND SECB

presented by Bahar Tuba Findik,

a candidate for the degree of doctor of philosophy,

and hereby certify that, in their opinion, it is worthy of acceptance.

Professor Linda Randall

Professor Michael Henzl

Professor Peter V. Cornish

Professor Gavin M. King

*To my family:*

*Zuhre and Mustafa Findik*

*Emine Sisman and Zehra Guleryuz*

## *ACKNOWLEDGEMENTS*

The successful completion of the work described in this dissertation certainly could not have been done singlehandedly. I would like to acknowledge and thank all those who have contributed to my success. I thank my mentor Lin Randall for her guidance and patience through this process. I would like to express my gratitude to her for investing the time and the effort in making me a better scientist and providing me an atmosphere full with enthusiasm for science. I acknowledge Jerry Hazelbauer for all his contributions during group meetings. I will miss the tea times and elegant membrane dining that Lin and Jerry have provided for us. I would like to thank my committee members: Mike Henzl, Peter V. Cornish and Gavin M. King for their contributions. I thank Wayne Hubbell and Christian Altenbach for assistance for interpretation of EPR results and for providing software. I thank the current and former members of the Membrane Group for assistance and their friendship in the lab and all they have done for me; Angie Lilly, Carl Edward Cheadle, Mingshan Li, Narahari Akkaladevi, Nick Bartelli, , Simon Hardy, Wenlin Pan, Wing-Cheung Lai and Yuying Suo. I especially thank Chunfeng Mao for her endless patience and helping me in various aspects of my research, Priya Bariya for being such a good friend and supporter; Mary Belle Streit for her endless favor and warm hugs that made me feel a part of her family, and Jennine Crane for critically reading and editing my thesis.

I thank my family for giving me a constant source of love and for supporting me in everything I do. The time that I spent studying abroad was a life time experience that cultivates life-long friendships. I thank all of my friends especially two wonderful

roommates Didem Onen and Eda Akdemir for their support and making the time that I spent in US precious and unforgettable.

TABLE OF CONTENTS

# *LIST OF FIGURES*

## *LIST OF TABLES*

INTERACTION OF SECRETORY PROTEIN SECA
WITH ITS BINDING PARTNERS: LIPIDS AND SECB

Bahar Tuba Findik

Dr. Linda L. Randall, Dissertation Advisor

## *ABSTRACT*

Thirty percent of proteins synthesized in the cytoplasm of *E.coli* are exported across or into the cytoplasmic membrane to reach their final destinations. The general secretory system exports precursor proteins through the heterotrimeric integral membrane protein complex, SecYEG, with the help of the myriad interactions that occur among SecA, the ATPase, SecB, the cytosolic chaperone, precursor and membrane. For efficient translocation, many precursor proteins are dependent on the chaperone SecB, which facilitates export by maintaining polypeptides in a nonnative conformation.

In this thesis, we describe three projects. Two are completed, and the third is still in progress. The first one, described in Chapter 2, reports the chromosomal level of SecB in *E.coli,* giving the details for proper preparation of standards for quantitative immunoblotting.

In Chapter 3, we investigated the interaction of SecA with lipids. We used three model systems: liposomes, liposomes assembled with SecYEG either alone or in the complex with SecA. We showed that the N-terminal ten residues of SecA interact with lipids integrally and these residues lie parallel to the plane of the membrane with a 6 Å

maximal depth of penetration into the bilayer. We also observed that these 10 residues in the membrane display a helical pattern that has a periodicity close to that of a π helix.

The other binding partner of SecA is SecB. When precursor-bound SecB interacts with two protomers of SecA, the precursor protein is trapped between the SecA and SecB in the complex, like a sandwich. Thus, transfer of the precursor presents an interesting topological problem. Nothing is known about the molecular details of the transfer of precursor along this pathway. In the project, described in Chapter four and still under investigation, we are trying to address the specific roles of each of the interaction sites of SecA:SecB complex. This knowledge will help us to elucidate the details of release of precursor within the complex. Current results indicate that the lack of the interaction between the N-terminal region of SecA with lipids results in a decrease in the rate constant of translocation; whereas, the interaction between the N-terminal region of SecA and the tail site of SecB has the greatest impact on the level of translocation.

# *CHAPTER ONE*

## *Introduction*

## Introduction

The barrier function of biological membranes, a universal structural feature, is fundamental in defining an individual cell by separating the inside of a cell from its environment. Membranes prevent the uncontrolled flow of ions, proteins and macromolecules into and out of a cell, which allows each cell to establish and maintain a specific ionic composition and a discrete complement of macromolecules. Eukaryotic cells differ from prokaryotic cells in having internal membranes that divide the cell into compartments that have unique compositions within the cells such as the nucleus, mitochondria and endoplasmic reticulum. Even though prokaryotes do not have internal membrane-bound organelles, the cytosol and the membrane are distinct compartments with specific functions. Gram-positive bacteria and archaea have only a cytoplasmic membrane; whereas, Gram-negative bacteria also have an outer membrane as well as the periplasm, the aqueous space between the inner membrane and outer membranes. As in all living cells, in Gram-negative bacteria, protein synthesis occurs in the cytoplasm, and proteins that function in different compartments have to be translocated into or across the inner membrane and, in some cases, the outer membrane to reach their final destinations. Many specialized pathways have evolved to deliver a wide range of proteins to their site of function without compromising the barrier function of the membrane. Of these, the general secretory, (Sec) system is ubiquitous and essential for viability in all three kingdoms of life, from single-cell organisms to mammals (Becker et al., 2009). In Gram-negative bacteria, the Sec system translocates proteins into, or through, the cytoplasmic membrane. Although for many proteins this is their final location, for others, this is the first step in secretion to the extracellular matrix or insertion into the outer membrane. The

Sec system is involved in the translocation of the great majority of proteins from the cytoplasm to their site of function. The interaction among the components of the Sec system in *Escherichia coli* is the subject of this thesis.

There are six known pathways in Gram-negative bacteria that insert proteins into the outer membrane or secrete them into the extracellular medium. The Sec system provides transport into the periplasm in four of these pathways (Thanassi & Hultgren, 2000). The secretion systems can be divided into two groups according to number of steps they use for translocation: either one step or two. In one-step secretion systems, proteins are exported to the extracellular space as a final destination in one step, skipping any periplasmic interaction. One-step export systems are divided into four sub-classes: type I, III, IV and VI (Costa et al., 2015). Type I secretion systems consist of three proteins in a complex that spans the cell envelope: An outer membrane protein that creates the pore, an ATP-binding cassette transporter and a membrane fusion protein that bridges the inner membrane and outer membrane. Type I secretion systems transport various size of proteins by recognition of a C-terminal uncleaved secretion signal (Thomas, Holland, & Schmitt, 2014). The type III secretion systems allow Gram-negative bacteria to export virulence factors from the cytoplasm directly into the host cell in one step. The protein complex is composed of approximately 20 proteins that span from the cytoplasmic membrane to well beyond the cell surface (Burkinshaw & Strynadka, 2014). The type IV secretion systems also span the whole cell envelope and reach the host cell. Evolutionarily, it is related to bacterial conjugation systems. It is responsible of exchanging genetic material between the bacteria, and protein, protein-DNA complexes from one bacterium to a eukaryotic host cell (Fronzes, Christie, &

Waksman, 2009). The type VI secretion system is a multipurpose export machinery that mediates interbacterial relationships including injection of virulence factors into eukaryotic cells and secretion of antipathogenic substrates into neighboring bacteria. The main system is formed by 13 conserved proteins and the structure resembles an inverted phage oriented to inject a target cell that is in contact with the bacterium (Filloux, Hachani, & Bleves, 2008, Records, 2011 #707).

During translocation that occurs in two steps, proteins are first exported across the inner membrane either through the general secretory (Sec) pathway, which is the subject of this thesis, as an unfolded protein (Randall & Hardy, 1986) or through the twin-arginine translocation (TAT) pathway as a stably folded protein (Palmer & Berks, 2012). After reaching the periplasm, classification differs according to the second step of translocation, depending on the destination. Proteins destined for translocation across the outer membrane are secreted via either the type II or type V pathways. In type II secretion, the first step of translocation across the cytoplasmic membrane is performed by either the Sec or the TAT pathways. Type II secretion is a specialized secretion system that exists in both pathogenic and nonpathogenic strains but not in all Gram-negative bacteria. This secretion system consists of 12-15 core components that create the machinery in the cytoplasmic membrane, the periplasmic space and the outer membrane. Substrates for the type II secretion include hydrolytic enzymes and toxins that help bacteria to survive and to grow in a host cell or in environmental niches (Korotkov, Sandkvist, & Hol, 2012). Proteins secreted by the type V system must be translocated across the cytoplasmic membrane by the Sec system. Autotransporter secretion pathways are sub-classes of the Type V secretion systems. Proteins that use this pathway have a

common ß-barrel structured C-terminal domain that inserts into the outer membrane and serves to translocate the N-terminal passenger domain to the bacterial surface (Henderson, Navarro-Garcia, Desvaux, Fernandez, & Ala'Aldeen, 2004).

The ß-barrel assembly machinery (BAM) complex in the outer membrane is responsible for insertion and proper folding of these precursor proteins into the outer membrane. The outer membrane proteins that have a ß-barrel structure are exported across the cytoplasmic membrane by the Sec pathway. Periplasmic chaperones accompany the proteins across the periplasmic space to maintain the protein in an unfolded conformation. It has homologous systems in eukaryotes: the sorting and assembly machinery (SAM) complex in mitochondria and the translocons at the outer envelope of chloroplasts (TOC) complex in chloroplasts (K. H. Kim, Aulakh, & Paetzel, 2012).

Although most proteins destined for the inner membrane, periplasm and outer membrane are exported by the Sec system, there are two independent pathways that deliver precursor proteins to the Sec translocons. Integral membrane proteins are inserted into the cytoplasmic membrane co-translationally while undergoing elongation on the ribosome. They are delivered to the Sec system by a particle homologous to the eukaryotic signal recognition particle (SRP). The SRP, a complex between a 4.5S RNA and a protein (Ffh), recognizes the signal sequence of a nascent chain (Saraogi & Shan, 2014). Another membrane protein that cooperates with Sec system, YidC, is also involved in insertion of cytoplasmic membrane proteins. YidC can also act as an insertase for membrane proteins independent of the Sec system (Dalbey, Kuhn, Zhu, & Kiefer, 2014).

## Sec System

The general secretory system (Sec) translocates 30% of the protein synthesized in the cytosol to their final destination in the inner cytoplasmic membrane, the periplasmic space, the outer membrane, or the extracellular milieu. Only unfolded proteins that carry a signal sequence, referred to as precursor proteins, can be translocated by the Sec system (Randall & Hardy, 1986). The Sec system includes multiple components: SecYEG, a membrane-embedded protein complex which provides the channel; SecA, a membrane-associated ATPase to supply energy to the system; SecB, a soluble cytosolic chaperone to keep the precursor protein in an unfolded conformation as well as other integral membrane proteins to provide protonmotive force and proteolytic cleavage to process precursor protein to the mature form.

## SecYEG Translocon

In the Sec system of *E.coli*, the channel through the membrane is formed by an integral heterotrimeric protein complex, SecY, SecE and SecG (75 kDa). The SecYE complex is highly conserved in all three kingdoms of life: bacteria, archaea, and eukaryotes. SecY and SecE are homologous to the Sec61α and γ in eukaryotes (Hartmann et al., 1994). The third subunit, SecG, does not show homology with the third subunit of other translocons. It is Sec61β in mammals, Sbh1p in yeast and Secβ in archaea. SecY and SecE, which are essential for cell viability, constitute the main domain of the channel (Akimaru, Matsuyama, Tokuda, & Mizushima, 1991). SecY consists of 10 α-helical transmembrane (TM) segments. TM1 through TM5 form half of the channel and TM6 through TM10 form the other half. The loop between TM5 andTM6 holds them

together. The channel formed by SecY has an hourglass shape. The narrowest part of the hourglass is formed by six hydrophobic amino acid residues, the pore ring, which closes the channel and prevents the passage of precursor proteins (Li et al., 2007; E. Park et al., 2014). A short, disordered helix creates a plug within the channel to seal the periplasmic side (Van den Berg et al., 2004). After insertion of a precursor into the channel, a conformational change occurs, and the plug is displaced. The sealing task of the plug is ended (Collier, Bankaitis, Weiss, & Bassford, 1988; Zimmer, Nam, & Rapoport, 2008). The diameter of the translocon is widened, allowing translocation of precursor proteins conjugated to hard, spherical organic molecules with diameters up to 22-24 Å (Bonardi et al., 2011).

SecE consists of 127 aminoacyl residues that form three TM helices. Only the C-terminal α-helix is required for viability. SecE acts like a clamp surrounding the SecY transmembrane helices to hold them together (Nishiyama, Mizushima, & Tokuda, 1992; Schatz, Bieker, Ottemann, Silhavy, & Beckwith, 1991; Van den Berg et al., 2004).

*E.coli* SecG contains three TM helices (Breyton, Haase, Rapoport, Kuhlbrandt, & Collinson, 2002). SecG stimulates the efficiency of translocation activity by undergoing inversion in the membrane in concert with the insertion-deinsertion cycles and ATP binding and hydrolysis that SecA undergoes during translocation. When the system is idle, the C-terminus of SecG is exposed on the periplasmic side of the membrane. When translocation of a precursor initiates, SecG inverts, and now the C-terminus of SecG is accessible from cytoplasmic side of the membrane (Sugai, Takemae, Tokuda, & Nishiyama, 2007).

## SecB

SecB, found in Gram-negative bacteria, is a homotetrameric chaperone with a molar mass of 68,600 Da (Weiss, Ray, & Bassford, 1988a). The monomeric unit of SecB consists of 155 aminoacyl residues (Kumamoto & Nault, 1989). Each monomer has four β strands localized on the surface of the SecB and two α-helices below the β strands. Two monomers associate to form a dimer with an eight stranded ß-sheets forming a flat surface on one surface (Dekker, de Kruijff, & Gros, 2003; Xu, Knafels, & Yoshino, 2000) . SecB is a stable tetramer with an equilibrium constant below 20 nM (Murén, Suciu, Topping, Kumamoto, & Randall, 1999) and is formed by dimerization of dimers through the α-helices(Xu et al., 2000). Hydrogen bonds formed between the dimers stabilize the interface of the tetramer (Dekker et al., 2003).

SecB has two binding partners during translocation; the unfolded precursor protein and SecA. Precursor proteins have a signal (also known as the leader) sequence at the amino- (N-) terminus that retards the folding of precursor to allow time for SecB to bind (S. Park, Liu, Topping, Cover, & Randall, 1988; Weiss et al., 1988a). The signal sequence is proteolytically removed by leader peptidase after translocation of the precursor across the cytoplasmic membrane (Kuhn & Wickner, 1985). The signal sequence, which consists of 20 to 25 amino acids, has three major regions: a short (five residues), positively charged N-terminal region (N region), a central hydrophobic core region (H region) and a polar carboxyl-terminal region (C region) which is the proteolytic cleavage site (von Heijne, 1983). SecB does not recognize the leader sequence. It recognizes the mature domain of precursor protein (Gannon, Li, & Kumamoto, 1989; Lecker et al., 1989; Randall, Topping, & Hardy, 1990). The precursor protein wraps

around SecB and binds to SecB with a high affinity but low specificity (Randall & Hardy, 1995; Randall, Topping, Suciu, & Hardy, 1998). A kinetic partitioning occurs between precursor folding and precursor association with SecB. The relative rates of these events determine whether SecB binds to precursor protein. Binding is near diffusion limited, so SecB can bind a precursor before it folds to final stable structure (Hardy & Randall, 1991).

The interaction between SecB and SecA is specific, and SecB binds SecA at two sites. The flat, negatively charged side of SecB binds the SecA C-terminus which contains a positively charged region. This region includes a zinc atom, which is coordinated by three cysteines and a histidine residue (Breukink et al., 1995; Fekkes, de Wit, Boorsma, Friesen, & Driessen, 1999; Kimsey, Dagarag, & Kumamoto, 1995). The second binding site is between the C-terminus of SecB and the N-terminus of SecA (Randall et al., 2005; Randall, Crane, Liu, & Hardy, 2004). The interaction between SecB and SecA will be discussed in further detail in Chapter 4. Although SecB binds SecA in solution with a Kd in the range of 1-2 μM (Hartl, Lecker, Schiebel, Hendrick, & Wickner, 1990), SecB has a higher affinity (Kd~30 nM) for the membrane bound SecA . The interaction is tighter if the SecB has precursor bound (Kd~10 nM)(Fekkes, van der Does, & Driessen, 1997) .

## SecA

SecA is a dynamic protein with a molar mass of 102,000 Da. SecA is essential for cell viability and plays crucial roles during protein translocation (Cunningham et al., 1989). It is an adenosine triphosphatase (ATPase) that provides energy for protein export

by binding and hydrolyzing ATP during translocation. With the help of protonmotive force, this energy is used for translocation of polypeptides. Multiple copies of SecA function for a single SecYEG translocon during translocation (Morita, Tokuda, & Nishiyama, 2012).

In solution, it is in equilibrium between monomer and dimer. The equilibrium is affected by salt concentration and temperature. The equilibrium is shifted toward dimer in low salt concentration and higher temperature. In physiologic salt conditions (buffer at pH 7.5, 5 mM $Mg^{+2}$ acetate, 300 mM $K^{+}$ acetate), Keq is 1 μM at 8°C. The strength of dimerization increases up to 14 nM at 20°C in low salt (Woodbury, Hardy, & Randall, 2002).

SecA contains 901 amino acid residues that create several domains. NBD1 and NBD2 are the two nucleotide binding domains. NBD1 has the main catalytic function while NBD2 has a regulatory role. Binding of nucleotide to the cleft between these two domains results in a conformational change (Karamanou et al., 2007; Keramisanou et al., 2006). A variable domain lies within the NBD2 and regulates the ATPase activity of SecA in *E.coli* (Das et al., 2012). It is referred to as variable because it is not present in all bacterial species. The preprotein binding domain (PBD) of SecA, interacts with precursor, SecYEG and SecB (Cooper et al., 2008). The α-helical scaffold domain (HSD) comprises three anti-parallel α-helices that interact with all other domains of SecA. The two short helices of the HSD, which are toward the C-terminus, form the Intramolecular Regulator of ATPase (IRA1) which makes contact with SecY and precursor proteins (Karamanou et al., 1999; Zimmer, Li, & Rapoport, 2006). The α-helical wing domain (HWD) is located between two helices in the HSD. The NBD2 and HSD are connected

by the Linker Helix that is formed by 10 residues (Cooper et al., 2008). The last 21 aminoacyl residues in the C-terminal domain, composed of residues 836 through 901, coordinate a required zinc ion and bind the flat β-sheet region on the side of SecB (Breukink et al., 1995).

In the cytoplasm, SecA recognizes the precursor (Lill et al., 1989) and binds it through the leader sequence and mature domains of precursor via HSD and PBD (Akita, Sasaki, Matsuyama, & Mizushima, 1990; Cooper et al., 2008; Lill, Dowhan, & Wickner, 1990). It delivers the precursor to the translocon on the membrane. The interaction of SecA with the membrane results in a conformational change from a closed state to an open state of SecA. In the open state, which is widely believed to be the active state, PBD rotates away from HSD and approaches NBD2 (Zimmer et al., 2008). Binding to the translocon with a high affinity stimulates the SecA ATPase activity. The SecA ATPase activity reaches a maximal level in the presence of precursor, the translocase and acidic phospholipids (Lill et al., 1989). Binding of ATP causes SecA insertion into the membrane (Economou & Wickner, 1994) and opening of the SecY channel. Hydrolysis of ATP results in deinsertion (Economou & Wickner, 1994) which is also coupled with SecG inversion to the original topology (Nishiyama, Suzuki, & Tokuda, 1996) and closing the SecY channel.

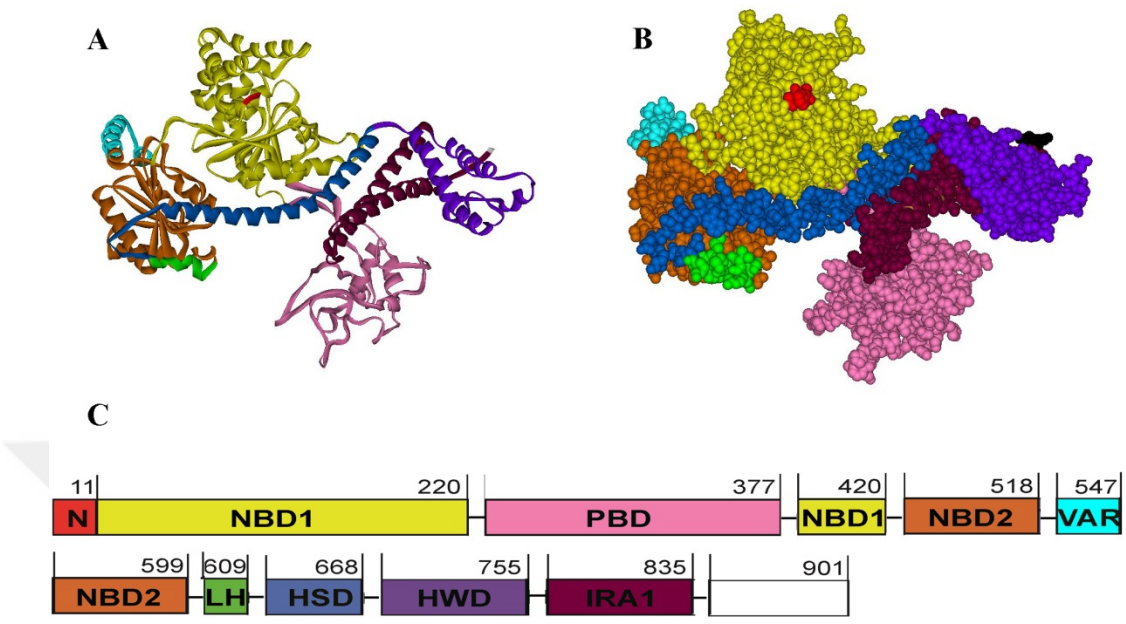


**Figure 1.** Structure of SecA. The structure of SecA is PDB code 2FSF with the PBD modeled in, based on the *B. subtilis* SecA PBD (PDB code 1TF5) (Papanikolau et al., 2007). A) *E.coli* SecA in ribbon representation B) The CPK representation of *E.coli* SecA shown in B. C) The color code for *E.coli* SecA domains displayed in panels A and B with the amino acid residues as in structure

SecA interacts with almost all of the components of the export system: the precursor, SecB, SecY and lipids. The *secA* gene was first identified by Oliver and Beckwith in 1981 and one year later, they determined that SecA associates with the cytoplasmic membrane (Oliver & Beckwith, 1981, 1982). In the early studies, this association was thought to be peripheral. In 1991, it was reported that 50 % of the SecA in the cell is associated with the membrane *in vivo*. Thirty percent of this membrane-associated SecA is found integrally associated with the membrane as shown by its resistance to high salt and urea washes (Cabelli, Dolan, Qian, & Oliver, 1991). The specific regions of SecA that associate with the membrane have not been determined. The characterization of the nature of the interaction is the topic of Chapter 3.

In the membrane, SecA binds both SecYEG with a high affinity (Kd ~ 40 nm) (Douville, Price, Eichler, Economou, & Wickner, 1995; Hartl et al., 1990) and binds lipids with a low affinity (Hendrick & Wickner, 1991). This interaction requires the presence of a physiological level of negatively charged lipids both *in vivo* and *in vitro* (X. Chen, Xu, & Tai, 1996; Hendrick & Wickner, 1991; Lill et al., 1990). There are three major phospholipids in *E.coli* membranes: phosphatidylethanolamine (PE) (67 %), phosphatidylglycerol (PG)(23%) and cardiolipin (CL) (9.8%). PE, the most abundant phospholipid in the cell membrane, is a neutral lipid at physiological pH, and can form hydrogen bonds. Also, it can undergo a transition between the lamellar and non-bilayer hexagonal ($Hex_{II}$) structure. PG is an anionic lipid at physiological pH, and forms the major acidic portion of the membrane. CL is made up of two phosphatidylglycerols connected by a glycerol backbone, and therefore has two negative charges. Both classes of lipids are necessary for efficient translocation of proteins across the cytoplasmic

membrane (de Vrije, de Swart, Dowhan, Tommassen, & de Kruijff, 1988; van den Brink-van der Laan, Antoinette Killian, & de Kruijff, 2004; van der Does, Swaving, van Klompenburg, & Driessen, 2000). Not only membrane insertion of SecA depends on presence of anionic lipids, but also full translocation ATPase activity of SecA requires presence of anionic lipids (Lill et al., 1990). Both the binding of SecA and its ATPase activity are inhibited in the presence of liposomes comprising neutral lipids: phosphatidylcholine (PC) and PE. SecA membrane association induces changes in conformation.

# *CHAPTER TWO*

## *Determination of the concentration of SecB expressed at the chromosomal level in E. coli*

## Introduction

The *secB* gene was first identified from *E. coli* mutants with pleiotropic defects in protein export (Kumamoto & Beckwith, 1983). The *secB* gene is not essential for cell viability. However, it is required for maximal-efficient protein export (Kumamoto & Beckwith, 1985). A *secB* null strain shows severe defects in export of many proteins. Fifteen proteins with known functions have been reported to utilize SecB (Baars et al., 2006; Collier et al., 1988; Kumamoto & Beckwith, 1985; Kusukawa, Yura, Ueguchi, Akiyama, & Ito, 1989; Powers & Randall, 1995) . There are other proteins with unknown functions that also require SecB (Baars et al., 2006). SecB is not absolutely crucial for all of the proteins classified as dependent on SecB, but rather it enhances the translocation efficiency. Two proteins, alkaline phosphatase (PhoA) and ribose binding protein (RBP) are exported normally in the SecB null (Collier et al., 1988; Collier, Strobel, & Bassford, 1990; Kumamoto & Beckwith, 1985). However, the physiological conditions of growth greatly change the requirement of SecB. The SecB dependence of PhoA alters with the change in the growth temperature (Kusukawa et al., 1989). When translocation is defective either by a mutation in the signal sequence of RBP (Teschke et al., 1991) or absence of protonmotive force due to existence of an uncoupler (J. Kim, Lee, Kim, & Park, 1992), SecB facilities translocation of RBP.

In contrast to other proteins of the Sec system, SecB shows no evidence of regulation of expression dependent on growth rate or growth phase. Two promoters control the transcription of the *secB* gene: the distal promoter, P1, and the proximal promoter, P2. Whereas the P1 promoter expresses *secB* constitutively, the P2 promoter is responsive to the carbon source via the regulatory protein CRP, the cyclic AMP (cAMP)

receptor protein. When glucose is used as a carbon sources, the level of CRP in complex with cAMP is reduced. CRP cannot bind target promoter (P2 protomer) to regulate transcription of *secB.* The cellular level of SecB is reduced in this condition. The *secB* gene is subject to catabolite repression. Cells grown with glycerol as the carbon source contain more SecB than do cells grown with glucose. It was also showed that the synthesis of SecB is not depended to growth rate and growth phase in glucose or glycerol media.(Seoh & Tai, 1999).

Investigations of the Sec system require knowledge of the concentrations of all components involved in in order to relate experiments carried on *in vitro* to the system *in vivo*. The concentrations of all other proteins in the Sec system have been determined and methods used have been published. However, there is no publication in the literature that reports the intracellular concentration of SecB produced at the chromosomal level. There are only three rough estimates in the literatures (Hardy & Randall, 1991; Seoh & Tai, 1997; Woodbury et al., 2000a). Two are cited by Dr. Randall as unpublished data and none give references to the techniques used. In this study, we have determined the cellular concentration of SecB on the chromosomal level by quantitative immunoblotting assay.

## Results and Discussion

We used quantitative immunoblotting as an approach to determination of the chromosomal level of SecB in *E. coli* K12 wild-type strain. Each immunoblot included a standard curve of pure SecB and multiple samples of the cultures being tested. We used whole cell cultures in this study. It was crucial to concentrate the cell culture so that the

sample gave a reaction within the linear range of immunoblots. Therefore, cell cultures were subjected to precipitation by addition of trichloroacetic acid (TCA) to a final concentration of 11%. The presence of cellular contents in the sample affected the recovery of SecB by TCA precipitation. When pure SecB was precipitated, approximately 97% was recovered. The presence of total cellular contents during TCA precipitation resulted in lower recovery (80-85%).

Whole cell cultures are highly complex containing many species of macromolecules such as lipopolysaccharide, proteins, and nucleic acids. We observed that the cellular content affects the intensity of the reaction with SecB on the immunoblots. In figure 2, the lanes were loaded alternately; the lanes 1, 3, 5 and 7 were loaded with the increasing amount of purified SecB (20-80 ng). The lanes 2, 4, 6 and 8 were loaded with the same amount of purified SecB with their pairs including the cell culture of SecB null strain to an optical density of 15 at 560 nm. It was observed that the presence of cellular contents in the sample affects the intensity of immunoblots. The effect of cellular contents is dominant in the presence of low amount of proteins. Recovery of the intensity increases linearly up to 62 % with the increasing amount of proteins. This finding states the necessity of proper standards when a quantitative immunoblot is carried out. To overcome the problem of comparing pure SecB in a standard to SecB in a cell culture that interferes with the intensity on immunoblots, we generated the standard curve by mixing purified SecB protein with the amount of cell culture of the SecB null strain equal to that in the samples to be quantified. The concentration of SecB was determined using at least three or four points that fell within

the range of the standard curve which includes at least four points in the linear range of reaction that is specific for SecB.

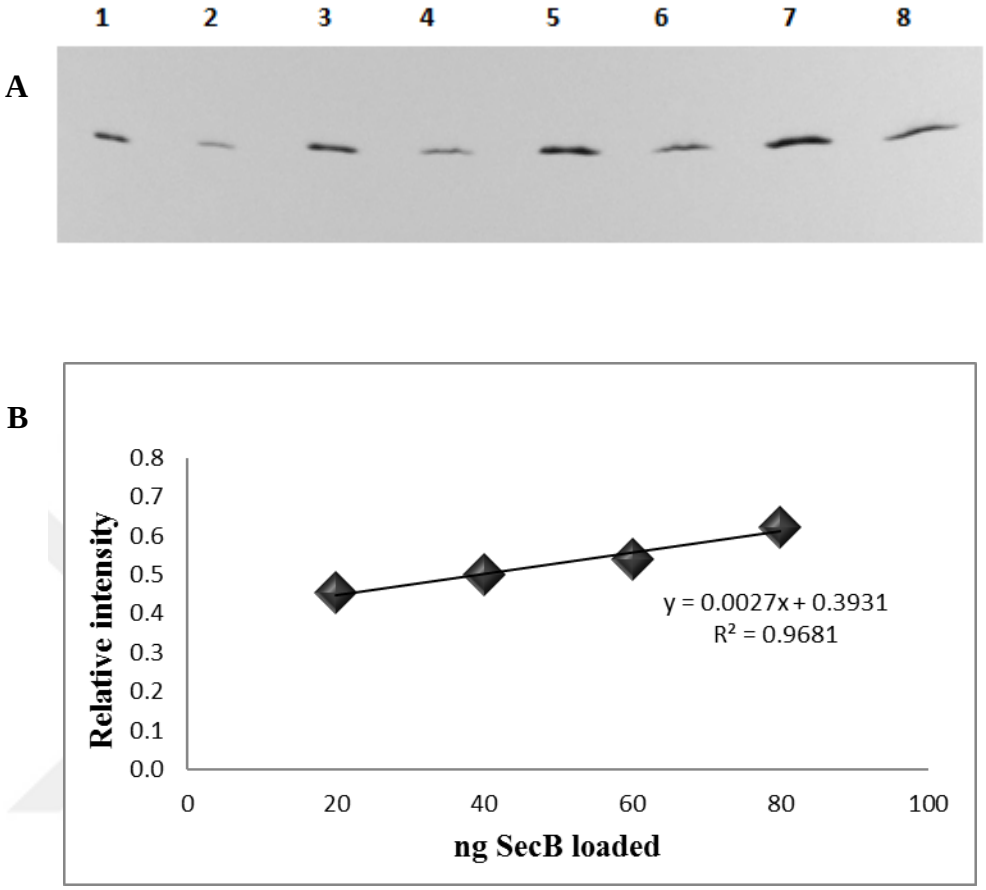


**Figure 2.** The effect of cellular content on the intensity of the reaction with SecB on the immunoblots. A) Lanes 1, 3, 5, 7 are pure SecB loaded at 20, 40, 60 and 80 ng, respectively. Lanes 2, 4, 6 and 8 were loaded with 20, 40, 60 and 80 ng of pure SecB in the presence of SecB null cell culture to an optical density of 15 at 560 nm. B) The relative intensity for each lane was plotted as a function of amount of purified SecB loaded.

The *E. coli* K12 strain (MC4100) was cultured at 35˚C both in rich media which includes tryptone and yeast extract, and in minimal media supplemented with 0.4 % glycerol as a carbon source. For each medium, three independent cultures were grown and subjected to quantitative immunoblotting. Growth was followed by measurement of OD at 560 nm. The doubling times of the *E.coli* cultures were 30 minutes in rich media and 80 minutes in minimal media.

We generated the standard curves for each growth medium using purified SecB mixed with a cell culture of the *secB* null strain that was grown in corresponding medium, LB or M9B. The amount of culture added to the purified SecB was equivalent to that in the culture of SecB to be quantified. The SecB was quantified using the ratio of slopes of the standard and SecB sample. The slope of the standard curve ($m_{std}$) is the increment of intensity of signal divided by the change in the mass of SecB.

$$m_{std} = \frac{\Delta Intensity}{\Delta\ mass\ (ng)}$$

The slope of the SecB sample curve ($m_{sample}$) is the change in the intensity of signal divided by the corresponding change in the volume of sample loaded.

$$m_{sample} = \frac{\Delta Intensity}{\Delta\ Volume\ (\mu l)}$$

The ratio of the slopes directly gives us the concentration of the SecB in the sample.

$$\frac{m_{unknown}}{m_{std}} = \frac{ng}{\mu l}$$

For the example in Figure 3, the concentration of SecB in the sample calculated is 4.3 ng/µl from the ratio of slopes.

$$\frac{m_{unknown}}{m_{std}} = \frac{20.0}{4.70} = 4.3\ ng/\mu l$$

The chromosomal level of SecB was calculated to be 8.2 µM as follows using the parameters below:

The concentration of SecB in the sample, $C_{SecB}$, is 4.3 ng/µl.

Total sample volume, $V_t$, is 0.085 ml.

The sample $OD_{560}$ is 15.

The molar mass of SecB tetramer is 69 x $10^3$ g/mole.

The volume of an *E.coli* cell is 1x$10^{-15}$ L, $V_{cell}$ (Milo R, 2016) .

The number of *E.coli* cells at an optical density of 1 at 560 nm ($OD_{560}$) was determined in our laboratory to be approximately 5x$10^8$ (cells/ml)/OD.

The number of *E. coli* cell in the sample:

$$((cells/ml)/OD)x\ OD\ x\ V_t = Total\ number\ of\ Cells$$

Total amount of SecB in the sample:

$$C_{SecB}x\ V_t = Total\ mass$$

Total amount of SecB in one *E. coli* cell:

$$\frac{Total\ mass}{Number\ of\ E.coli\ cells} = ng/cell$$

Molarity of SecB in the sample:

$$\frac{Total\ amount\ of\ SecB\ (\frac{g}{cell})}{Molar\ mass\ of\ SecB\ (\frac{g}{mole})\ x\ V_{cell}} = M$$

**A**

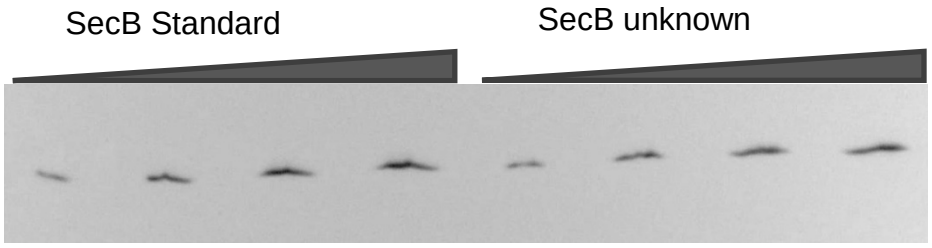
SecB Standard
SecB unknown

**B**

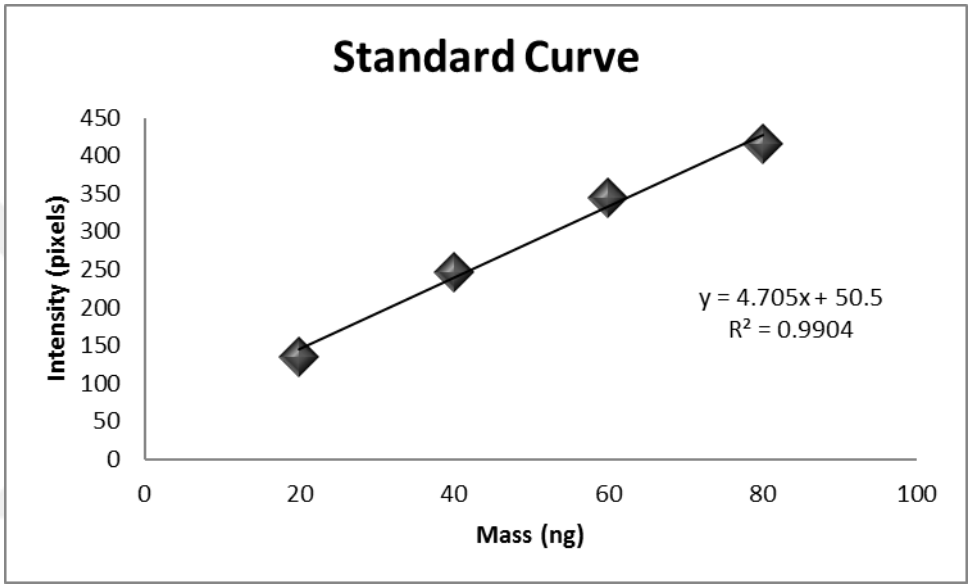
Standard Curve
Intensity (pixels)
450
400
350
300
250
200
150
100
50
0
0
20
40
60
80
100
Mass (ng)
y = 4.705x + 50.5
R² = 0.9904

**C**

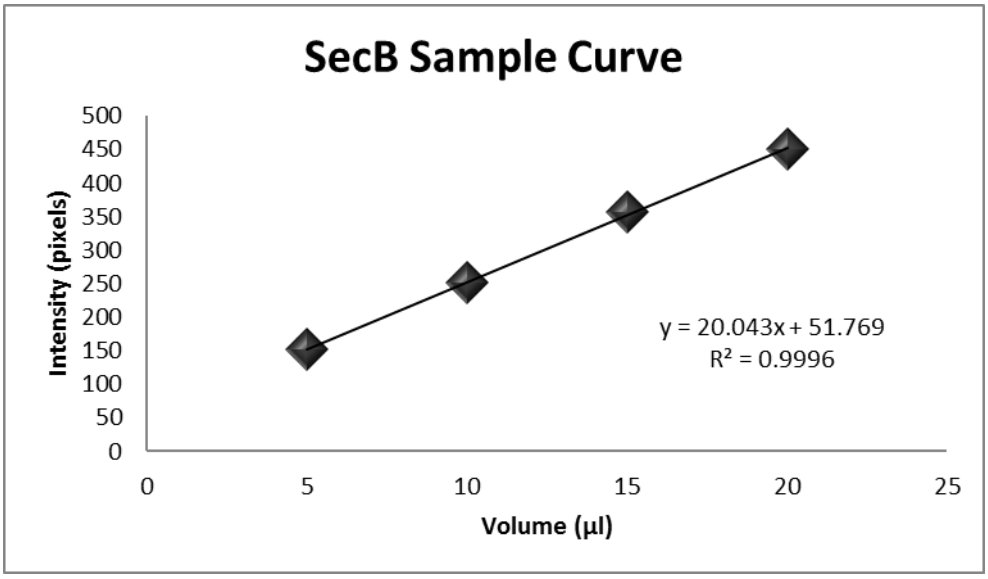
SecB Sample Curve
Intensity (pixels)
500
450
400
350
300
250
200
150
100
50
0
0
5
10
15
20
25
Volume (µl)
y = 20.043x + 51.769
R² = 0.9996

**Figure 3.** Determination of the cellular concentration of SecB. The example shown is the determination for the growth in minimum media. A standard graph created by adjusting purified SecB to contain the same amount of total cellular content of the unknown sample by addition of SecB null cell culture a) Quantitative immunoblots: lanes 1-4 contain purified SecB loaded at 20, 40, 60, 80 ng mixed with SecB null culture with the appropriate amount. Lanes 5-8 contain the SecB cell culture loaded at 5, 10, 15, 20 µl. b) Quantification of lane 1-4 of blot in a. c) Change in the intensity of immunoblots with the increasing volume of SecB cell culture loaded.

The cellular concentration of SecB was first estimated as approximately 4 μM by S. Hardy and L. Randall based on a published paper (Watanabe & Blobel, 1989), that described the purified SecB. A rough estimation was made from the yield of purification with many assumption (Hardy & Randall, 1991). Later, it was estimated around ~20 μM, based on unpublished results collected from immunoblots with an inappropriate standard (Woodbury et al., 2000a). In another study, the concentration of SecB as a monomer was estimated to be around 1000 copies per cell in glucose minimal medium which equals to 0.25 μM of SecB tetramer, and in the presence of glycerol minimal media, the cellular amounts of SecB was found ~2 fold higher (Seoh & Tai, 1997). However, the calculation was based on immunoblots in which purified SecB used as a standard directly.

In this study, we found that the cellular concentration of SecB was 4 μM in rich media. The concentration of SecB expressed at the chromosomal level in *E. coli* differs at least 2.5 fold dependent on the growth media. Concentration of SecB was found to be ~10 μM in minimal media in which glycerol was the carbon source. The results are unexpected that the level of SecB is higher in a scarce media that causes a slow growth rate. The expression of *secB* gene is known to be subjected to catabolic repression depending on the carbon sources. The cellular level of SecB is reduced when glucose is used as carbon source. It was also shown that the synthesis of SecB is not depended to growth rate and growth phase in glucose or glycerol media. There is no further investigation about *secB* regulation in the rich media without a carbon sources neither glucose nor glycerol. It is not clear why the synthesis of SecB is lower in a rich media, whether it is downregulated in rich media or not. It requires further investigation.

**Table 1.** Concentration of cellular SecB in rich and minimal media

| | **Concentration of cellular $SecB_4$ (μM)** | | | |
|---|---|---|---|---|
| **Medium** | **1** | **2** | **3** | **Average** |
| Rich | 4.4 | 3.6 | 3.8 | 3.9 ±0.4 |
| Minimal | 8.1 | 8.3 | 13 | 9.8 ±2.7 |

## Materials and Methods

### Bacterial strains and plasmids

The *E.* coli strains used for this study are listed in Table 1. MC4100 was used as an example of a wild-type *E.coli* K-12 strain. A *secB* null mutation in MC4100 (Ullers et al., 2007 PNAS 104:3101-06) that does not have any apparent polarity on *gpsA* was a gift from Pierre Genevaux. Wild-type SecB was purified from HB1042, which is BL21(DE3) harboring plasmid pJW25.

### SecB Purification

The SecB used as a standard for immunoblots was purified as previously described (Randall, L. L., 2004). The cells were disrupted by passage through a French press at 8,000 psi. The cellular lysate was centrifuged at 362,000*g in a 6*0Ti rotor, (Beckman) for 3h at 4° C. The protein was purified from the high-speed supernatants, using a QAE column (TosoHaas). The concentration of SecB was determined spectrophotometrically at 280 nm using 47,600 $M^{-1}$ $cm^{-1}$ as the extinction coefficient of the SecB tetramer.

**Table 2.** The *E. coli* strains used in the study

| **Strain** | **Plasmid** | **Genotype** |
|---|---|---|
| MC4100 | | $F^-$ $[araD139]_{B/r}$ Δ (argF-lac)169 $lambda^-$ e14-flhD5301 Δ(fruK-yeiR)725(fruA25) relA1 rpsL150(strR) rbsR22 Δ (fimB-fimE)632(::IS1) deoC1 |
| MC4100 (A251) | | MC4100 Δ *secB*::CmR |
| HB1042 | pJW25- SecB WT under T7 RNA polymerase control, bla (ApR) | $F^-$ ompT gal dcm Ion $hsdS_B(r_B^- m_B^-)$ λDE3 [lacI lacUV5-T7 gene 1 ind1 sam7 nin5] |

**Cell Growth**

To determine the intracellular concentration of SecB, three independent cultures of MC4100 and MC4100ΔSecB were grown in both *Luria-Bertani* (LB) broth and M9 minimal medium supplemented with 0.4% glycerol and 0.4% vitamin B1. All optical densities were measured at 560 nm unless otherwise noted. Cultures were inoculated to an optical density of 0.08-0.1 and grown at 35°C. The growth was stop in logarithmic growth phase when the culture reached an optical density of between 1 and 2 by placing the culture on ice. The culture was frozen by dripping into liquid nitrogen and stored at -70°C.

**Sample Preparation**

The protein in each cell culture was precipitated by addition of trichloroacetic acid (TCA) to a final concentration of 11% (w/w), collected by centrifugation (16,000 x g, 15 minutes at 4°C, Eppendorf benchtop centrifuge) washed with acetone and suspended in sample buffer to a final $OD_{560}$ of 20. SDS polyacrylamide (0.5 mm, 14% w/w) gel electrophoresis was performed on each sample.

The standards were generated by mixing purified SecB protein with the amount of cell culture of the SecB null strain equal to that in the samples to be quantified, TCA precipitation was carried out immediately to avoid proteolysis.

**Quantitative Immunoblotting**

Immunoblots of the gels were used to quantify the cellular concentration of SecB. SecB was transferred from the gel to a nitrocellulose blotting membrane (pore size: 0.45 µm) for 2h at 12 V. The membrane was immersed in powdered milk, 2% in 20 mM Tris, pH 7.0, 0.5 M NaCl (PM-TBS) and placed on a shaker at 35 °C for 15 min. Then, the membrane was incubated with a rabbit antiserum, raised to purified SecB, at a dilution of 1:1000 in PM-TBS on a shaker at 35 °C for 2h. After washing with TWEEN, 0.05 % (vol/vol)) in PM-TBS for 15 min, the membrane was immersed in a 1:2000 dilution of the secondary antibody that is a goat antiserum raised to rabbit immunoglobulin G and conjugated with horseradish peroxidase. The washing step was repeated, and the blot was developed with a solution of 4-chloro-1-napthol created by dissolving 15 mg in 5 ml of methanol, mixing with 25 ml TBS and adding 15 µl of 30 % $H_2O_2$ immediately before use. The membranes were photographed using a KODAK EDAS 290 digital camera system. The intensity of the bands was quantified using TotalLab. The amount of SecB was calculated from the intensity of each band using a standard curve of pure SecB present on the same blot.

## Notes

1. Angela Lilly constructed the SecB used as a standard in this study.
2. Yuying Suo purified the SecB used in this study.
3. The *secB* null strain was a gift from Pierre Genevaux.
4. The manuscript of this chapter is in preparation.

# *CHAPTER THREE*

## *Characterization of SecA association with the lipid bilayer*

## Introduction

SecA is a dynamic protein that plays a central role in the export of proteins into and across the cytoplasmic membrane. It is essential for the viability of the cell (Cunningham et al., 1989), and it is found distributed almost equally between the membrane and the cytosol (Akita, Shinkai, Matsuyama, & Mizushima, 1991; Cabelli et al., 1991; Chun & Randall, 1994). SecA binds to the membrane through both low affinity interactions with acidic phospholipids and high affinity interactions with SecY of the SecYEG translocon (Douville et al., 1995; Hartl et al., 1990; Matsumoto, Yoshihisa, & Ito, 1997). The ATPase activity of SecA is maximally stimulated by its interaction with acidic phospholipids, precursor proteins, SecYEG translocase (Lill et al., 1990) and SecB (Miller, Wang, & Kendall, 2002). The membrane-associated SecA not only binds the surface of the membrane but also penetrates into the hydrocarbon region (Breukink, Demel, De Korte-Kool, & De Kruijff, 1992; X. Chen, Brown, & Tai, 1998; Rajapandi & Oliver, 1994; Ulbrandt, London, & Oliver, 1992). This penetration requires the presence of anionic lipids (Breukink et al., 1992). The physiological significance of the interaction between SecA and the lipid bilayer has been shown, but the details of the interaction remain elusive.

In 1993, Breukink and colleagues (Breukink, Keller, & Kruijff, 1993) showed that incubation of SecA with lipid vesicles resulted in an increase in the turbidity indicating vesicle aggregation. They demonstrated that SecA has at least two lipid binding sites that

cause interaction between vesicles. They concluded that at least one of the interactions is electrostatic since the SecA-induced vesicle aggregation was disrupted in the presence of high salt concentrations. Further, deletion mutations in SecA demonstrated that the C-terminus of SecA is the lipid binding site responsible for the electrostatic interaction (Breukink et al., 1995). They also showed that SecA insertion into the lipid monolayer could not be inhibited by increasing salt concentration and concluded that the second interaction is hydrophobic (Breukink et al., 1992). By visual examination of the sequence of SecA, they proposed that N-terminus 25 aminoacyl residues could be responsible of this hydrophobic interaction (Breukink et al., 1993).

The N-terminal residues 2 through 11 of SecA and the Linker Helix residues 600 through 609 were chosen as candidates that are likely to interact with the membrane. First residue, Met1 was removed in the cell. A previous study using continuous wave (CW) electron paramagnetic resonance spectroscopy (EPR) showed that two residues (K4 and V9) in N-terminal region of SecA interact with liposomes (Cooper et al., 2008). Residues S600, D601, R602, M607 and K609 in the Linker Helix showed slight increases in mobility in the presence of liposomes (Cooper et al., 2008).

The N-terminal 10 aminoacyl residues have several important roles in protein export. SecA undergoes a monomer-dimer equilibration (Woodbury et al., 2002) and these residues contribute to the dimerization of SecA by making intersubunit contacts (Jilaveanu, Zito, & Oliver, 2005). In addition, this N-terminal region binds the C-terminal 13 residues of SecB (Randall & Henzl, 2010). The wild-type complex between SecA and SecB has two protomers of SecA and one tetramer of SecB (A2B4); however, deletion of

these residues (SecAdN10) results in a complex that has only one protomer of SecA and a SecB tetramer (A1:B4) (Randall et al., 2005). Also, in a competition assay using analytical velocity sedimentation centrifugation, addition of a synthetic peptide of the first 10 residues of SecA to a wild-type complex (A2B4) causes the release of one protomer of SecA from the complex (L.L. Randall unpublished data). SecAdN10 variants also show an intermediate level of activation of SecYEG when SecA and SecYEG are co-assembled into liposomes (Mao et al., 2013). The aminoacyl residues 600-610 that form the Linker Helix of SecA make contact with the C-terminal 13 residues of SecB (Suo, Hardy, & Randall, 2011).

To date the region of SecA that penetrates the bilayer has not been identified. In this work we directly demonstrated using the technique of electron paramagnetic resonance (EPR) power saturation that the N -terminal 15 residues of SecA penetrates to a depth of approximately 6 Å into the hydrocarbon region.

**The Approach**

Electron paramagnetic resonance (EPR) spectroscopy is a well-characterized approach to gain knowledge about structural and dynamic properties of soluble and membrane proteins. EPR was first reported by Zavoisky in 1945 (Zavoisky, 1945) and has become a powerful method to investigate materials that have a paramagnetic center. EPR is a spectroscopic technique based upon the absorption of electromagnetic radiation by paramagnetic matter. Most proteins do not have a paramagnetic center, but combining EPR with site-directed spin labeling (SDSL) allows the introduction of an artificial

paramagnetic center at a specific site on the protein of interest. The strategy of SDSL requires that only one cysteine is available for modification by the spin label reagent. Thus, the first step is to substitute any native cysteines with another residue that does not perturb the structure or function of the protein. An accessible cysteine is introduced to a site of interest using standard recombinant DNA techniques and covalently modified by a spin label reagent (C. Altenbach, Flitsch, Khorana, & Hubbell, 1989). The spin label that was used in this study was a nitroxide spin label that has the unpaired electron predominantly localized to the N-O bond.

Atoms have different energy states in which transitions occur between a lower energy state and a higher state by absorbing energy. According to Planck's law, absorption occurs if the energy difference between two states is equal to $h\nu$, where $h$ is Planck's constant and $\nu$ is the frequency of the radiation. We can measure this energy difference by spectroscopic techniques. In EPR, introducing a magnetic field causes a splitting in the energy levels of unpaired electrons. This effect is called the Zeeman Effect. Even an isolated electron has an intrinsic angular momentum because of its charge and it creates its own magnetic field in the absence of any external forces. It behaves like a small magnet. In an applied magnetic field, the lowest energy state of an unpaired electron is aligned with the magnetic field (-1/2) and the highest energy state is aligned against the magnetic field (+1/2) (Figure 4). The difference in the energy states is proportional to the strength of magnetic field. When the energy difference between the states equals the energy of the applied electromagnetic radiation, a transition from one spin state to the other occurs by absorption of energy. This absorption of energy by an

unpaired electron is monitored. The EPR spectrum represents the first derivative of the absorption curve (Figure 5).

The unpaired electron in the spin label is not only affected by the applied magnetic field but also by the magnetic field of a nucleus. A nucleus with nuclear magnetic moment in close proximity interacts with the unpaired electron of the spin label to give a hyperfine coupling resulting in multi-line EPR spectra. The number of lines in the EPR spectrum can be determined by the formula: $2I + 1$, where $I$ is the spin quantum number. In the nitroxide spin label that is used in this study, the electron interacts with the nucleus of the $^{14}N$ atom, which has a spin quantum number of 1. Thus, the resulting spectrum has three lines (Figure 6).

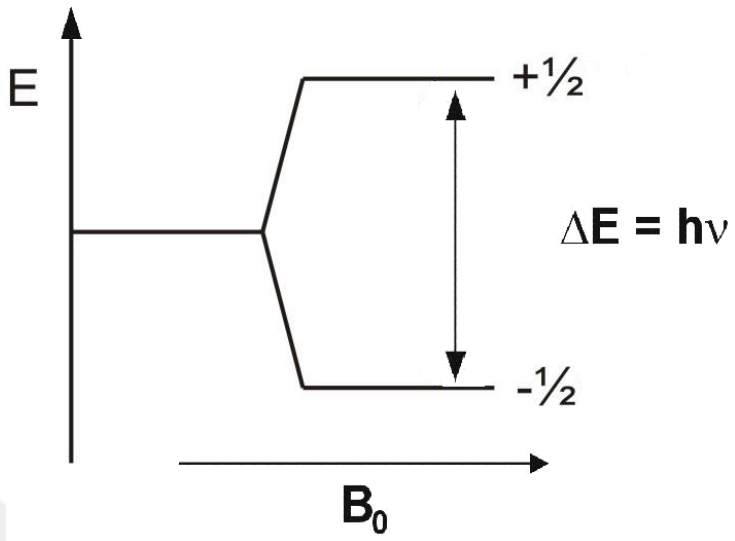


**Figure 4.** Splitting of the spin state energies of an electron as a function of the magnetic field, B0.Transition from lower spin state to the higher occurs by absorption of energy when the energy difference between the spin states equals the energy of radiation.

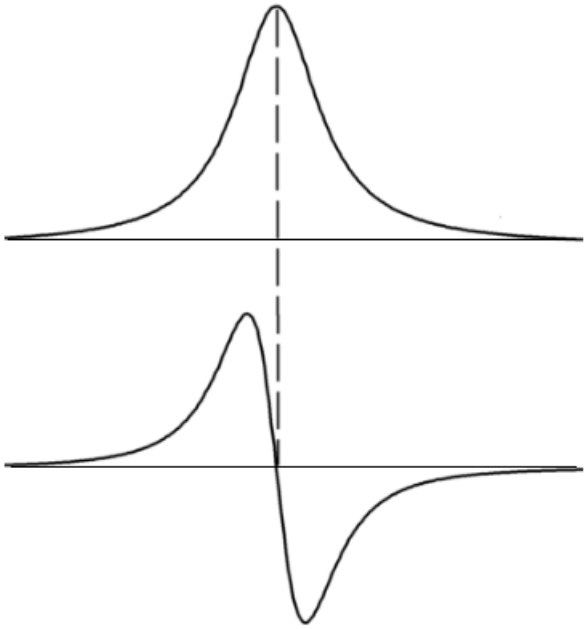

**Figure 5.** A schematic representation of an absorption curve (upper) and its first derivative (lower), as seen in EPR.

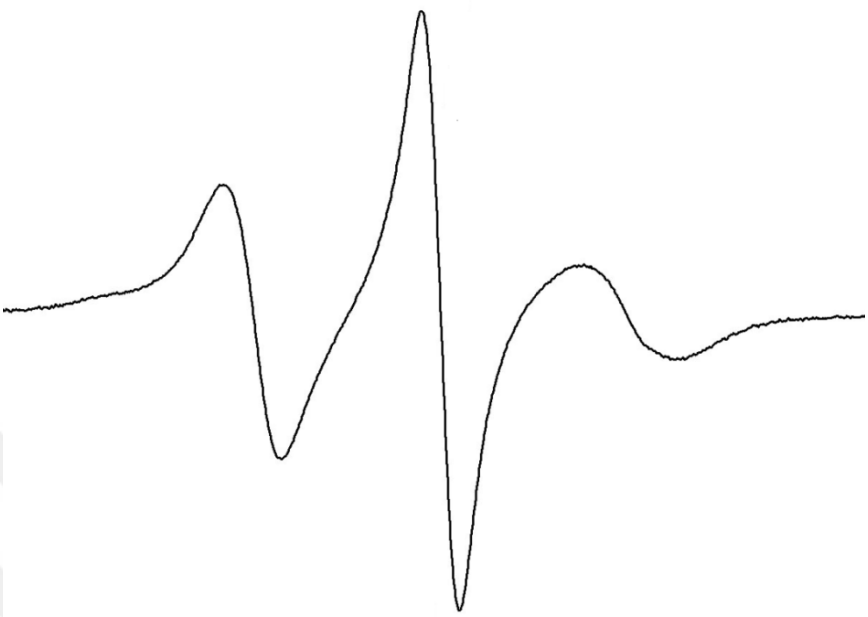

**Figure 6.** A representative hyperfine splitting of the EPR spectrum of a nitroxide. The splitting of the resonance line arises from interaction of the unpaired electron with the nitrogen nucleus.

An excited electron in the higher energy state transfers energy to the surroundings in the form of heat to reach thermal equilibrium with its environment, referred to as spin-lattice relaxation, resulting in a transition from the higher energy state to lower energy states. The time that an electron spends in the higher energy state is the spin-lattice relaxation time, T1. The value 1/T1 expresses how fast a spin system equilibrates with its surrounding. Presence of a paramagnetic reagent in the system affects the relaxation rate of the spin. When a nitroxide spin and a paramagnetic reagent that has a very short spin-relaxation time collide, 1/T1 will be increased. Paramagnetic relaxation reagents transfer the excess energy of the nitroxide spin to the environment by Heisenberg exchange. The exchange rate for a nitroxide can be measured by the method of power saturation and used to determine the accessibility of the nitroxide to the solvent in the system.

Using continuous wave EPR power saturation, the solvent accessibility of the nitroxide can be determined by the relative exposure of the nitroxide to paramagnetic relaxation reagents. The intensity of the EPR signal is proportional to the square root of the incident microwave power (P) and increases linearly. At some point, the nitroxide spin cannot relax fast enough to return to the lower energy state and no further absorption of energy occurs. The population of nitroxide spin at the lower and higher energy states becomes equal. Under this high power condition, the intensity of EPR signal does not increase further. This condition is called power saturation. When a paramagnetic relaxation reagent is introduced to the system, it increases the relaxation rate of the nitroxide spin. As a result, the amount of power needed for saturation increases. The

change in the saturation power is proportional to the Heisenberg exchange rate of a nitroxide spin due to collision with paramagnetic relaxation reagent.

**Determination of P1/2**

A power saturation curve is generated by measuring the intensity of a series of spectra collected at increasing incident microwave power (P) (Figure 7). The height of the center line of the first derivative EPR spectrum is plotted as a function of the square root of P. This curve is fitted to the equation below to calculate the power saturation parameter:

$$A = I.\sqrt{P}.[1+\left(2^{\frac{1}{\varepsilon}}-1\right).P/P_{(1/2)}]^{-\varepsilon}$$

where A is the line height of the central line signal, I is a scaling factor and ε represents the homogeneity of the saturation line. $P_{1/2}$ is directly proportional to the inverse product of the spin-lattice relaxation time (T1) and spin-spin relaxation time (T2).

$$P_{1/2} = \frac{1}{T_1.T_2}$$

T2 is spin-spin relaxation time and can be measured by changes in spectral line width ($\Delta H_{pp}$) (Figure 8). Dividing $P_{1/2}$ by the line width ($\Delta H_{pp}$) give us a value that is simply proportional to $T_1$.

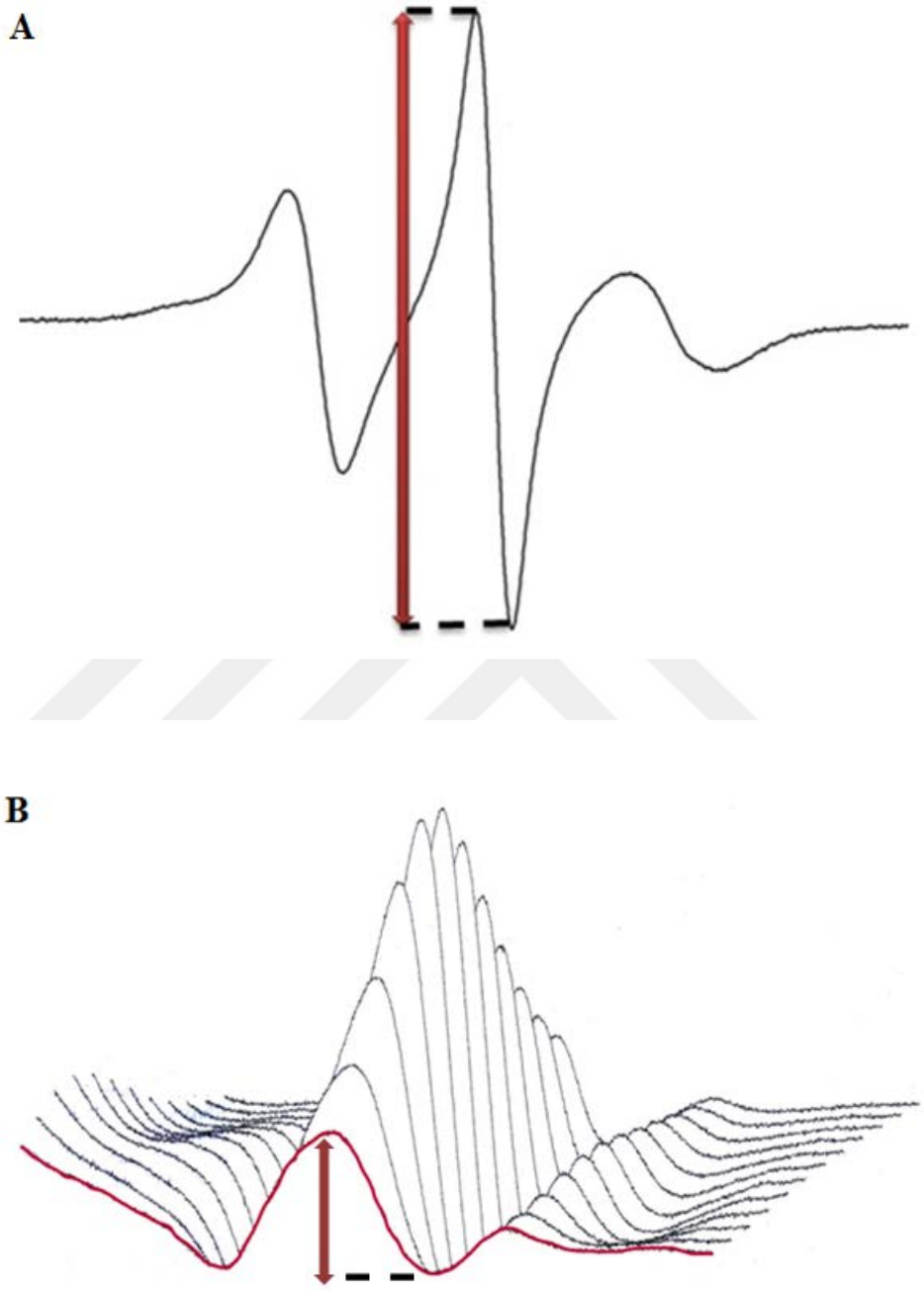
A
B

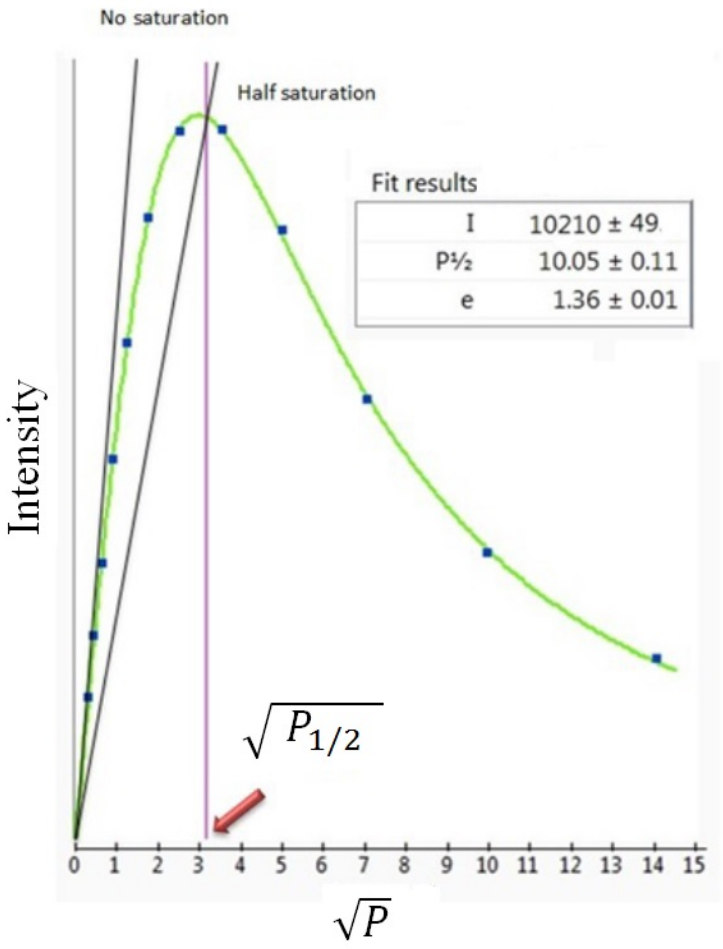


**Figure 7.** Power Saturation A) The peak-to-peak first derivative height of the central resonance line, intensity. B) An example of a power saturation series of spectra shown as the center line of first derivative EPR spectra plotted at increasing microwave power. The red spectral line is the spectrum recorded at the highest microwave power (100 mW). C) The power saturation curve plotted from data in B. The height of the central line of the first derivative EPR spectrum is plotted against the square root of the incident microwave power. $P_{1/2}$ is the power at which the intensity of the central line is half of its unsaturated intensity. The parameters calculated from the fit are shown on the inset.

Two paramagnetic relaxation reagents were used in this study. $O_2$ is a hydrophobic paramagnetic relaxation reagent. It is lipid soluble and its concentration increases through the lipid bilayer, reaching a maximal level at the center of lipid bilayer. On the other hand, nickel (II) ethylenediamine diacetate (NiEDDA) is a water soluble, hydrophilic paramagnetic relaxation reagent and shows an opposite concentration profile. It is at highest concentration the aqueous phase. The concentration of decreases through lipid bilayer and is lowest at the center. $N_{2,}$ which contains no paramagnetic species, is used to determine the natural relaxation rate of the nitroxide spin in the absence of relaxation reagents. This value is used as background and subtracted from both the $P_{1/2}$ of $O_2$ and the $P_{1/2}$ of NiEDDA. Gas permeable TPX capillaries are used to allow equilibration of the gas through the sample. Power saturation spectra for each spin-labelled sample are collected in all 3 conditions: $N_2$, $O_2$ and NiEDDA. The system is equilibrated with the gas for at least 10 minutes for each condition before collecting data. First, N2 is blown through the resonator and $P_{1/2}$ ($N_2$) is calculated from the power saturation curve to be used for background correction. In the second condition, compressed air is blown through the resonator to introduce $O_2$ into the system. For NiEDDA, the sample is incubated with NiEDDA three hours 30 minutes at room temperature. In the case of protein in liposomes, the sample is subjected to three cycles of freezing and thawing to ensure NiEDDA reaches the lumen of the liposomes. To equilibrate proteoliposomes with NiEDDA, the sample is. N2 is blown through the resonator containing NiEDDA. When the experiment is carried out in the presence of the relaxation reagents, $O_2$ and NiEDDA, the amount of power needed for saturation

increases according to the degree of accessibility of the nitroxide spin to the reagents. The spectra collected in the presence of $N_2$, air and NiEDDA are used to calculate $P_{1/2}$ ($N_2$), $P_{1/2}$ ($O_2$) and $P_{1/2}$ (NiEDDA). The power saturation parameter corrected for background for $N_2$, $\Delta P_{1/2}$ is calculated following equation: $\Delta P_{1/2}(x) = P_{1/2}(x) - P_{1/2}(N2)$, where X is air or NiEDDA. Dividing $\Delta P_{1/2}$ by the line width, $\Delta$Hpp, of the first derivative EPR signal gives the accessibility parameter, $\pi$. To eliminate variation between resonators, $\pi$ values are normalized to the accessibility of 2,2-diphenyl-1-picrylhydrazyl (DPPH), determined in our lab using a sample of crystalline DPPH (Farahbakhsh, Altenbach, & Hubbell, 1992).

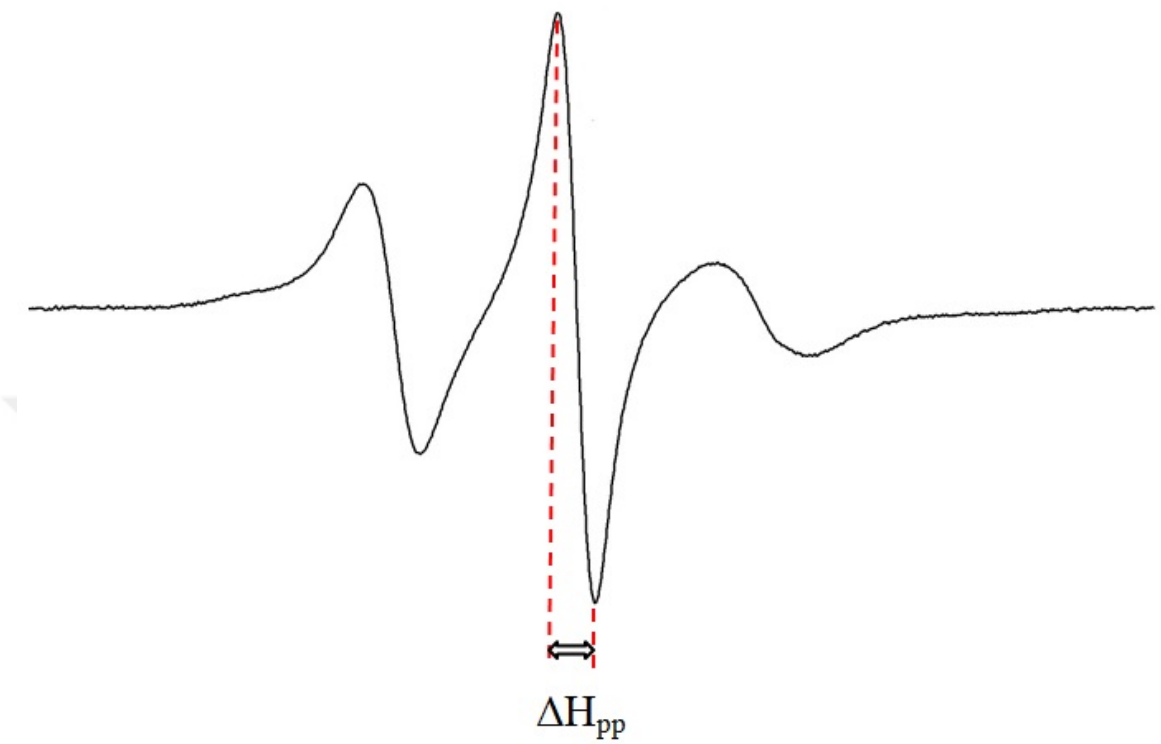


**Figure 8.** The peak-to-peak first derivative width of the central resonance line, ΔHpp.

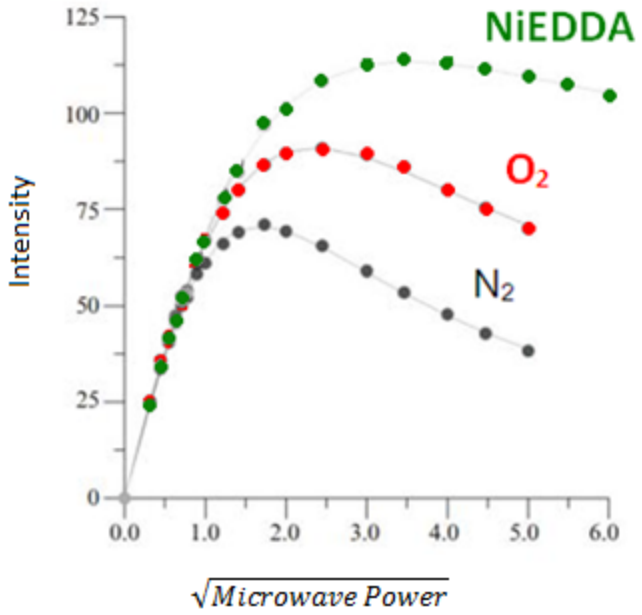


**Figure 9.** An example of power saturation curves in the presence of N2, O2 and NiEDDA. It is clear that the residue being analyzed is more accessible to NiEDDA than to $O_2$ because the power needed to achieve saturation is higher in the presence of NiEDDA.

A plot of the accessibility values of sequential residues in a polypeptide as a function of the position number can provide information about the secondary structure of the protein of interest and its environment. An α-helical structure shows a periodicity of three to four residues whereas a β strand gives a periodicity pattern of every other residue. If a polypeptide is exposed to a lipid environment, the accessibility of $O_2$ and NiEDDA should be out of phase. A polypeptide in a homogeneous aqueous environment shows an in-phase accessibility pattern.

The immersion depth of a nitroxide spin attached to a membrane-associated peptide can be determined using accessibility data. The differential solubility of $O_2$ and NiEDDA in the lipid bilayer results in opposite concentration gradients through the lipid bilayer. If the nitroxide spin is deep in the bilayer, it will have a high accessibility for $O_2$, and low accessibility for NiEDDA. The depth parameter (Φ) of the spin label is calculated from the equation;

$$\Phi = \ln \pi(O_2)/\pi(\text{Ni-EDDA}).$$

A calibration curve of depth (Φ) is produced by using species of phosphatidylcholine spin labelled lipids at the phosphate head group or at positions C5, C7, C10 or C12 in the hydrocarbon chain esterified to C2 of the glycerol backbone. Each spin-labelled species of phosphatidylcholine was mixed with *E.coli* polar lipids at a molar ratio of 1:100. The phospholipids carrying spin labels were assembled into pure lipid liposomes, liposomes containing SecYEG, and liposomes co-assembled with SecYEG and SecA. Calibration curves were determined independently for each type of liposome

and the accessibility of the spin label at each position was calculated. The calculated Φ from accessibility values for each position in the phospholipid is plotted against the known depths for each labeled carbon.

## Results and Discussions

Site-directed spin labeling (SDSL) in combination with electron paramagnetic resonance (EPR) spectroscopy is a well-characterized, powerful approach used to gain knowledge about the structure, location and environment of soluble and membrane proteins (Fajer, 2000). In this study, we examined two regions of SecA that were likely to interact with the hydrocarbon region of the lipid bilayer using the EPR method of power saturation.

We created a collection of 20 SecA variants, each containing a single cysteine at the site of interest by cysteine substitution mutagenesis. The cysteine was covalently labeled with a nitroxide spin label. The label (1-oxyl-2,2,5,5-tetramethylpyrroline-3-methyl)-methanethiosulfonate (MTSL) is the most well characterized sulfhydryl specific spin label that is used for EPR studies. However, since it is attached through a disulfide bond, it is released by mild reducing reagents (Berliner, Grunwald, Hankovszky, & Hideg, 1982). Free spin in the system would give us an artifactual saturation profile, since the collision rate of a free spin is faster than that of a spin bound to the protein. To eliminate the problem, a maleimide derivative spin label was used in this study, 1-oxyl-3-(maleimidomethyl)-2,2,5,5-tetramethyl-1-pyrrolidine (maleimide), designated Rm. The reactive group forms a stable, irreversible thioether bond with the available sulfhydryl

group of the targeted cysteine in the protein even in the presence of reducing reagents. Maleimides react with amino group under alkaline conditions. All spin labelling process were carried out at pH 7.0 where the maleimide reaction is specific for sulfhydryl groups. At pH 7.0, maleimide labels sulfhydryl groups 1000 times faster than amine groups (Hermanson, 2008).

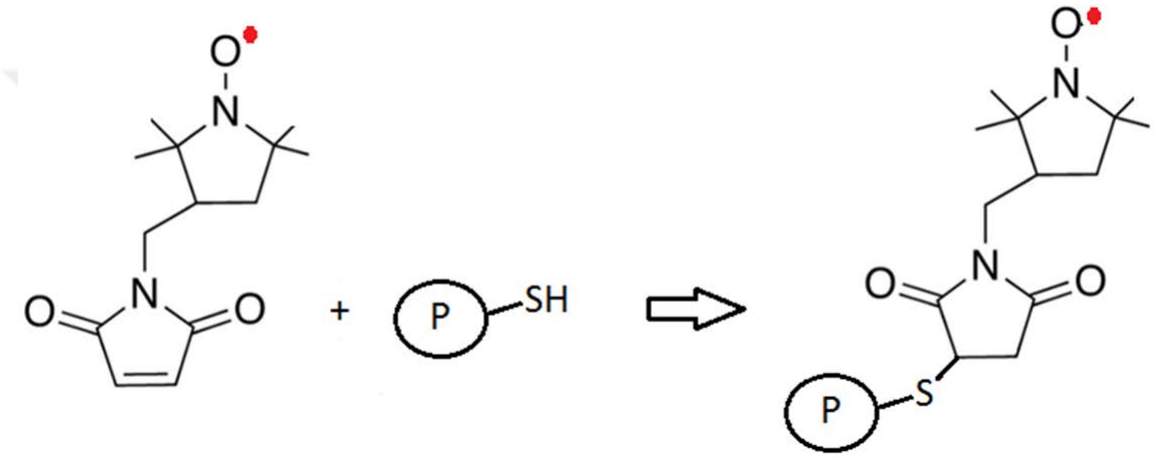


Figure 10. Illustration of the reaction between 1-oxyl-3-(maleimidomethyl)-2,2,5,5-tetramethyl-1-pyrrolidine spin label and a cysteine residue via thioether chemistry at pH 7.

The strategy of site-directed spin labeling requires that a reactive cysteine at the site of interest be the only available residue for modification. A wild type SecA contains four native cysteines (C98, C885, C887, C896), three of which are involved in coordinating a necessary zinc ion in the extreme C-terminal region of SecA. We have previously shown that SecA and SecB form two types of complexes that differ in stoichiometry depending on whether a zinc ion is present in the zinc-binding domain of SecA (J. M. Crane et al., 2005; Randall et al., 2004). If zinc is bound, the domain binds the flat β-sheets that form the sides of SecB and a complex is made that has two protomers of SecA and one tetramer of SecB (A2:B4). If zinc is missing, then only one protomer of SecA is able to bind SecB tetramer (A1:B4) (J. M. Crane et al., 2005; Randall et al., 2004).

In order to preserve the zinc-binding domain, the base protein for the variants in the N-terminal region of SecA (residues 2 – 15) was made by replacing only the cysteine at position 98 with serine (C98S). The spin label reagents do not react with the zinc-coordinating cysteines (Cooper et al., 2008), thus, only the cysteine introduced in a region of interest was available for labeling. For the Linker Helix region, we used single-cysteine variants in the Linker Helix that were made for a previous EPR study (Cooper et al., 2008). The base protein for these variants is SecA that has all four native cysteine replaced with serine (SecAC4). Thus, because the three zinc-coordinating cysteines were removed, these variants do not have a zinc ion bound. In addition, some of these variants were labelled with MTSL (Cooper et al., 2008). For ease of discussion, the spin-labeled variants were designated by the amino acid and residue number that was substituted and

the spin label used to modify the protein, Rm for the maleimide derivative and R1 for the MTSL. For example, SecAC98SL2Rm indicates that the leucine residue at position 2 in the base protein with one cysteine removed (SecAC98S) was converted to cysteine and reacted with the maleimide spin label Likewise, SecAC4G605R1 indicates that the glycine residue at position 605 in the base protein with all four cysteines removed (SecAC4) was converted to cysteine and reacted with the MTSL spin label.

**Size-exclusion chromatography of SecA species and its binding partner, wild-type SecB**

All SecA variants, with and without the spin-labelled, were analyzed by size-exclusion chromatography to ensure that neither substitution of the native residue with cysteine nor the subsequent introduction of a spin label disrupted the structure of SecA or its ability to bind SecB. Both the cysteine-substituted and the spin-labeled forms of the SecA variants were analyzed by size-exclusion chromatography (see Materials and Methods). The absolute molar mass of the proteins was determined directly using static light scatter by passing the eluent through a detector for UV absorbance, a multi-angle laser light scatter detector followed by a differential refractometer. Figure 11, A shows the elution profile of wild-type SecA applied to the size-exclusion column (6 µM dimer). The molar mass was approximately156 kDa at the apex of the peak where dimers would be most populated, and it decreased towards the tail of the peak, consistent with a self-associating protein. SecB (6 µM tetramer) applied alone eluted from the column with a molar mass of 69 kDa at a position later than SecA. When an equimolar mixture of wild-type SecA and wild-type SecB (6 µM each) was applied to the column, they eluted as a

complex ahead of the individual proteins, and the molar mass for the complex was approximately 190 kDa.

All SecA variants having cysteine substitution were folded, demonstrated a monomer-dimer equilibrium, and were shown to bind SecB. Some of the spin-labelled variants derived from the SecAC98S base protein had a small amount of aggregate that eluted in the void volume of the column, but were otherwise well-behaved. The spin-labeled variants derived from the SecAC4 base protein were previously characterized by size-exclusion chromatography (Cooper et al., 2008) and shown to be folded and bind SecB. Figure 11 shows examples of cysteine-substituted SecA variants compared to wild-type SecA. SecAC98SI3C elutes with a molar mass of 178 kDa at the highest point of the apex of the peak and it makes a complex with SecB which elutes with a molar mass of 213 kDa. The higher molar mass relative to that observed with wild type SecA indicates that the replacement of isoleucine at position 3 with cysteine shifted the equilibrium toward dimer (Figure 11, B).

Each of the spin-labelled SecA variants was assessed for folding and complex formation by size-exclusion chromatography. Some variants showed small amount of aggregation and eluted in the void volume However, these variants were still able to bind SecB and make a complex of two protomer of SecA and a tetramer of SecB (data is not shown).

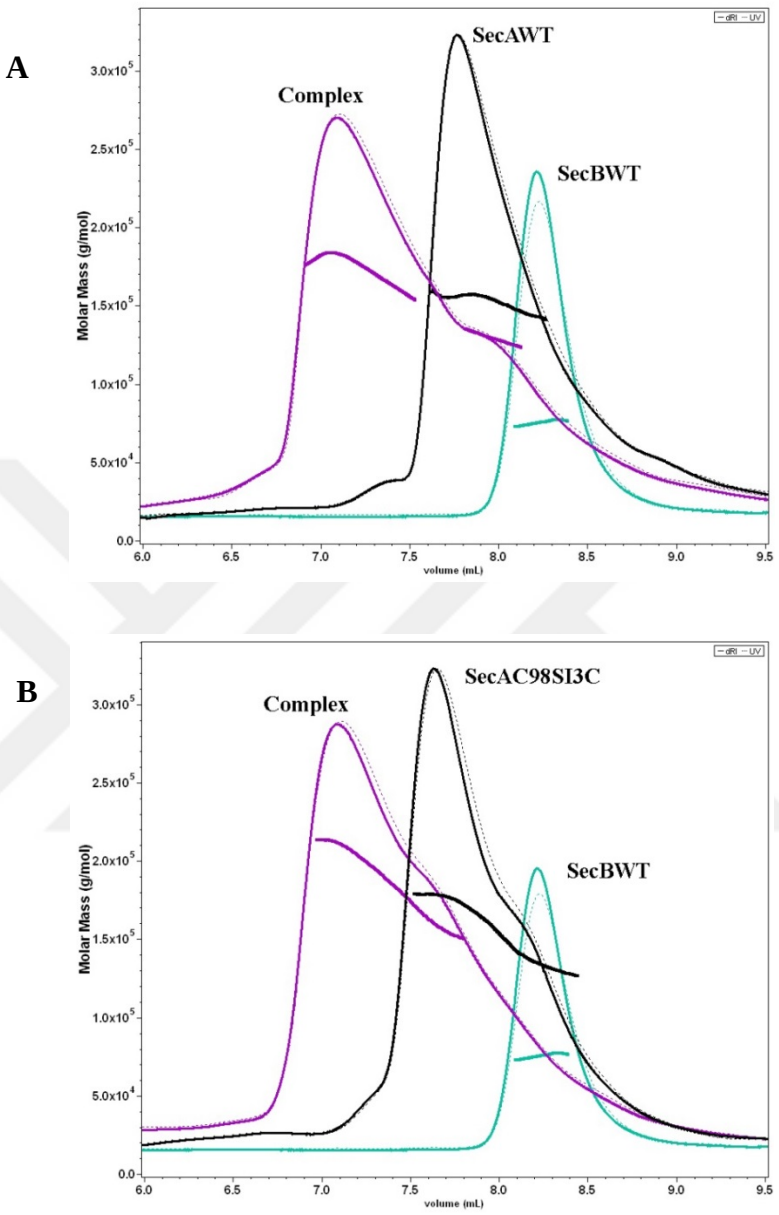


**Figure 11.** Size-exclusion chromatography of SecA and its specific binding partner, SecB. SecA alone, black; SecB alone, green; complex of secA and SecB, puerple. (A) Wild-type SecA and wild-type SecB were applied individually or as a mixture. B) Cysteine substituted SecA and wild-type SecB were applied individually or as a mixture.

The shoulder on the tailing edge of the peak is likely to be uncomplexed SecA or a small % of A1B4 complex caused by loss of zinc.

### *In vitro* Translocation Activity of SecA Variants in Translocation

An *in vitro* translocation assay was performed to demonstrate that the spin-labeled SecA variants were able to translocate the precursor of outer membrane protein A (OmpA), proOmpA into proteoliposomes, which are used an *in vitro* model of the Sec system. Standardly, proteoliposomes are prepared by reconstituting SecYEG into liposomes (referred to as as proteoliposomesYEG, PLYEG) followed by an addition of SecA (PLYEG+A). These proteoliposomes show only 10% of the number of active translocons as compared to the number of active translocons in native membranes. We developed a new method for preparing proteoliposomes in which SecYEG and SecA are simultaneously reconstituted into liposomes (PLYEG•A) (Mao et al., 2013). Co-assembly of SecYEG and SecA increased the number of active units of SecYEG to a level that corresponds to the level of units observed in the native environment of inner membrane vesicles (Mao et al., 2013).

To determine whether spin-labelled SecA variants were able to activate SecY in the same way as wild-type SecA does, proteolipsomes were prepared using both the standard method of adding spin-labeled SecA after the reconstitution of SecYEG in liposomes and the enhanced method of reconstituting co-assembled spin-labeled SecA and SecYEG into liposomes. The translocation activity of SecAC98SK4Rm is shown in the two types of proteoliposomes (PLYEG+A and PLYEG·A) and is compared with the

translocation activity of wild-type SecA (Figures 13). The data were fit to a single exponential rise to maximum to determine the final level of translocation. The level of translocation of proOmpA when wild-type SecA was added to PLYEG was ~ 232 nM at the plateau (Mao et al., 2013). When SecAC98SK4Rm was added to PLYEG (red) ~ 178 nM proOmpA was translocated. The final level of translocation using co-assembled PLYEG·SecAC98SK4Rm (blue) was ~523 nM compared to ~675 nM when wild-type SecA was used to make PLYEG·A (black). Therefore, the spin-labelled species assessed when co-assembly (PLYEG·SecAC98SK4Rm) or added exogenously (PLYEG+SecAC98SK4Rm) preserved 77% of the translocation activity observed for wild-type SecA. We concluded that the spin-labeled SecA variants activated SecY in the same manner as does wild-type SecA.

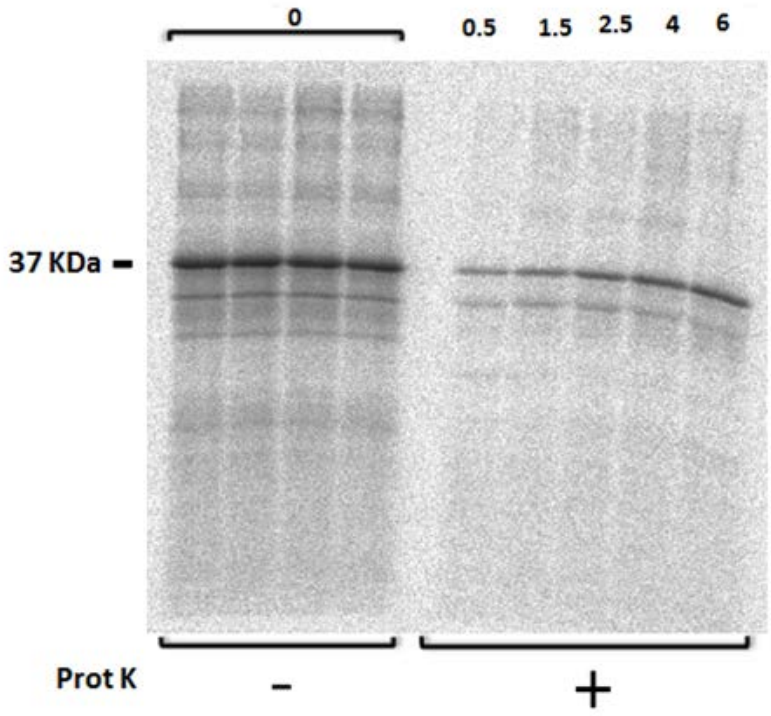


**Figure 12.** A representative image of the primary data of translocation of radiolabelled proOmpA ($^{14}$C-proOmpA) in PLYEG·SecAC98SK4Rm. The bands at 37 kDa are full length proOmpA. The first four lanes are the input that were sampled at 0 minute on ice and were not treated with proteinase K. The last five lanes were sampled at the times indicated during incubation at 35 °C (t = 0.5, 1.5, 2.5, 4, 6 minutes). All sample applied in the lanes were treated with proteinase K (see Materials and Methods for details).

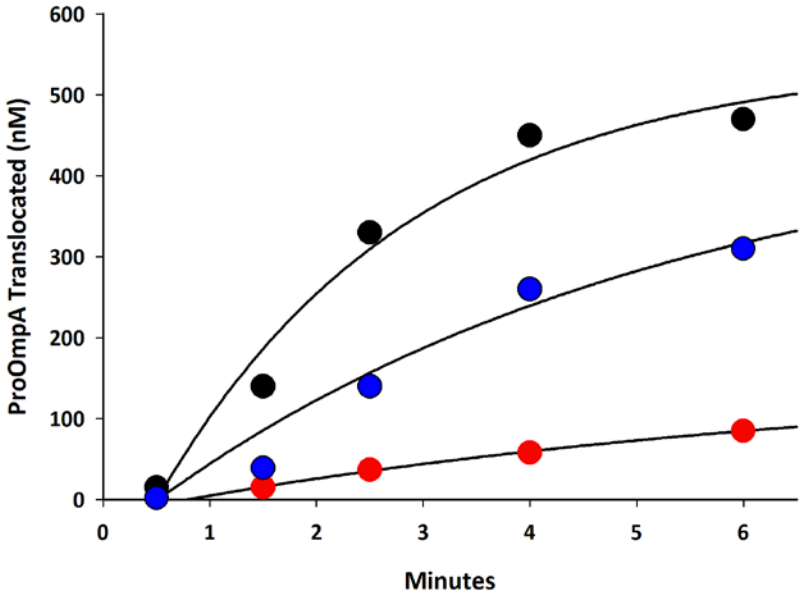


**Figure 13.** Translocation activity of SecA species. Translocation of $^{14}$C-proOmpA was assayed *in vitro* (see Materials and Methods). Red, SecAC98SK4Rm was added to the reaction with PLYEG; black, when wild-type SecA co-assembled with SecYEG into the liposomes (PLYEG·SecAWT); blue, when SecAC98SK4R was used to co-assembled with SecYEG into the liposomes (PLYEG·SecAC98SK4R).

**Solvent Accessibility**

The solvent accessibility ($\pi$) of a nitroxide side chain at the residue of interest in SecA was determined from measurement of the biomolecular collision rate of the nitroxide with paramagnetic reagents. Two paramagnetic reagents were used in this study: oxygen, a hydrophobic reagent; and nickel (II) ethylenediamine diacetate (NiEDDA), a hydrophilic reagent. $N_2$ was used as a control to eliminate $O_2$ from the samples. Air which is ~ 20 % oxygen was introduced to the sample as the oxygen paramagnetic reagent. The NiEDDA concentrations were at 20 mM for the solvent-exposed residues and at 100 mM for the lipid-exposed residues.

At a high local concentration, NiEDDA causes a measurable broadening of the line width of a residue (Christian Altenbach, Froncisz, Hemker, McHaourab, & Hubbell, 2005). To eliminate the broadening of line width ($\Delta$Hpp), low concentrations of NiEDDA are used for residues that are solvent-exposed. We measured the line with of the nitroxide spectrum under different concentrations of NiEDDA (2, 5, 10, 20, 25, 50 and 100 mM) and determined that 20 mM NiEDDA is the proper concentration for residues exposed to the solution. Figure 14 illustrates the line broadening caused by a high concentration of NiEDDA on the spectra of nitroxide-labelled proteins: SecAC98SR13Rm, in solution; SecAC98SF10Rm, in the presence of phosphatidylcholine liposomes which do not interact with SecA; and SecB T46R1, a soluble protein, which does not interact with liposomes, in the presence of *E.coli* liposomes. A comparison of spectra for proteins in solution at 20 mM NiEDDA showed no line broadening. On the other hand, at 20 mM NiEDDA the residues that are in the lipid bilayer do not reach saturation because of the

low solubility of NiEDDA in the lipid bilayer (data not shown). Therefore, for the residues in the lipid bilayer NiEDDA at 100 mM was used.

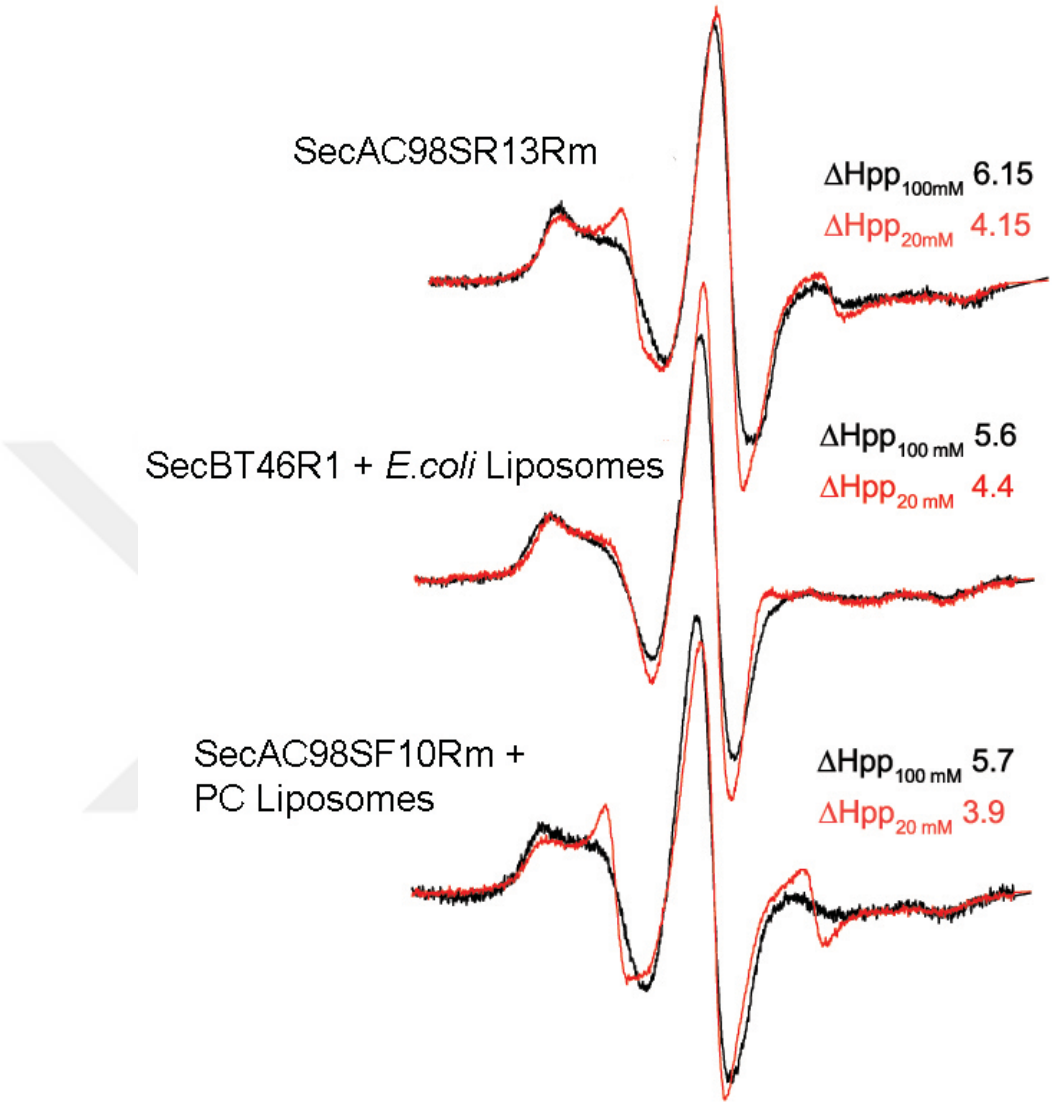


**Figure 14.** Illustration of line broadening of the solvent exposed residues at 100 mM NiEDDA.

Solvent accessibility of a nitroxide side chain provides information about the local environment of specific sites on a protein. Patterns of accessibility are different for proteins in solution as compared to patterns for membrane proteins. The residues that are completely solvent exposed show a relatively higher accessibility to NiEDDA and a lower accessibility to $O_2$. Accessibility of a series of consecutive side chains in solution have the same phase if the environment is a homogeneous environment which means all the residues are on the surface with no contacts. If a residue is in the protein interior packed on other residues, its accessibility for both NiEDDA and $O_2$ are low because both reagents are similarly excluded from the protein interior. If residues in structural elements on the surface make contacts, they also show reduced accessibility to both relaxation reagents. A residue deep in a lipid bilayer shows the opposite pattern compared to a residue that is in aqueous solution: low NiEDDA accessibility and high $O_2$ accessibility. In an environment with an asymmetric distribution of the paramagnetic reagents such as a lipid bilayer, residues show a periodicity that is out of phase by 180° because of the opposite concentration gradients of NiEDDA and $O_2$ in the lipid bilayer. The periodic dependence of solvent accessibility as a function of sequence position can be used to determine the secondary structure of a protein. In the present study, we collected the solvent accessibility data for the nitroxide side chains at the sites of interest to obtain detailed information about the interaction of SecA with the lipid bilayer.

Solvent accessibility data also allows one to determine the depth of penetration into the lipid bilayer of a nitroxide side chain on an integral membrane protein. The depth parameter (Φ) is given by the natural logarithm of the ratio of the solvent accessibilities

(ln ($\Pi_{Air}$/ $\Pi_{NiEDDA}$). A standard curve is generated to calibrate $\Phi$ using spin-labelled lipids with known depths in the bilayer. Phosphatidylcholine (PC) lipids carrying spin labels at the head group or at the hydrocarbon chains were mixed with an *E.coli* polar lipid extract at a ratio of 1 to 100. We used PC lipids spin labeled on the phoshate head group by TEMPO, and spin labeled with doxyl groups at the positions of C5, C7, C10-, and C12 of the hydrocarbon chains (Figure 15).

A separate standard curve must be generated for investigations using liposomes, liposomes with secYEG integreted, and liposomes with SecYEG and SecA co-assembled because the presence of protein within the bilayer changes the accessibilty parameters measured.

Three independent standards were generated using five separate preparations of each type of liposomes, each have one of the spin-labelled lipids species, each contained a mixture of *E.coli* polar lipids and spin-labelled PC at a position of interest at the ratio of 100:1. The $\Phi$ values determined using accessibility data were plotted as a function of known-depth of the carbon positions from the phosphate group of the lipid (Kyrychenko & Ladokhin, 2013). The standard graph for PLYEG·A is shown in Figure 17 as an example. Each data point was done at least three times. Using the equation obtained from a linear fit to the data, depths in the lipid bilayer for each residue on SecA were determined.

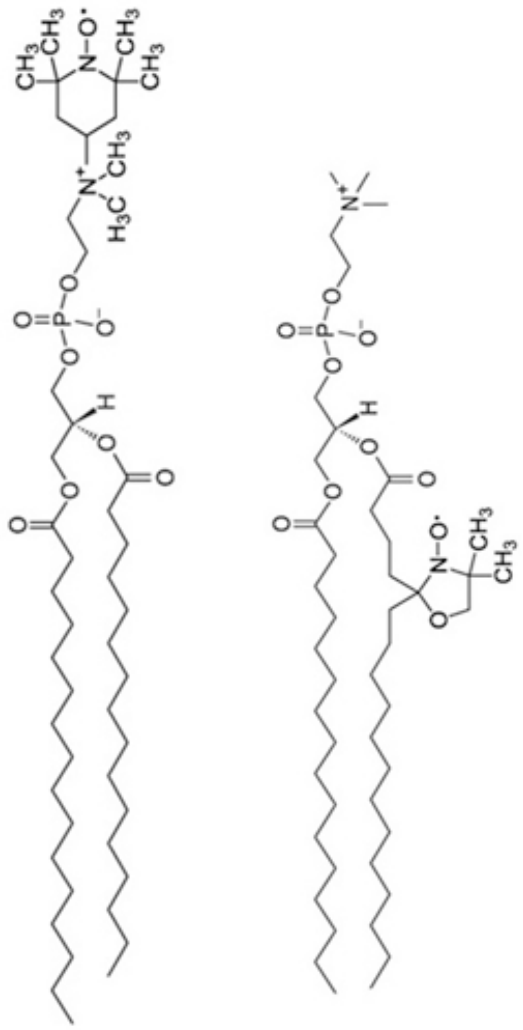

**Figure 15.** Two examples of spin-labelled lipids. 1,2-dipalmitoyl-*sn*-glycero-3-phospho(tempo)choline is on the left and 1-palmitoyl-2-stearoyl-(5-doxyl)-*sn*-glycero-3-phosphocholine is on the right. In all cases the chain that is spin labelled is esterified to the C2 hydroxyl of the glycerol backbone.

**Investigation of the N-terminal residues of SecA in PLYEG·A**

We began our survey by investigating the N-terminal region of SecA when SecYEG was assembled into the liposomes in the presence of a spin-labeled SecA species (PLYEG·A). Figure 16 shows the solvent accessibility pattern of these residues of SecA in PLYEG·A as a function of sequence positions. The solvent accessibility of the residues that form the extreme amino terminal region of SecA in proteoliposomes, PLYEG·A, shows an out-of-phase pattern that is characteristic of protein inserted into a lipid bilayer. While the accessibility of $O_2$ for a residue increases, accessibility of NiEDDA decreases and vice versa. The residues I3 and G11 break the out-of-phase pattern. Their accessibility to both $O_2$ and NiEDDA are decreased indicating that access of these residues is likely to be blocked directly or indirectly because of a tertiary contact. The residues I3 and G11 might make a contact with another domain of SecA or with SecYEG or lipid head groups. It was previously suggested that G11 might make contact with the lipid head groups (Cooper et al., 2008).

The standard graph for PLYEG·A is shown in figure 17. Results show that these residues lie parallel to the plane of the membrane with a maximum depth of 6.2 Å penetrations into the bilayer (Figure 18).

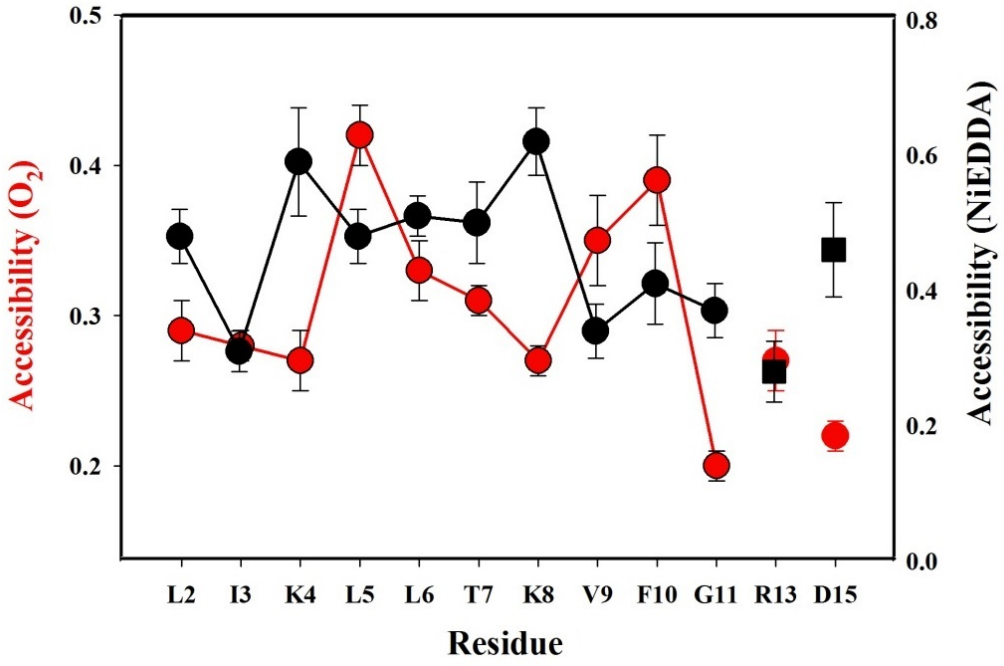


**Figure 16.** Solvent accessibility of residues 2 through 15 of SecA in PLYEG·A. Red, oxygen accessibility; black, NiEDDA accessibility.

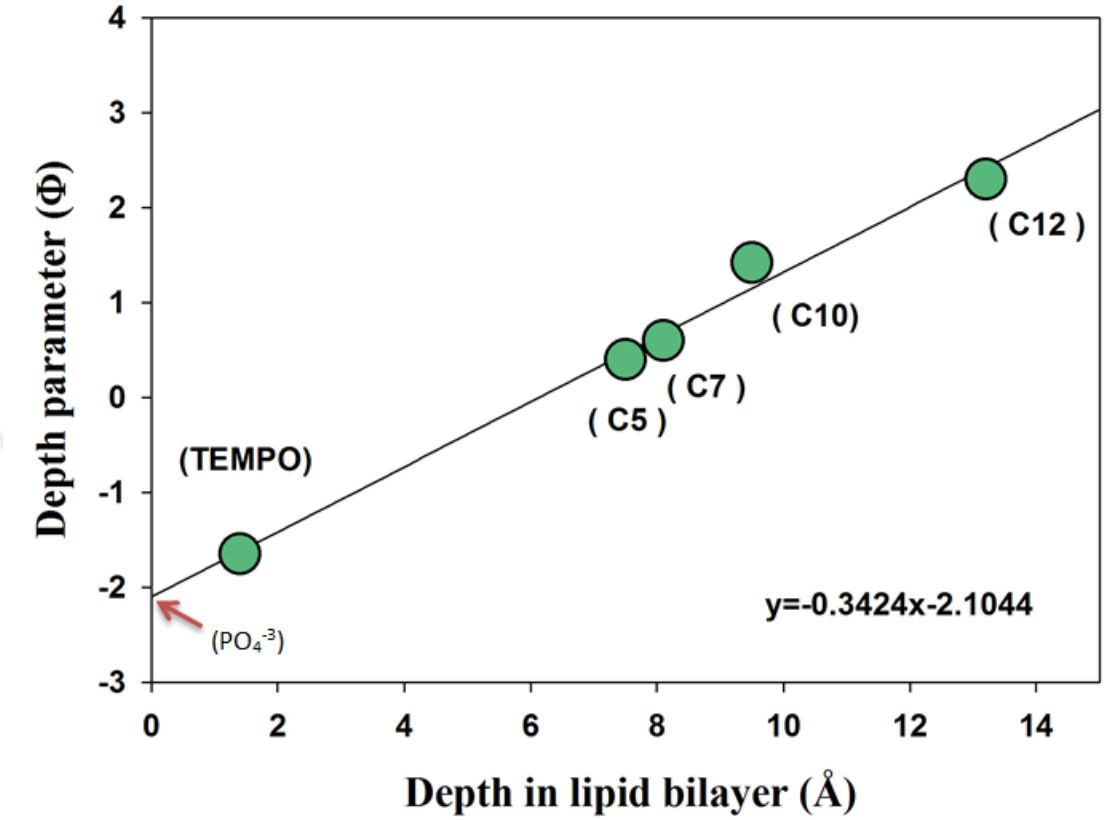


**Figure 17.** Standard curve for PLYEG·A. The depth of the nitroxide spin labels from the phosphate group on PC are taken as follows; at the head group, 1.4 Å; C5, 7.5 Å; C7, 8.1 Å; C10, 9.5 Å; C12, 13.2 Å (Kyrychenko & Ladokhin, 2013).

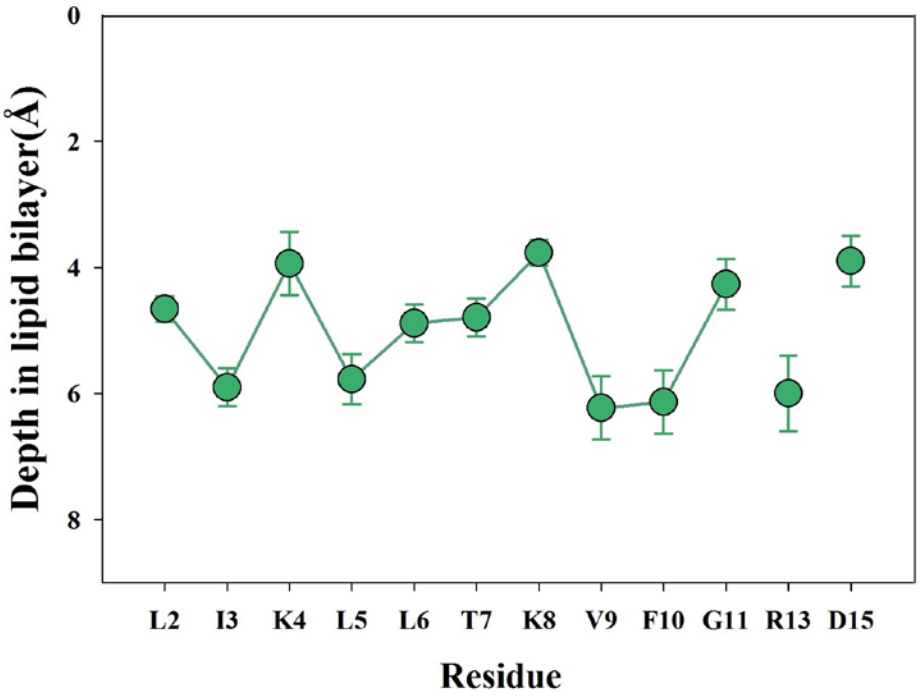


**Figure 18.** Depth of N-terminal residues taken phosphate group as zero.

The orientation of a protein or peptide relative to the plane of the membrane can be determined from the pattern of depth. For an α-helical transmembrane protein perpendicular to the plane of the membrane, the depth would increase 1.5Å for each residue through the center of bilayer. We do not see any directional pattern of increase from N-terminal L2 to residue R15. Figure 18 indicates that these residues of SecA lie parallel to the plane of the membrane. The residues on the hydrophilic side of the amphipathic helical wheel have the shallowest depth in the lipid bilayer. L2, a hydrophobic residue, showed a lower degree of penetration because it is the N-terminal aminoacyl residue of SecA and carries a positively charged amine group.

**Investigation of the N-terminal residues of SecA in PLYEG+A and liposomes+A**

The co-assembly of SecYEG and SecA in PLYEG·A showed a six-fold increase in the number of active translocons as compared to PLYEG +A in which SecA is added to the system after reconstitution of SecYEG into liposomes. PLYEG·A is the most active *in vitro* system in the literature. However, the mechanism of activation is not known (Mao et al., 2013). The enhanced activity of PLYEG·A might arise from the difference in the membrane association of SecA when SecA makes a complex with SecYEG in the early stages of assembly. To sort out whether the interaction of first 10 residues of SecA with the lipid bilayer is different, we compared the results of solvent accessibilities of these residues which we obtained when SecYEG and SecA were co-assembled, described in the previous section, with the accessibility of spin-labelled SecA added to SecYEG, assembled into liposomes (PLYEG), immediately before the assay.

In addition to binding SecY at the membrane with a high affinity, SecA binds phospholipids nonspecifically with low affinity (Douville et al., 1995; Hartl et al., 1990; Matsumoto et al., 1997). To determine if SecA interacts differently with membrane alone than it does with membrane plus SecYEG, we analyzed the effect of adding spin-labelled SecA to liposomes without SecYEG present (Liposomes+A). The solvent accessibility of the first 10 aminoacyl acid residues of SecA in the PLYEG+A and Liposomes+A is shown in Figure 19 and 20, respectively. All residues were analyzed at least three times for $N_2$, NiEDDA and $O_2$ in both systems. The solvent accessibility plots of PLYEG+A and Liposomes+A show out-of-phase periodicity which indicate that the first 10 residues of SecA are immersed into the lipid bilayer in both PLYEG and liposomes. However, the residues that break the out-of-phase pattern, which are likely contact sites, differ in all three systems. As discussed in the previous section, in PLYEG·A, residues I3, G11 are the breaking points. In PLYEG+A, in addition to I3 and G11, residue L6 shows low accessibility to both relaxation reagents. On the other hand, in Liposomes+A, only residue I3 has a reduced accessibility to the relaxation reagents. In liposomes, the only possible contacts for SecA are SecA itself or lipids. The residue I3 in all three systems might make an intramolecular contact with SecA. The residues G11 in PLYEG·A and the residues L6 and G11 in PLYEG+A might make a contact with SecYEG that causes a reduced accessibility to the relaxation reagents.

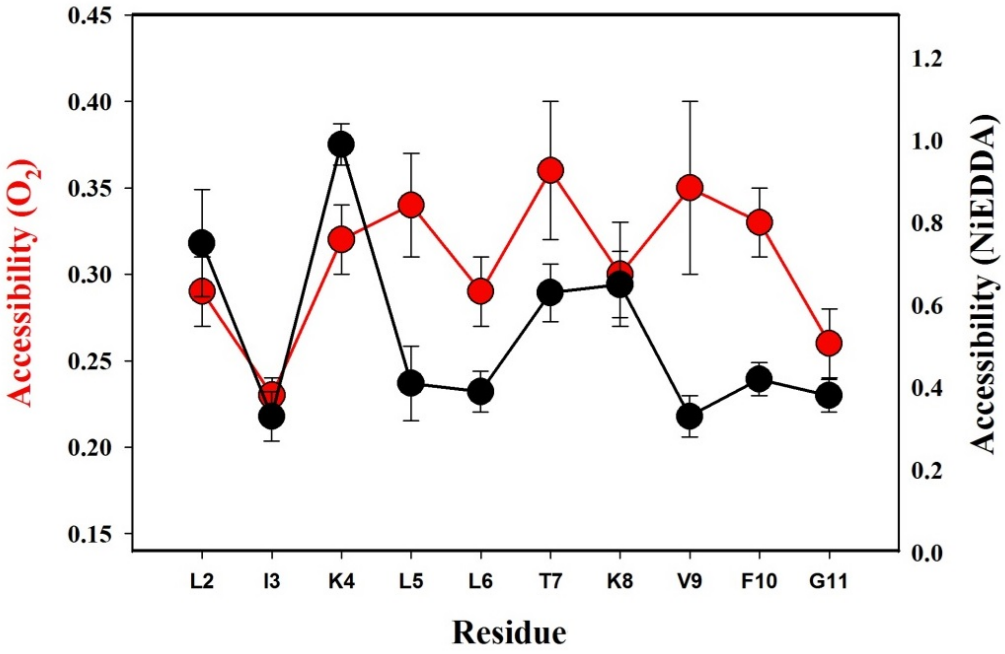


**Figure 19.** Solvent accessibility of residues 2 through 11 of SecA in PLYEG+A. Red, oxygen accessibility; black, NiEDDA accessibility.

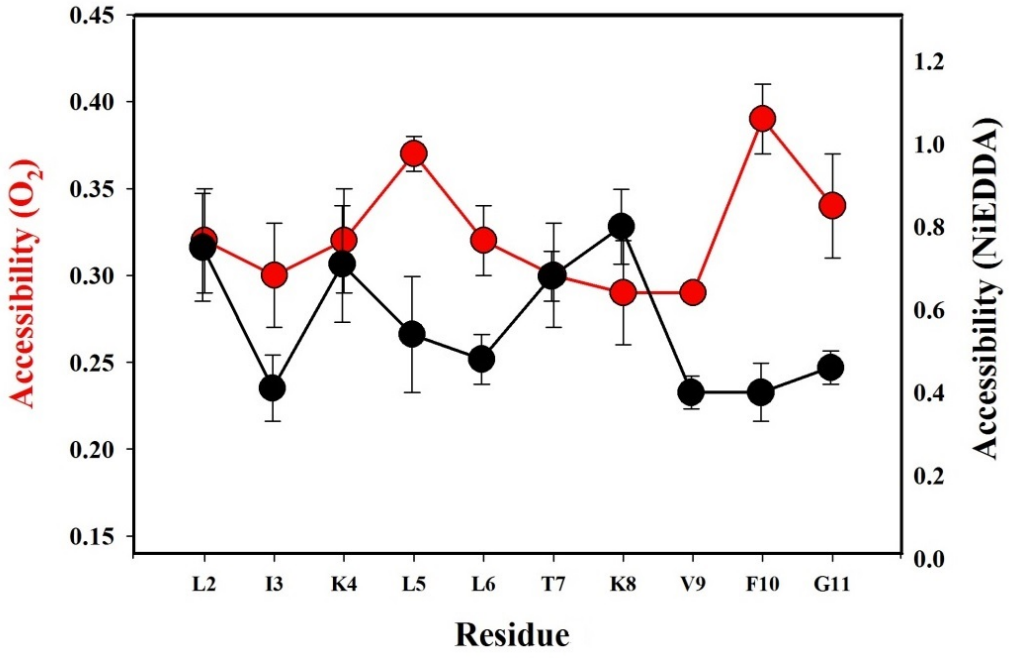


**Figure 20.** Solvent accessibility of residues 2 through 11 of SecA in Liposomes+A. Red, oxygen accessibility; black, NiEDDA accessibility.

The equations of calibration curves generated for PLYEG+A and Liposomes+A are y=-0.3671x+4.5452 and y=-0.3324x+4.2851, respectivly. Figure 21 shows the depth in the lipid bilayer for all three systems. The observed penetration depths of the first 10 residues of SecA did not show a dramatic difference among the three systems. When SecA is added to PLYEG (Figure 21, blue), it penetrated into the bilayer with a maximum of 2 Å deeper than did the SecA which was co-assembled with SecYEG (Figure 21, green) or added to liposomes without SecYEG (Figure 21, pink). The actual differences in the penetration depths among the systems might be larger than we observed. The results generated by EPR power saturation are a weighted sum of the population of the spin-labelled SecA.

Imaging studies using atomic force microscopy (Mao et al., 2013) showed that SecA added to liposomes or to liposomes containing SecYEG have a wide distribution of heights above the bilayer which indicates a heterodisperse population of multiple binding modes. If these different binding modes penetrated to different depths in the bilayer, the EPR results would reflect the weight average. In contrast to this situation when SecA is added after liposomes are found, preparations of PLYEG·A showed a sharp distribution of height centered at 40 Å which corresponds to the height of a SecA:SecYEG complex determined by X-ray crystallography . In this case there is one population, but studies in our laboratory have shown that the SecA in these proteoliposomes exchanges with SecA in solution. Therefore depending on the time constants for the exchange, EPR might underestimate the depth of penetration. Averaging can only decreased the observed

depth. Therefore, we know that the N-terminal region of SecA goes at least 6.2 Å deep in the bilayer.

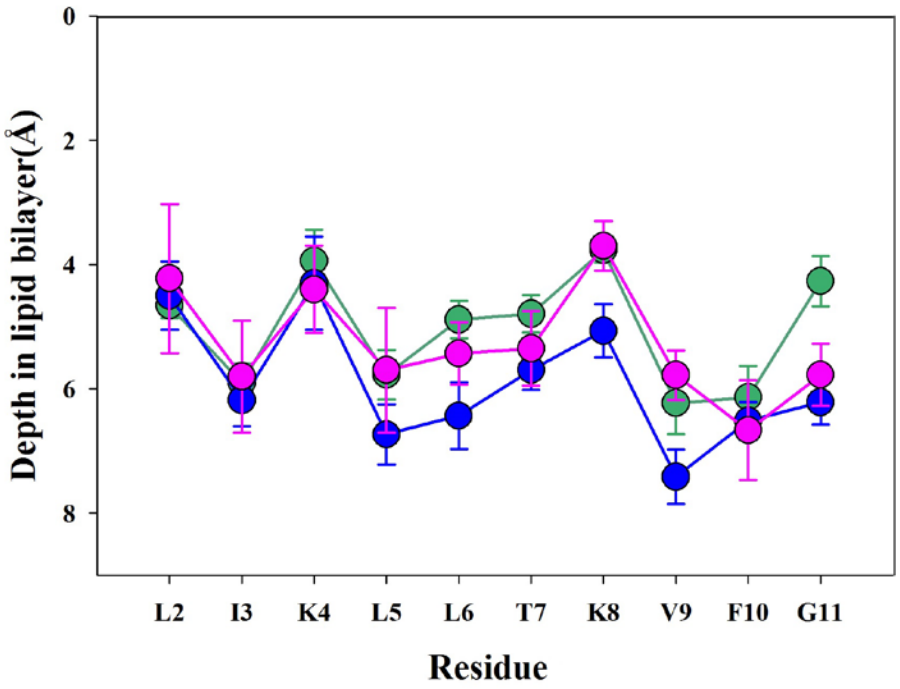


**Figure 21.** Depth of N-terminal residues 2 through 11 of SecA in the bilayer in PLYEG·A (green), PLYEG+A (blue), liposomes+A (pink). The phoshate head group is taken as zero.

**Secondary Structure Determination**

Secondary structure of a region of a protein can be obtained from the periodicity of solvent accessibilities of residues in consecutive sequences. While the alternating pattern of solvent accessibility for a β-sheet shows a periodicity of 2.0, the pattern for an ideal α-helix displays a periodicity of 3.6 with an angular increment of 100°. Disordered regions, without regular secondary structure, do not display a periodicity on accessibility plots. To determine if a periodic pattern existed, we fit the accessibility data of O2 as a function of fractional residue location for all three types of association between SecA and lipids: Liposomes+A, PLYEG+A and PLYEG·A.

Ten amino acids could only form 2 turns of α-helix. Nonetheless, all three systems showed weakly helical patterns for these residues (Figure 22). The helices were not the standard α-helix commonly observed in proteins. The angular increment of the residues is approximately 85° in PLYEG·A and PLYEG+A, corresponding to 4.2 aminoacyl residues in a turn which is similar that in a π-helix (4.1 residues per turn). A π-helix has an angular increment of 87°. The π-helix, consider to be a rare element of secondary structure, has been proposed to function in the formation or stabilization of specific binding sites and to be more common than thought (Weaver, 2000). In Liposomes+A (absence of SecYEG) the helical structure becomes wider, with a periodicity of 4.9 aminoacyl residues in a turn and an angular increment of 73°. The N-terminal 10 residues of SecA are flexible and have not been resolved in crystal structures. In solution, these residues might be disordered or be in equilibrium among multiple conformations. If the equilibrium occurs on the EPR time scale, the EPR spectrum

represents the weighted sum of the individual conformations resulting in an average conformation.

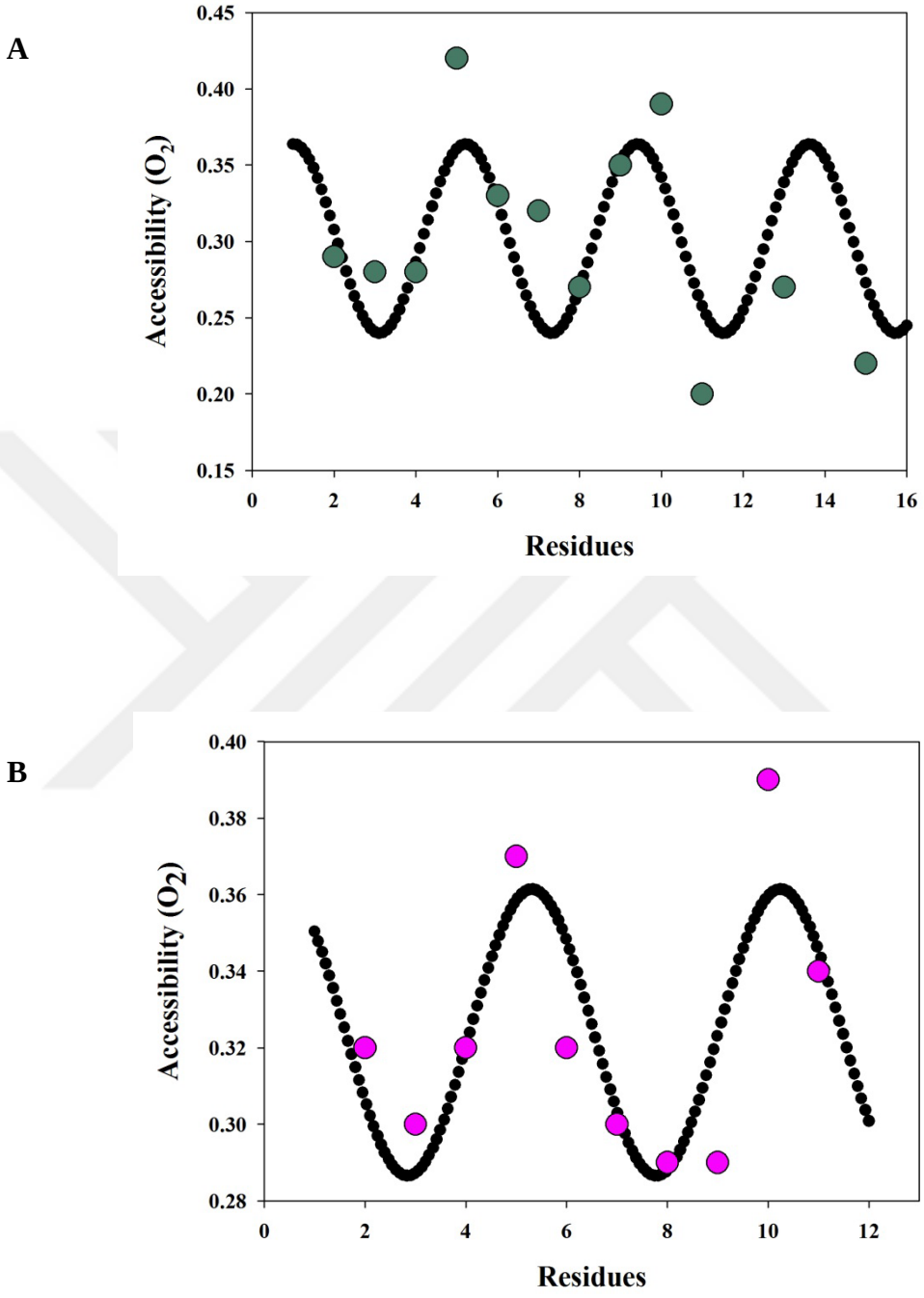


**Figure 22.** Accessibility to O2 is plotted with the periodicity function in PLYEG·A (A) and Liposomes+A (B).

Circular dichroism (CD) was performed to determine the structure of a synthetic peptide (A2/11) mimic of the first 10 amino acid residues of SecA in collaboration with Virginia F. Smith, United States Naval Academy. CD, a well-defined method for characterization of secondary structure of a protein, depends on the sensitivity of far-UV CD to the backbone conformation of proteins. The first 10 amino acid residues were predominantly disordered in the absence of lipid (Figure 23). However, the structure of the synthetic peptide became more α-helical as increasing amount of lipids were added. In the presence of 1 mM *E.coli* liposomes, 70% of the structure was α-helical. All of the EPR experiments reported here were done with lipids at 5 mM.

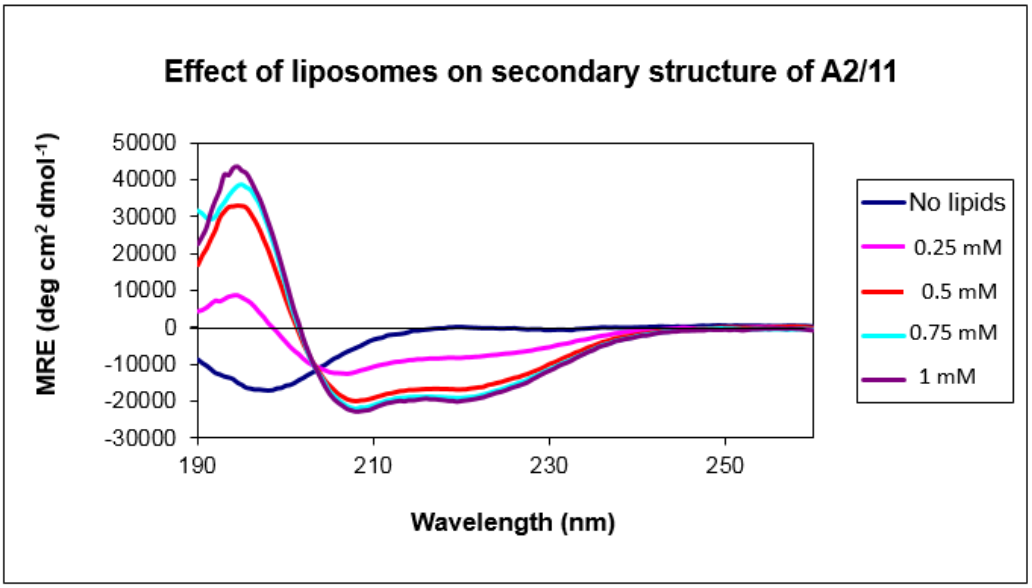


**Figure 23.** Effect of liposomes on secondary structure of the synthetic peptide A2/11.

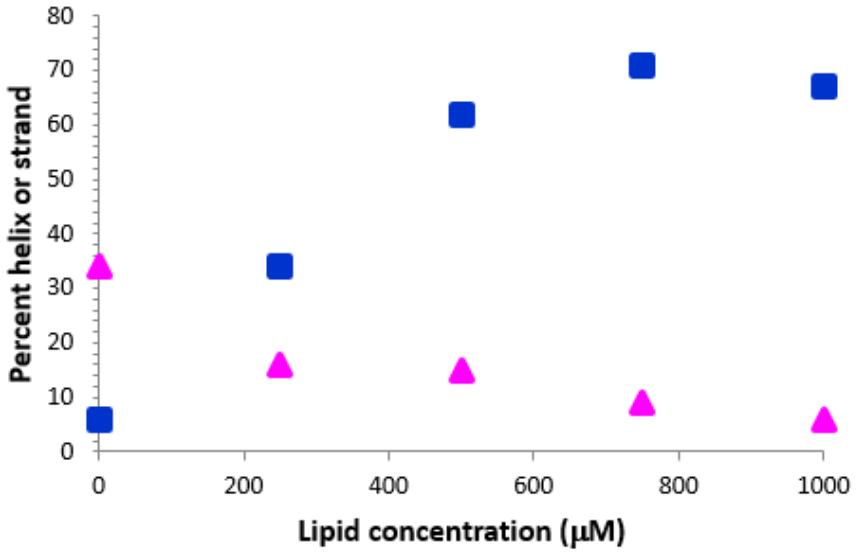


**Figure 24.** Changes in secondary structure as a function of lipid concentration. Blue squares represent the percentage of total helical structure; pink triangles represent the percentage of total strand.

Plotting the residues of the synthetic A2/11 peptide, which formed an α-helix in the presence of lipids, onto a helical wheel for an ideal α-helix shows that the helix is amphipathic (Figure 25, A). The first 10 residues which did not show α-helical periodicity were also plotted on helical wheels adjusted for the angular increments that were observed in PLYEG·A (Figure 25, B. PLYEG+A had similar angular increments with PLYEG·A and is not shown.) and in Liposomes+A (Figure 25, C). It is worth noting that residues which broke the in phase pattern of accessibility for PLYEG·A and for PLYEG+A lie on the same side of the helices as shown in Figure 25, B: residues SecAI3 and SecAG11 in PLYEG·A and residues SecAG11 and SecAL6 in PLYEG+A. These residues might define a face that is in the contact face.

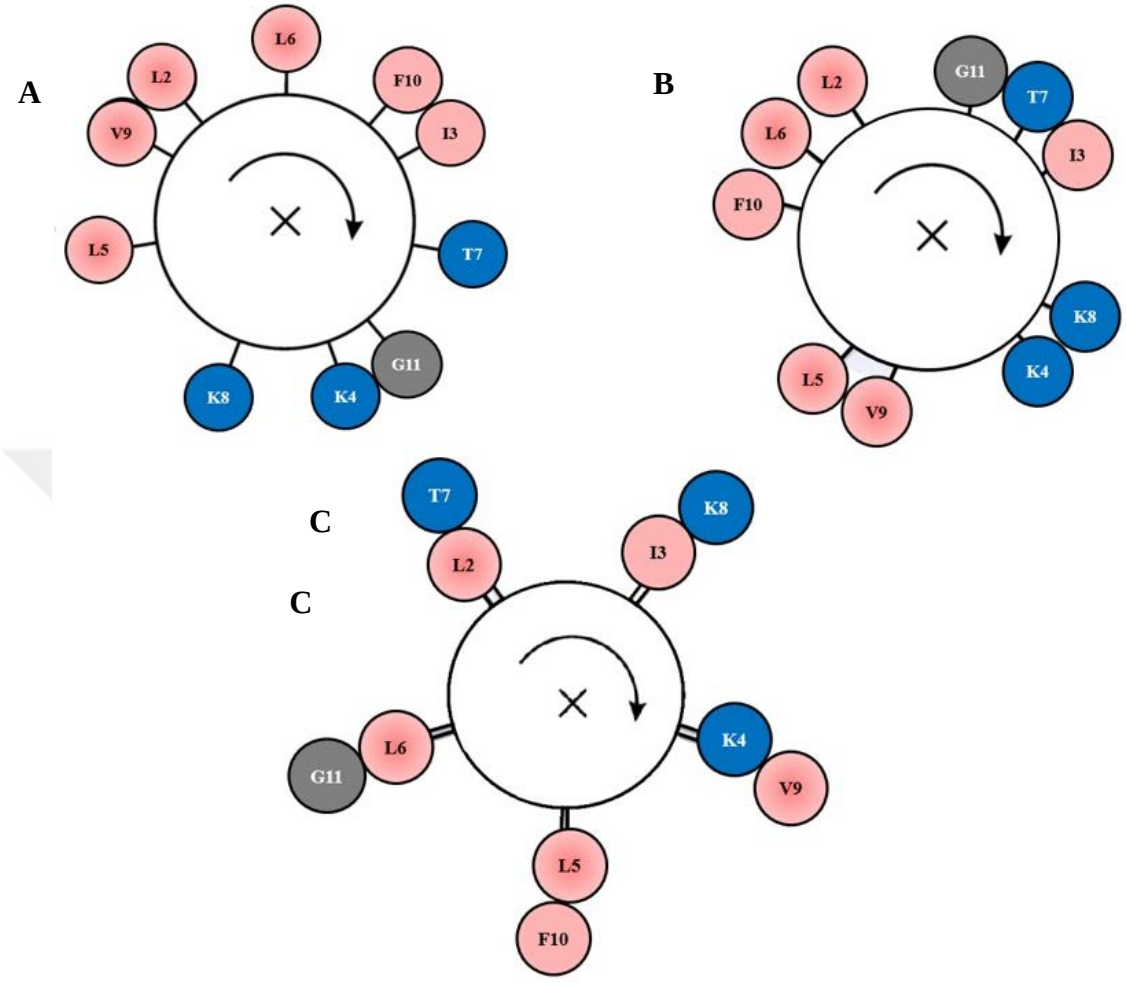


**Figure 25.** Helical wheels showing distribution of the N-terminal residues of SecA. The color schemes are as follows: pink, the hydrophobic residues; blue, the hydrophilic residues; gray, the glycine which is considered neutral. A) An amphipathic α-helical wheel of an ideal α-helix. B) A helical wheel of first 10 residues in PLYEG·A with an 85° angular increment. C) A helical wheel of first 10 residues in Liposomes+A with a 73° angular increment.

**Solvent Accessibility of the Linker Helix of SecA in PLYEG·A, PLYEG+A and liposomes+A**

We used power saturation EPR to gain insight into the interaction of the Linker Helix, residues 600 through 609 with the membrane. As described for the amino-terminal region, solvent accessibilities of the Linker Helix of SecA were examined in the three systems: Liposomes+A, PLYEG+A, and PLYEG·A. Because this region was a candidate for the lipid-exposed site, NiEDDA was used at a concentration of 100 mM. Broadening of the spectral line width was observed for all the residues in all three systems and the solvent accessibility plots showed a periodicity pattern that was in phase (Figures 26). These results indicate that the Linker Helix is solvent exposed in the presence of liposomes. Therefore, we examined the accessibility of Linker Helix of SecA in solution in the absence of liposomes using NiEDDA at 20 mM which is the standard used for solvent exposed sites (Figure 27). Comparison of the accessibility of the residues to oxygen for SecA free in solution, in PLYEG+A, in PLYEG•A and in Liposomes+A showed that the accessibility patterns are similar (Figure 28). The highest accessibility to the oxygen was seen when SecA was free in solution. The reason for lower accessibility to oxygen in the presence of liposomes might be that the contacts are made between these residues and lipid head groups. It was previously shown that residues 600, 601, 604, 605 and 608 interact with the lipid head groups at 6°C (Cooper et al., 2008). It is important to remember that even if the Linker Helix is a solvent exposed region, it would be in proximity to lipids because SecA is tethered to the membrane by the penetration of the N-

terminal region of SecA into the lipids. This close proximity to the membrane might result in a reduced accessibility to relaxation reagents.

The periodicity of accessibility does not correspond to a common secondary structure. In the X-ray structures of SecA, this region has an α-helical conformation, with the exception of a structure of *B. subtilis* SecA that was crystallized as a dimer (PDB 2IBM) (Zimmer et al., 2006). In this structure the 600 to 609 region of one protomer is α-helical; whereas, the same region of the other protomer is part of a three-stranded β-sheet that forms between the two protomers to stabilize the dimeric form. If this region is in equilibrium between different conformations, it is possible that we observed the average; thereby, masking any characteristic pattern.

**A**

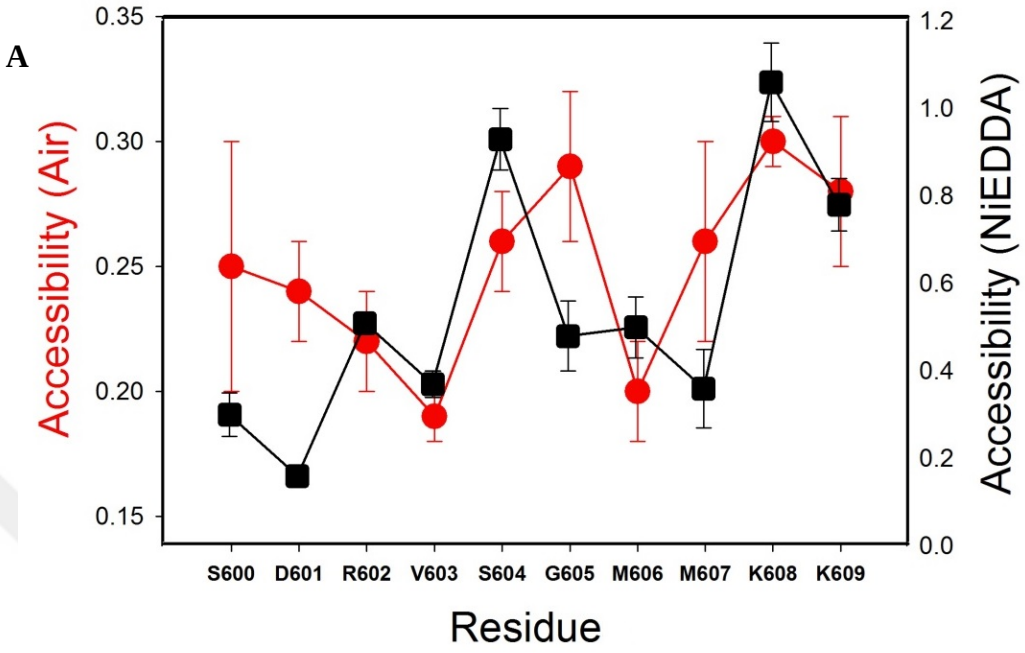
Accessibility (Air)
Accessibility (NiEDDA)
0.35
0.30
0.25
0.20
0.15
1.2
1.0
0.8
0.6
0.4
0.2
0.0
S600 D601 R602 V603 S604 G605 M606 M607 K608 K609
Residue

**B**

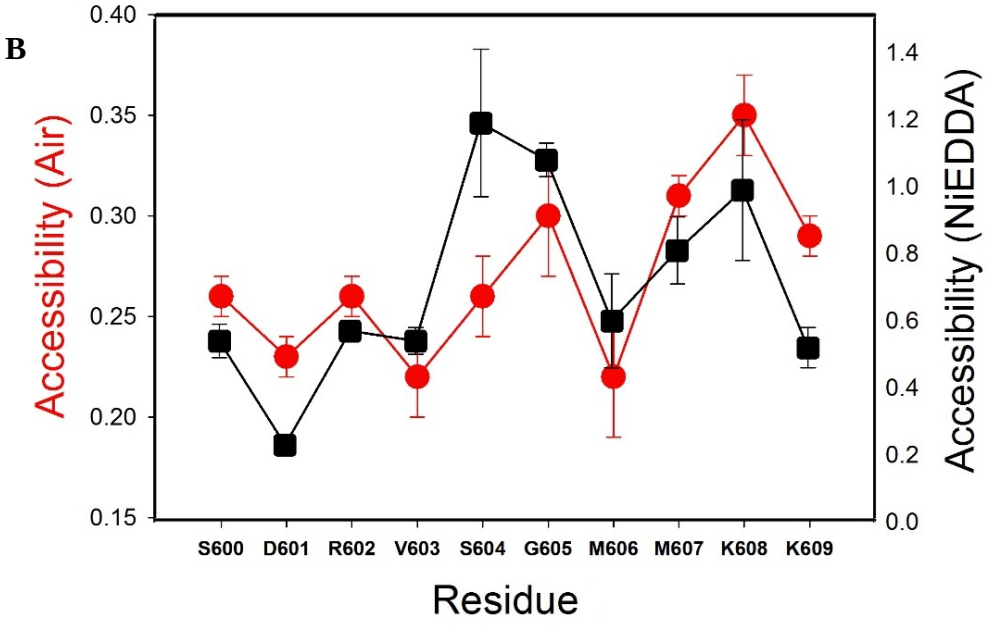
Accessibility (Air)
Accessibility (NiEDDA)
0.40
0.35
0.30
0.25
0.20
0.15
1.4
1.2
1.0
0.8
0.6
0.4
0.2
0.0
S600 D601 R602 V603 S604 G605 M606 M607 K608 K609
Residue

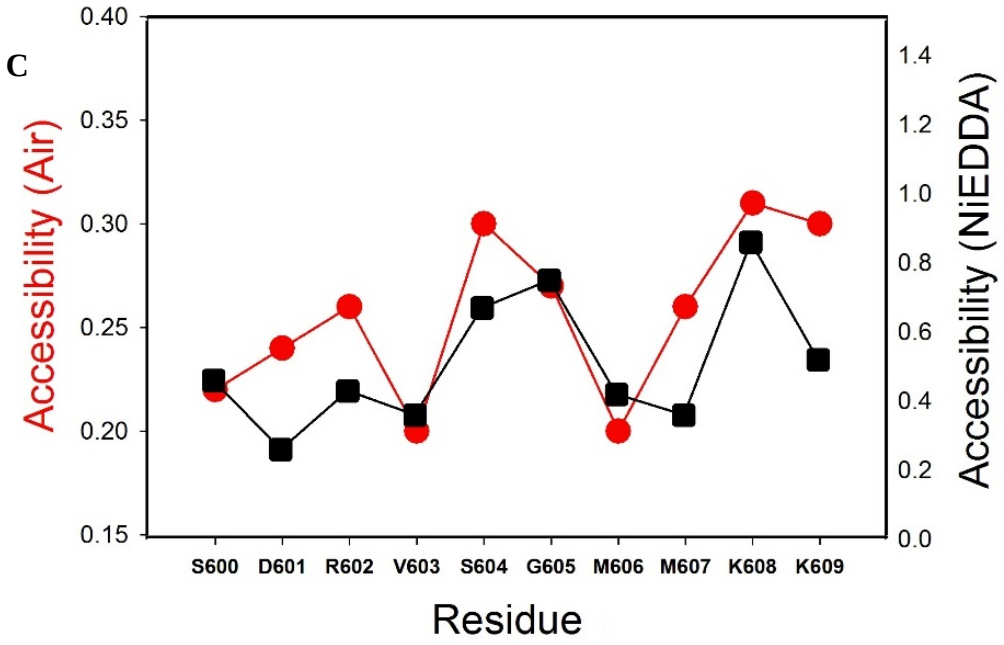


**Figure 26.** Solvent accessibility of residues 600 through 609 of SecA. Red, oxygen accessibility; black, NiEDDA accessibility. A) PLYEG·A B) PLYEG+A C) Liposomes+A

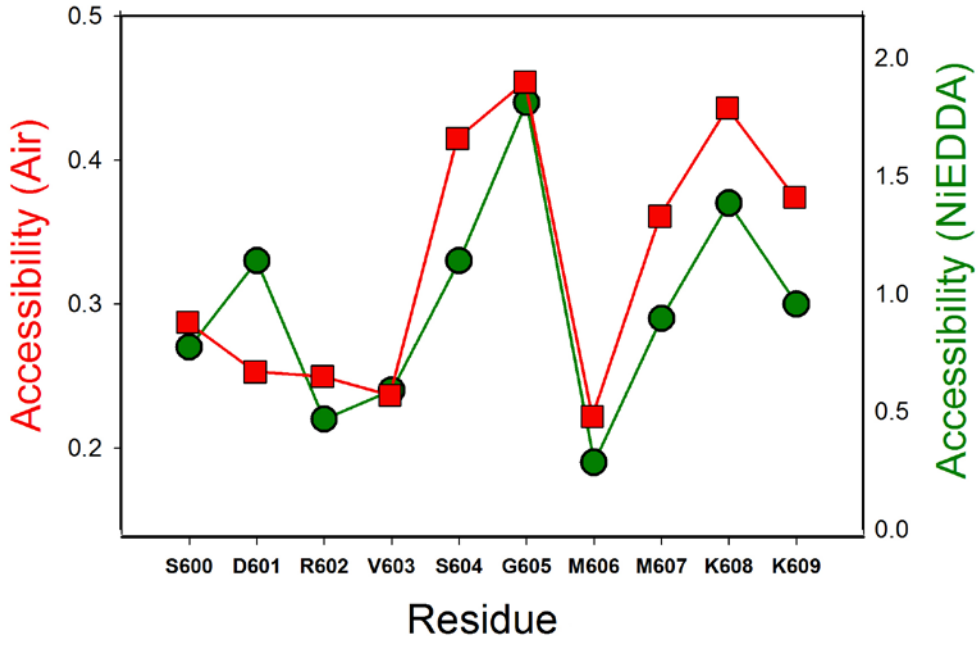


**Figure 27.** Solvent accessibility of residues 600 through 609 of free SecA in solution. Red, oxygen accessibility; green, NiEDDA, used at 20 mM, accessibility.

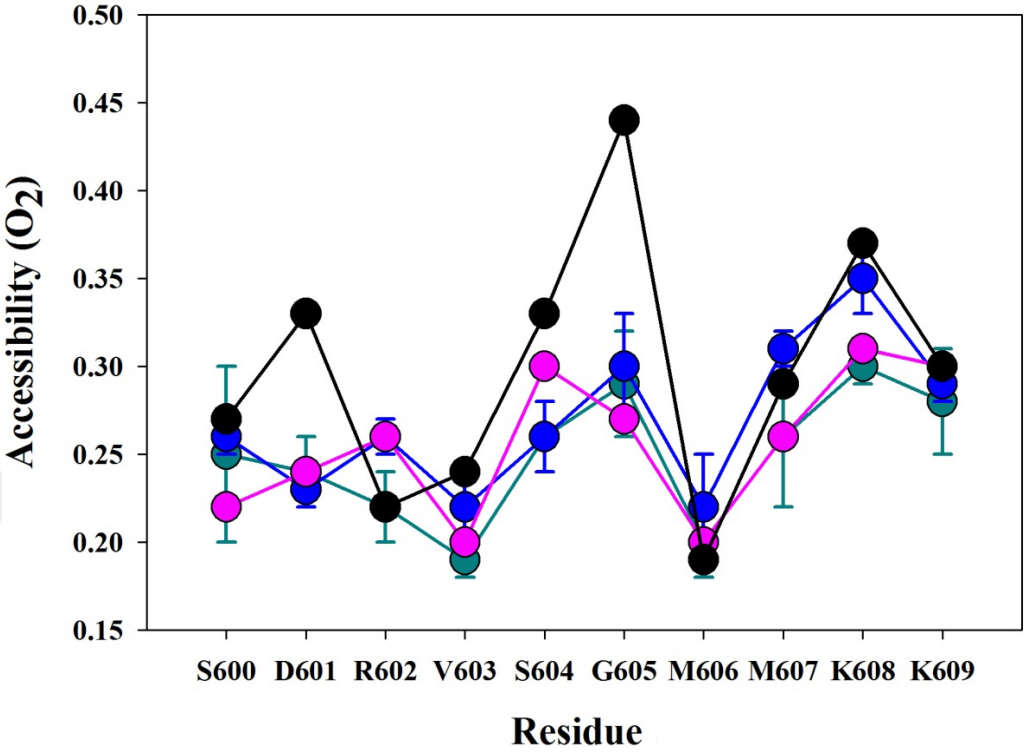


**Figure 28.** Comparison of solvent accessibilities to oxygen of the Linker Helix. Black, SecA free in solution; green, in PLYEG·A; blue, in PLYEG+A and pink, Liposomes+A.

**Validation of determination of depth in our system by EPR power saturation**

To test the validity of EPR power saturation with our system to determine depth we selected residues that were known to be found in different enviromnents with respect to the membrane (Figure 29). Firstly, we selected the residue L20 of Tsr, a transmembrane chemoreceptor for serine in *E. coli,* which, based on the model of $Tar_E$ (Peach, Hazelbauer, & Lybrand, 2002), is exposed on the surface of the helix and at the center of the lipid bilayer. The estimation of depth from the model of the chemoreceptor (Peach et al., 2002) agrees closely with the depth (10.6 Å) determined here by power saturation (pink diamond). Secondly, we tested two residues on SecA that are likely to be solvent exposed according to an *E.coli* homology model of the SecYEG-SecA structure (a generous gift from Ian Collinson). The residues SecAC98SE699 and SecAC98SE729, in the α-helical wing domain (HWD) were examined to determine their solvent accessibilty in PLYEG·A. The purple triangles represent the residues of SecAE699 and SecAE729 which are 0.1 and 0.6 Å below the phosphate head group. These residues are on SecA which immerse the lipid bilayer. Even though they do not interact with lipids, they will be in the close proximity to the lipids. We also selected SecAC98SC896 because it should lie near the phosphate head group of lipids. The C-terminal region of SecA was shown to interact with membranes electrostatically (Breukink et al., 1995). Spin-labeled SecAC98SC896 in the C-terminal region was chosen as a candidate that should lie near the phosphate head group of lipids. The depth results show that the residue of SecAC896 (black triangle) is 2.2 Å below the phosphate head group. It is on the lipid-water interface where the electrostatic interaction occurs.

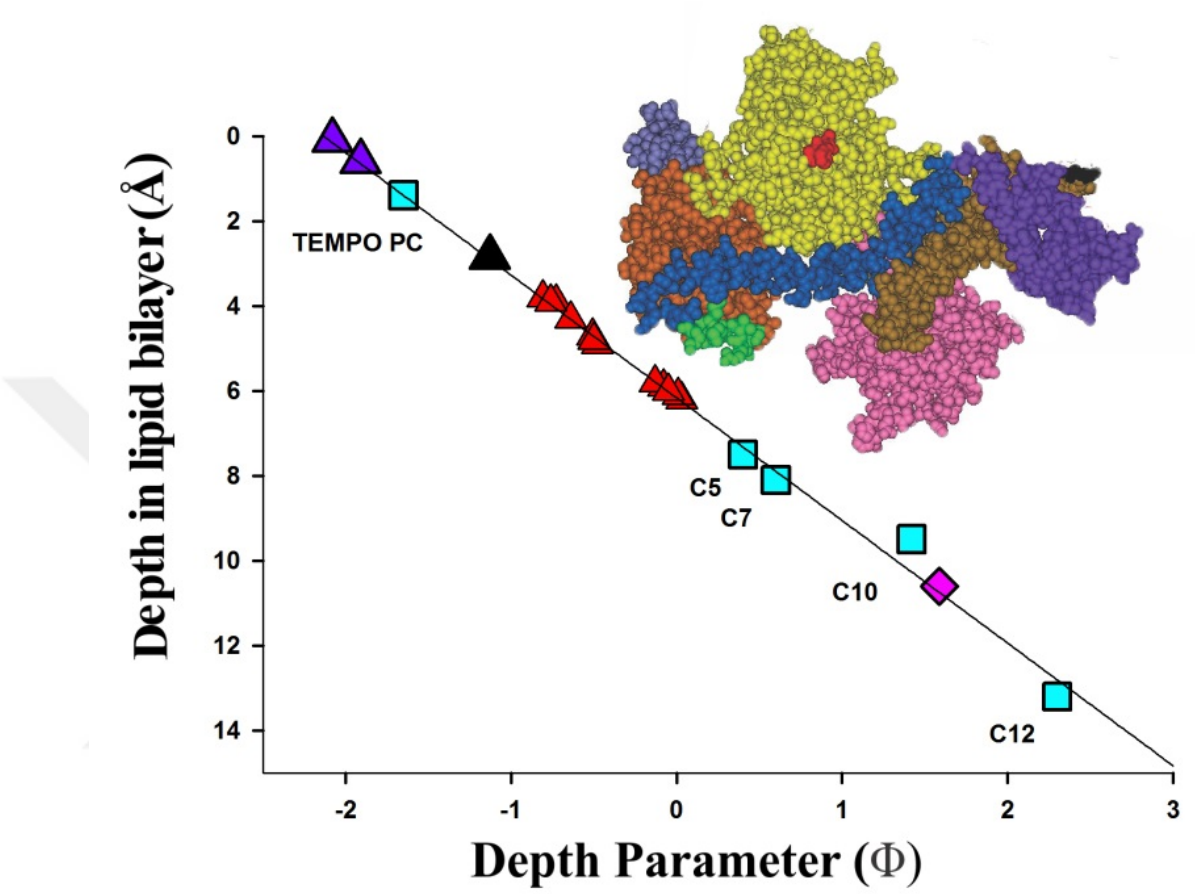


**Figure 29.** Depth in the bilayer. Cyan squares are the spin labelled lipids at the positions indicated in the figure. For the residues in SecA the symbols represent a residue located in a domain at the same color: red triangles, first 15 residues; black triangle, residue 896 in the C-terminal region (not shown in the structure); purple triangle, residues E699 and E729 in the HWD of SecA. Pink diamond represents the TsrL20 which is a chemotaxis transducer.

We also carried out EPR power saturation for residues that are expected to be in solution and not to have any interaction with lipids. All of these residues showed broadening of line widths with 100 mM NiEDDA which indicates the residues are exposed to the solvent as discussed earlier. Therefore, we used NiEDDA at 20 mM. SecB, a cytosolic chaperone, is used as a control for a protein in the solution with no affinity for lipid. SecB spin-labelled at residue T46R1 was examined in the presence of liposomes. Interaction of SecA with membranes requires the presence of acidic lipids. SecA does not bind liposomes made with neutral lipid such as phosphatidylcholine (PC). We examined the interaction of SecAC98SF10Rm with PC liposomes. We also examined SecAC98SF10Rm and SecAC98SG11R free in solution (in the absence of liposomes).

A simple representation that distinguishes residues on proteins that are in a homogenous aqueous environment from those that are in the bilayer is given in a type of phase diagram also called a topographical plot (Figure 30). The accessibility parameter for NiEDDA ($\pi_{NiEDDA}$) is plotted versus the accessibility parameter for oxygen ($\pi_{O2}$) for the results of the proteins mentioned above. The spread of the data points along the axis for $\pi_{O2}$ results from the increase in the concentration of $O_2$ as the environment becomes more hydrophobic. The higher concentration results in an increase of the rate of collision with $O_2$. In the absence of tertiary contacts, the collision rate determines $\pi$. The spread of data points along the axis for $\Pi_{NiEDDA}$ does not result from differences in concentration of either NiEDDA or O2, since there are no gradients in the solution phase. What differs is whether the residue on a given protein is in contact with other atoms or constrained in any way to prevent collisions with the paramagnetic reagents. The data points clearly

cluster in two areas that correspond to a soluble phase and a lipid phase. The three values for the phosphate head groups in the three liposomes systems can be taken as indicating the interface between the hydrocarbon phase and the aqueous phase. Lines are drawn through these data points to illustrate the interfacial region where the concentration of NiEDDA and $O_2$ would be intermediate.

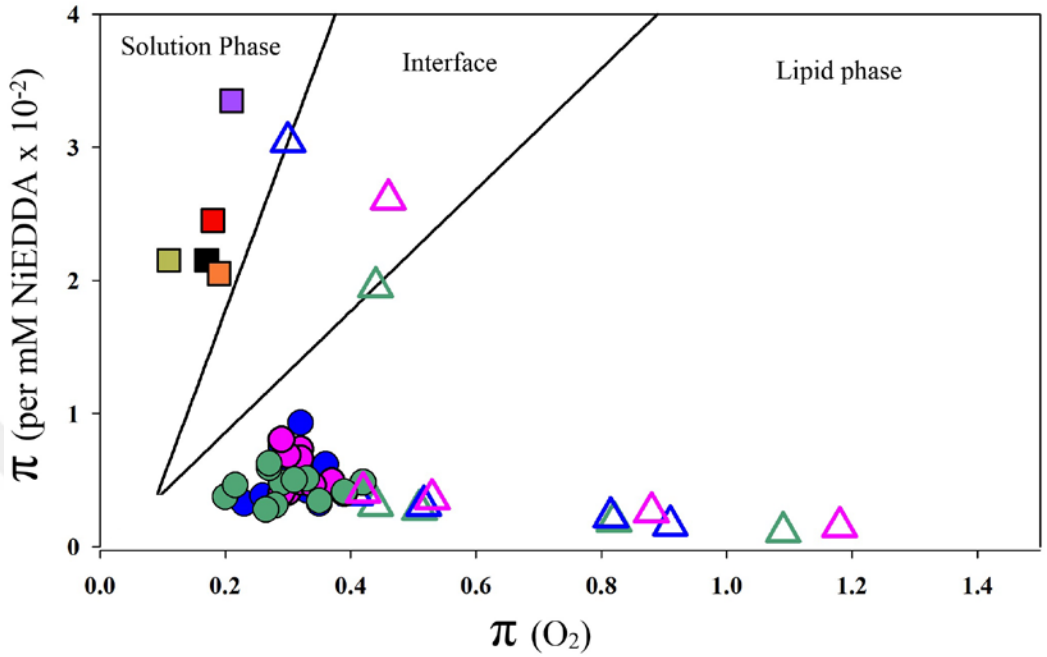


**Figure 30.** Phase diagram. Accessibility of NiEDDA is normalized for per mM NiEDDA since two concentrations of NiEDDA (20 and 100 mM) were used. The color scheme is as follows: green, SecA is co-assembled into the liposomes in the presences of SecYEG (PLYEG·A); blue, SecA is added into the liposomes containing SecYEG (PLYEG+A); pink, SecA is added to liposomes (Liposomes+A). The symbol key is as follows: Δ, lipids spin-labeled at different positions; ○, first 10 residues of SecA. Square symbol represents the residues; black, SecAR13 in solution; orange, SecAG11 in solution; yellow, SecAF10 in solution; red, SecAF10 in the presences of neutral PC liposomes, purple, SecBT46 in the presence of *E.coli* liposomes.

These findings establish the nature of interaction of the N-terminal first 10 residues of SecA with lipid bilayer. We showed that this region of SecA penetrates the lipid bilayer and that the interactions differ when SecA is reconstituted into the liposomes in the presence of SecYEG (PLYEG·A). The co-assembly of liposomes results in an increase in the number of active units of SecYEG bringing it to the same level as that observed in native membrane vesicles. This work provides a foundation for further investigation of the activation mechanism of co-assembly of SecA and SecYEG. We also showed that possible conformational change of the Linker Helix of SecA in the presence of lipid bilayer.

## Materials and Methods

### Bacterial Strains and Plasmids

Site-directed spin labeling requires one available cysteine that the targeted residue to modify. Wild-type SecA includes four native cysteines: 98, 885, 887, and 896. The last three cysteine residues bind zinc and are not available for labeling. Therefore, only residue 98 was replaced with serine amino acid (SecAC98S) by site-directed mutagenesis (Quick Change, Stratagene). The resulting construct was used as a template to prepare all variants used in this study (see table 3). Each mutation was confirmed by DNA sequencing.

**Table 3.** The *E. coli* strains used in the study

Ampicillin was used as the antibiotic for all strains. IPTG was used as the inducer for all strains except SecYEGL58C for which L-arabinose was used.

| | Parent/Host | Base Plasmid | Plasmid | Promoter |
|---|---|---|---|---|
| SecAC98SL2C | JM109(DE3) | pMAN400 | pAL741 | Lac |
| SecAC98SI3C | | | pAL742 | |
| SecAC98SK4C | | | pAL773 | |
| SecAC98SL5C | | | pAL743 | |
| SecAC98SL6C | | | pAL744 | |
| SecAC98ST7C | | | pAL745 | |
| SecAC98SK8C | | | pAL746 | |
| SecAC98SV9C | JM109 | | pAL608 | |
| SecAC98SF10C | JM109(DE3) | | pAL747 | |
| SecAC98SR13C | | | pAL787 | |
| SecAC98SD15C | | | pAL788 | |
| SecAC4Q520C | BL21(DE3) | pT7secA2C4 | pAL537 | T7 |
| SecAC98SS600C | JM109 | pMAN400 | pAL641 | Lac |
| SecAC4D601C | BL21(DE3) | pT7secA2C4 | pAL436 | T7 |
| SecAC4R602C | | | pAL514 | |
| SecAC4V603C | | | pAL592 | |
| SecAC4S604C | | | pAL593 | |
| SecAC98SG605C | JM109 | pMAN400 | pAL604 | Lac |
| SecAC4M606C | BL21(DE3) | pT7secA2C4 | pAL594 | T7 |
| SecAC98SM607C | JM109 | pMAN400 | pAL607 | Lac |
| SecAC4R608C | BL21(DE3) | pT7secA2C4 | paL515 | T7 |
| SecAC4K609C | | | pAL516 | |
| SecAC98 E699C | JM109(DE3) | pJC1 | pAL924 | Lac |
| SecBT46C | BL21(DE3) | pJW25 | pAL297 | T7 |
| SecYEGL58C | | pBAD | pAL716 | |

**SecA Purification**

Wild-type SecA was purified from RR1/pMAN400 (Kawasaki et al., 1989). Wild-type SecB was purified from HB1042, which is BL21(DE3) harboring plasmid pJW25 (Weiss et al., 1988). The translocon, SecYEG, was purified from a strain C43(DE3) suitable for overexpression of membrane protein harboring a plasmid encoding *secE* with a His-tag at the N-terminus, *secYC329S, C385S*, and *secG*. For all single cysteine variants, following protocol was used. Cells were grown in LB media at 35° C with shaking to an optical density of 0.5 at 560 nm. $ZnSO_4$ was added to a final concentration of 0.1 mM and growth continued for 10 minutes, at which time Isopropyl-1-thio-β-D-galactopyranoside (IPTG) was added to 0.2 mM and growth continued for 2.5 hrs. Cells were harvested, washed and suspended in 20 mM Tris-Cl, pH 8.0, 2 mM DTT at 120 OD. The cell suspension was frozen by dripping into liquid nitrogen and stored at -70° C.

The cell suspension was thawed by adding 2x the weight of pellet of 20 mM Tris-Cl pH 8.0, 1 mM phenylmethylsulfonyl fluoride (PMSF), 2 mM DTT, 0.15 mg/ml lysozyme. Cells were frozen by rapid dripping into liquid nitrogen and thawed by incubating at 40° C in a water bath. Cycles of freeze and thaw were repeated twice. After breaking the cells, the cell suspension was incubated on ice for 20 min with DNAse (10 µg/ml) and $MgAc_2$ (3 mM). The cell suspension was centrifuged at 542,000 × g, 32 min at 4 °C, in a TL100.4 rotor (Beckman). The supernatant was removed and filtered using a Milipore Steriflip membrane (size: 0.2 µm). A 5 ml Hitrap Blue HP affinity column (GE

Healhcare) was equilibrated in 10 mM HEPES pH 7.6, 0.1 M NaCl, 2 mM DTT. The supernatant was applied and washed with the running buffer. SecA was purified by applying a gradient from 0.1 M NaCl, 0 % ethylene glycol, to 1.5 M NaCl and 50 % ethylene glycol. All contaminants are eluted in the gradient. SecA elutes during a continues wash with 1.5 M NaCl and 50 % ethylene glycol. The fractions containing SecA were pooled, concentrated and stored at -80° C.

**Spin Labeling of SecA Variants**

SecA variants were labelled with 1-oxyl-3-(maleimidomethyl)-2,2,5,5-tetramethyl-1-pyrolidine (Toronto Research Chemicals, Iinc) in methanol . Reducing agent was removed just before spin labeling using a Nap10 column (GE Healthcare). The exchange buffer was 10 mM HEPES pH 7.0, 0.3 M KAc. A three-fold molar excess of spin labeling reagent was added from a stock of 50 mM in MeOH and stored in the dark at -80° C. The MeOH concentration was kept below 1%. The sample was rotated in the dark at room temperature for 3 hours and placed on ice in the dark for 1 hour 30 min to complete the reaction. A Nap10 column equilibrated in 10 mM HEPES pH 7.6, 0.3 M KOAc was used to remove free spin. Fractions of 4 drops (~200 µl) were collected. Fractions containing spin-labelled SecA were identified by EPR and pooled. Pooled SecA was washed twice to minimize free spin and concentrated using Amicon 30K MWCO with 10 mM HEPES pH7.6, 30 mM KOAc, 1mM $Mg(OAC_2)$ and stored at -80° C.

**Proteoliposomes**

Unilamellar liposomes were prepared by extrusion of *E.coli* polar lipids (Avanti) suspended in 10 mM HEPES at pH 7.6, 30 mM KOAc, 1 mM $Mg(OAC_2)$ using a lipofast (Avestin) with a membrane of 100 nm pore diameter. The liposomes were swelled for 3 hours at room temperature in the presence of dodecyl beta-D-maltoside (DβM) at a ratio of 4.65 mM DβM to 5 mM lipids. For PLYEG•A, 10 µM SecYEG and 10 µM $SecA_1$ were assembled into the liposomes simultaneously. For PLYEG, only 10 µM SecYEG was added. The mixture was rotated at room temperature for 1 hour. Biobeads SM-2 (BioRad) in 10 mM HEPES at pH 7.6, 30 mM KOAc were added to the mixture with a 1.4 fold of sample volume to remove detergents. The sample was rotated around 1.5 hours at room temperature. Biobeads were removed by centrifugation at 2050 x g, 5 min at 9 °C in a GH-3.8 rotor (Beckman Coulter, Allegra 6R). The proteoliposomes were centrifuged at 436,000 × g, 20 min at 4 °C, in a TL100.1 rotor (Beckman). The pellet was washed in 10 mM HEPES pH 7.6, 0.3 M KOAc, 1 mM $Mg(OAc_2)$ and centrifuged again. The final pellet was suspended in a volume to give a 200 fold higher concentration over the initial in order to have a good EPR signal (around 60 mM spin label).

***In vitro* translocation assay**

The translocation assay was carried out at 30° C. Translocation of 1 µM proOmpA labelled with a $^{14}C$-L-amino acid mixture was carried out under conditions of limiting SecY (1 µM SecYEG) and 1.2 µM $SecA_2/SecB_4$. For an ATP regeneration system, 7.5 mM phosphocreatine and 37 mg/ml of creatine phosphokinase was present in

the reaction mixture. Samples of 8 µl were taken from the reaction mixture at time as indicated. At the zero time point (on ice), two 8 µl samples were taken to count the radioactivity of total input. All samples except inputs were incubated with proteinase K (5 units/ml) for 15 min on ice to degrade the untranslocated precursors. To stop digestion, tricholoroacetic acid precipitation was carried out. The washed precipitate was suspended in gel sample buffer with DTT and subjected to SDS-polyacrylamide gel electrophoresis to count the amount of radioactivity of the translocated precursor. A Fujifilm FLA 3000 phosphoimager was used to measure the radioactivity of the proteins.

**Size exclusion chromatography**

All SecA variants (both cysteine-substituted and spin-labeled) were analyzed by size exclusion chromatography to be certain that they were properly folded and could make complexes with the binding partner of SecB.

High performance liquid chromatography was performed on a TSK G3000SW (TosoHaas) size exclusion column (7.5 mm inner diameter x 60 cm) in 10 mM HEPES–KOH (pH 7.6), 300 mM KOAc, 5 mM $Mg(OAc)_2$ at 7º C. The absolute molar mass of proteins were determined directly using static light scatter by passing the eluent through a multi-angle laser light scatter detector followed by a differential refractometer (DAWN-EOS and Optilab, respectively; Wyatt Technology Corporation). The molar mass was determined using a specific refractive index increment (dn/dc) of 0.182 ml/g and the Debye plotting formalism of the Astra software supplied with the instrument. The

relationship between the weight average molar mass (Mw) and the excess Rayleigh ratio R(θ) at the low protein concentrations used here is given by:

$$\frac{K^{*}c}{R(\theta)} = \frac{1}{[M_w P(\theta)]}$$

where

R(θ) is the light scattered by the solution at an angle θ in excess of that scattered by pure solvent divided by the incident light intensity, c is the concentration of protein, P (θ) is the form factor that describes the angular dependence of the scatter, and K* is a constant dependent on the parameters of the system used in the study. Further details are given by Woodbury et al.(Woodbury et al., 2002)

**EPR Experiments**

EPR spectroscopy was performed on an X-band Bruker EMX spectrometer with a dielectric EPR resonator (ER4123D-CW-Resonator Bruker). A sample of 4 µl was loaded into a capillary made of gas-permeable methyl-pentene polymer referred to as TPX (Molecular Specialties, Inc.). Before collecting data, $N_2$ or compressed air was flow through capillary at least 5 min to remove air from the capillary. For NiEDDA, 8 µl of sample was incubated with a final concentration of 100 mM NiEDDA for 3 hour 30 min. Then the sample was frozen and thawed 4 times so that NiEDDA concentration would be the same through the both side of the lipid bilayer. During the assay, $N_2$ was run through capillary to keep $O_2$ out of the system. To measure inverse central line width values

(ΔHpp), spectra were collected using incident microwave power at 3 mW and a 100 kHz modulation frequency of 1 to 3 G as appropriate. For each spectral line, 8 scans were run through a 100.0 G sweep width with a center field: 3474.0 G. For power saturation, EPR spectra were collected at microwave powers over the range of 0.1 to 200 mW with a modulation of 1 to 3G as appropriate. From these spectra, $\Delta P_{1/2}$ values were calculated using the Labview programs written by Christian Altenbach (University of California, Los Angeles).

**Circular dichroism spectroscopy**

Spectra were recorded from 190 to 260 nm using a 1 mm pathlength quartz cuvette at 8 °C using a JASCO J-815 spectrophotometer. The step-size was 0.5 nm, the bandwidth was 1 nm and the scan rate was 20 nm/min. Smoothed, background-corrected spectra were fit using the CDSSTR secondary structure analysis method (Sreerama & Woody, 2000) accessed through the DichroWeb web-interface (Whitmore & Wallace, 2008) located at ttp://dichroweb.cryst.bb.ac.uk. Reference set 4, which is optimized for the spectral region between 190 and 240 nm was used for all. The peptide concentrations were 45 μM, and total lipid concentration was varied between 0 and 1 mM.

## Notes

1. Chunfeng Mao and Weijiang Ying synthesized the NiEDDA used in this study.
2. Angela Lilly constructed all of the SecA single cysteine variants used in this study.
3. Wing Cheung constructed and purified TsrL20.
4. The interpretation of EPR data were done in collaboration with Wayne Hubbell at the Jules Stein Eye Institute, University of California, Los Angeles.
5. The LabVIEW program for the analysis of EPR spectra of nitroxide spin labels were developed by Christian Altenbach at UCLA in the Lab of Professor Wayne L. Hubbell.
6. The fits to calculate periodicity of accessibility data were done by by Christian Altenbach at UCLA.
7. The Circular Dichroism analyses were done by Virginia F. Smith, United States Naval Academy.
8. The synthetic A2/11 peptide was synthesized by Fabio Gallazzi, Structural Biology Core, University of Missouri-Columbia.
9. The E.coli homology model of the SecYEG-SecA structure used in this study was a generous gift from Ian Collinson at University of Bristol, UK.
10. The manuscript of this chapter is in preparation

# *CHAPTER FOUR*

## *Preliminary studies of defective species of both SecA and SecB within complexes during translocation*

## Introduction

The chaperone, SecB, is a homotetramer which is organized as a dimer of dimers with an equilibrium constant ($K_{eq}$) well below 20 nM (Murén et al., 1999; Topping, Woodbury, Diamond, Hardy, & Randall, 2001). SecB functions in the export process to bind unstructured polypeptides and keep them competent for translocation (Thom & Randall, 1988). Precursor-bound SecB binds SecA, the ATPase of the system, and this ternary complex is directed to the translocon by the affinity of SecA for SecYEG (Hartl et al., 1990).

SecB binds precursor proteins with high affinity. The Kd for precursor galactose binding protein is in the range of 35-100 nM. However, the binding exhibits low-specificity (Hardy & Randall, 1991; Topping & Randall, 1994). Precursors wrap around SecB and a continuous stretch of approximately 150 amino acyl residues of the precursor proteins make contact with SecB (Khisty, Munske, & Randall, 1995; Smith, Hardy, & Randall, 1997; Topping & Randall, 1994). Sites of contacts are distributed over all surface of SecB: in the deep cleft at the dimer interface, on the ß-sheets at the sides and on the C-terminal region of SecB (J. M. Crane et al., 2006; Lilly, Crane, & Randall, 2009). The large area of contact on SecB suggests that there are numerous available pathways for a ligand binding (J. M. Crane et al., 2006; Xu et al., 2000).

SecB has two binding sites for SecA (Figure 31). The flat eight-stranded β-sheets on each of the dimers of SecB (referred to as the side site,) bind the C-terminal region of SecA that contains a coordinated zinc atom (Breukink et al., 1995; Fekkes et al., 1999; Kimsey et al., 1995). The second site on SecB is C-terminal 13 residues that interact both

with the N-terminal 10 residues of SecA (Randall et al., 2004) and the Linker Helix of SecA ( amino acyl residues 600-610) (Suo et al., 2011).

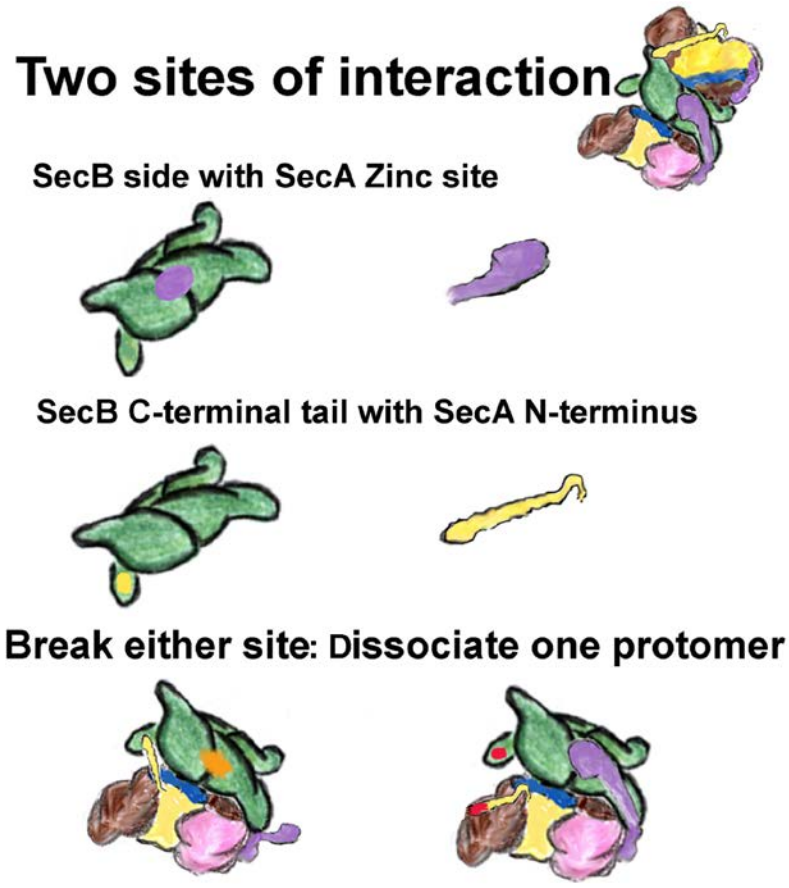


**Figure 31.** Representative schematic cartoons for the sites of interaction in the A2B4 complex (drawn by L.L. Randall). The SecB tetramer is green. The side site of the SecB tetramer is marked in purple. The cognate binding site on SecA, the C-terminal region that contains zinc, is also purple. The extreme C-terminal tail of the monomer of SecB is marked in yellow. The SecA N-terminal region is yellow.

Maximal efficiency in translocation occurs when SecB is bound to two protomers of SecA forming a symmetric complex (referred to as A2B4) (Mao, Hardy, & Randall, 2009). The interactions that stabilize this symmetric complex are distributed asymmetrically. Breaking the contact between the SecA C-terminus and the side site of SecB releases only one protomer of SecA (Randall et al., 2005). A model that explains the asymmetry within the A2B4 complex was proposed based on data collected by size-exclusion chromatography, calorimetry, sedimentation velocity centrifugation (Suo, Hardy, & Randall, 2015) and electron paramagnetic resonance spectroscopy (Cooper et al., 2008; J. M. Crane et al., 2006). It is suggested to the reader to follow the text with the guidance of Figure 32. The model (Figure 32) suggests that the first protomer of SecA (black protomer) interacts through its C-terminal zinc-containing region with the side site of the SecB tetramer (black circle) to bind SecB. The Linker Helix of that protomer of SecA (Fig. 34, indicated by a green area) binds the SecB tail site (Fig. 34, red circle) that is on the same dimer of SecB that is occupied at the side site. The N-terminal 10 residues of SecA (Fig. 34, indicated by N) bind to the SecB tail (Fig. 34, yellow circle) on the opposite dimer directly across the interface within the tetramer. Thus, the first protomer of SecA occupies three sites (red, yellow and black circles) of one SecB tetramer in the complex: one side site and two tail sites. The second protomer of SecA (Fig. 34, pink) binds the opposite face of SecB in the complex. The second protomer of SecA is rotated 180° around the x-axis relative to the first protomer of SecA. However, there are no available SecB tail sites to bind either the N-terminal region of SecA or the Linker Helix of the second SecA protomer. Therefore the binding of the second protomer to join in the complex is stabilized by the interaction of side site (pink circle). Thus breaking

interaction at the side sites releases one protomer, but not the other because its binding also stabilized by interactions at the tails of SecB.

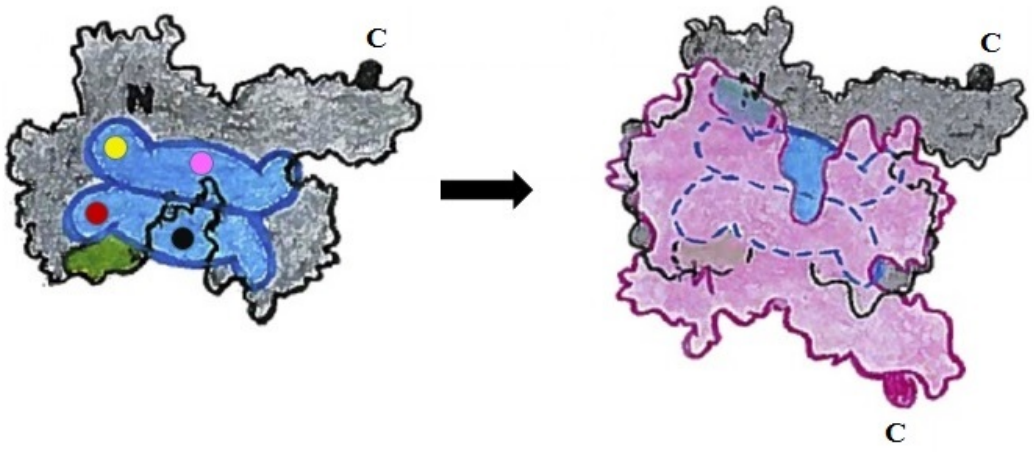


**Figure 32.** Representative schematic cartoons for asymmetric binding of two protomers of SecA and a tetramer of SecB The first protomer of SecA which binds SecB is shown in black, the second protomer of SecA which binds SecB is shown in pink; the tetramer of SecB, blue (Suo et al., 2015). The tail sites on SecB are represented by yellow and red circles, the side sites by pink and black circles. The amino terminal regions of SecA are indicated by N in the color of the corresponding SecA protomer. The extreme C-terminal zinc-containing region was not resolved in the X-ray structure on which this cartoon is based, but it emerges from the positions indicated on the SecA protomers by the black or red protrusion, indicated by C.

The cycle of translocation of precursor by the Sec system is complex and involves many steps. Initially the unfolded precursor is bound to SecB. Precursor bound SecB then binds two protomer of SecA that binds the translocon via specific interaction between SecA and SecY. When two protomers of SecA interact with the precursor-bound SecB, the precursor protein is trapped between SecA and SecB in the complex, like a sandwich. Precursor is released first from SecB to SecA then into the channel of SecYEG and crosses the membrane. Nothing is known about the molecular details of the transfer of precursor along this pathway: how the precursor is transferred from SecB to SecA, whether the transfer occurs within the complex, through solution or when the complex binds the translocon. It is not even known which of the many steps is rate-limiting.

Transfer of precursor from SecB to SecA might occur within the complex if the affinity of the precursor for SecA were higher than for that SecB. However, this is not the case in solution. The precursor has higher affinity for SecB, in the nM range. That the precursor binds SecA was demonstrated by EPR studies. However, the interaction is weaker than that with SecB to be observed directly by size exclusion chromatography.

In the work here, we aim to determine which step limits the rate. To achieve this goal, we assessed the activity of the Sec system *in vitro*, and determined the rate constant (k) of the translocation reaction. It must be remembered that a change in k can reflect either a change in the step that limits the rate, or a change in the limiting reaction itself that results in a different rate constant. There are several steps that might be rate-limiting; release of precursor from SecB to SecA; interaction of SecA with the channel on the membrane; release of precursor from SecA to the channel in SecY; or opening the channel. Therefore changes in SecA, SecB, SecYEG and precursor are candidates for

changing the limiting step. The effect of precursors on the rate constant of translocation is currently under study by Chunfeng Mao and Priya Bariya in our laboratory.

In this project, we use our extensive collection of altered variants of SecB and SecA to determine whether they are involved in the step that limits the overall rate. We have previously characterized the sites of interactions among SecA, SecB and precursors (Jennine M. Crane, Lilly, & Randall, 2010; Lilly et al., 2009; Patel, Smith, & Randall, 2006; Randall & Henzl, 2010) and now we will extend our experiments to address the specific roles which each interaction plays along the pathway of secretion.

## Results and Discussion

### The Assay

The activity of the Sec system is assessed *in vitro* by examining translocation of a radiolabeled precursor of the outer membrane protein OmpA, $^{14}$C-proOmpA (37.2 KDa), into inverted membrane vesicles isolated from *E.coli*. *In vivo,* protonmotive force is required for transfer; whereas, *in vitro* if sufficient ATP is present, protonmotive force only shows stimulation. In our system, we generate protonmotive force by addition of NADH. In order to test the effect of protonmotive force on translocation, *in vitro* translocation assays are done ± NADH. A time course of translocation is generated for each condition by sampling the reaction mixture at the times given (see Materials and Methods). The total amount of precursor translocated is plotted as a function of time. The data are fit using an equation for a single exponential rise to maximum. From the plot, we obtain the rate constant (k) of the rate-limiting step of translocation and the final level of translocated precursors (A) (see Figure 33 for an example). Some assays were done fewer

than three times, therefore more work must be done to draw reliable conclusions. Nonetheless, the results presented here are valuable and will guide us in determing which direction to follow in the continuation of this work.

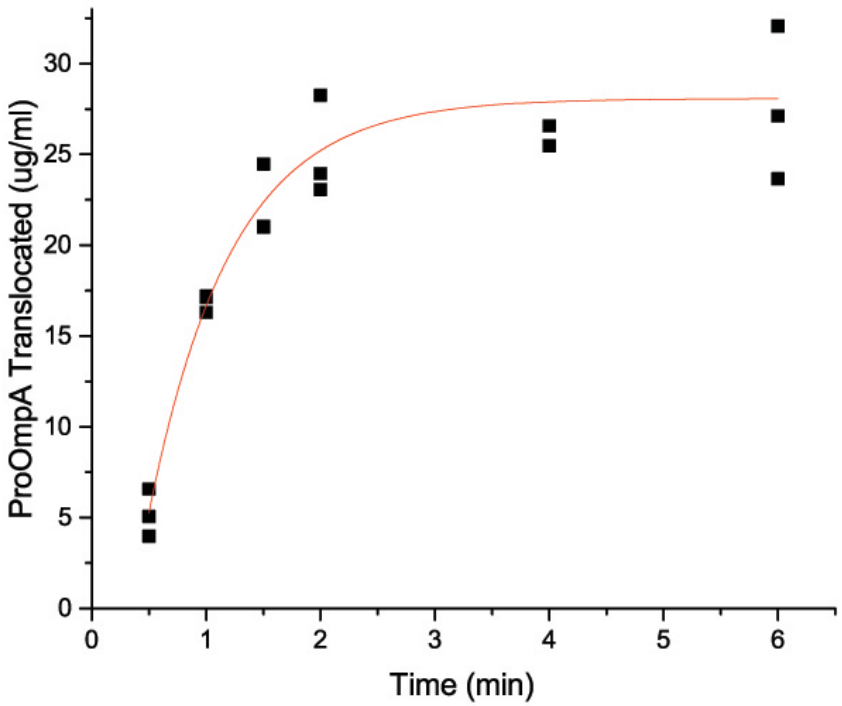


**Figure 33.** Translocation activity in the presence of wild-type SecA without SecB. Translocation of $^{14}$C-proOmpA was assayed in IMV in the presence of NADH by protection from proteinase K (see Materials and Methods). The line shows the fit which gives a plateau of 28.1 ± 1 μg/ml (750 nM) and a rate constant of 1.38 ± 0.24 min$^{-1}$. The precursor in the assay was 1.2 μM; therefore, 63% was translocated. The assay illustrated here was performed 3 times (n).

We started our investigation using SecA variants to elucidate the region of SecA that might change either the rate constant or the rate-limiting step. Four different SecA variants were tested in the translocation assay: SecA880, which is truncated to remove the C-terminal 21 aminoacyl residues that coordinate zinc; SecAC4, which lacks zinc because the coordinating cysteines are replaced by serine; SecAdN10, which has aminoacyl residues 2–11 deleted; and SecAdN10/880, which has both aminoacyl residues 2–11 deleted and C-terminal 21 aminoacyl residues deleted.

SecB functions to keep precursors competent and thus would be expected to increase the extent of translocation. Addition of SecB into the system might also change the rate constant. It is possible that the release of precursor from wild-type SecB to SecA is rate-limiting. In that case, the rate constant of the system would decrease. To demonstrate whether this is the case, we assayed translocation with and without SecB present.

**Translocation of proOmpA in the presence of different SecA species with and without SecB**

In the absence of wild-type SecB (SecB), the rate constants (k) of translocation for all SecA variants tested were between 0.82 min¯1(for SecAdN10) and 1.4 min¯1(for wild-type SecA) (Figure 34, red square). Addition of wild-type SecB to the translocation reactions decreased the rate constants for all SecA species (Figure 34, blue square). The smallest effect of addition of SecB was observed for wild-type SecA with a decrease of 30% in the rate constant. However, SecB stimulated the final level of translocation 1.4 fold (from 28 µg/ml (750 nM) to 44 µg/ml (1.18 µM)).

The greatest effect of the addition of SecB on the rate constant occurred with SecAdN10/880. Presence of SecB decreased the rate constant 10 fold relative to that observed in the absence of SecB but the extent of translocation was only changed slightly. SecAdN10/880 is a species that does not make a complex with SecB. In this situation, the precursor must be passed from SecB to SecAdN10/880 through solution. The extremely low rate constant observed (0.11 $min^{-1}$) when SecB was added indicates that to transfer precursor from SecB to SecA efficiently, the formation of a complex is required.

The lowest rate constant and level of translocation were observed with SecAdN10 (0.82 $min^{-1}$, 40% of wild-type SecA, and 15 μg/ml (403 nM), 54% of wild-type SecA) in the absence of SecB. Addition of SecB to SecAdN10 restored the final level of translocation to near the wild-type level even though the rate constant was decreased 4.3 fold (0.32 $min^{-1}$). We did not observe recovery of the level of translocation by addition of SecB for the other SecA variants.

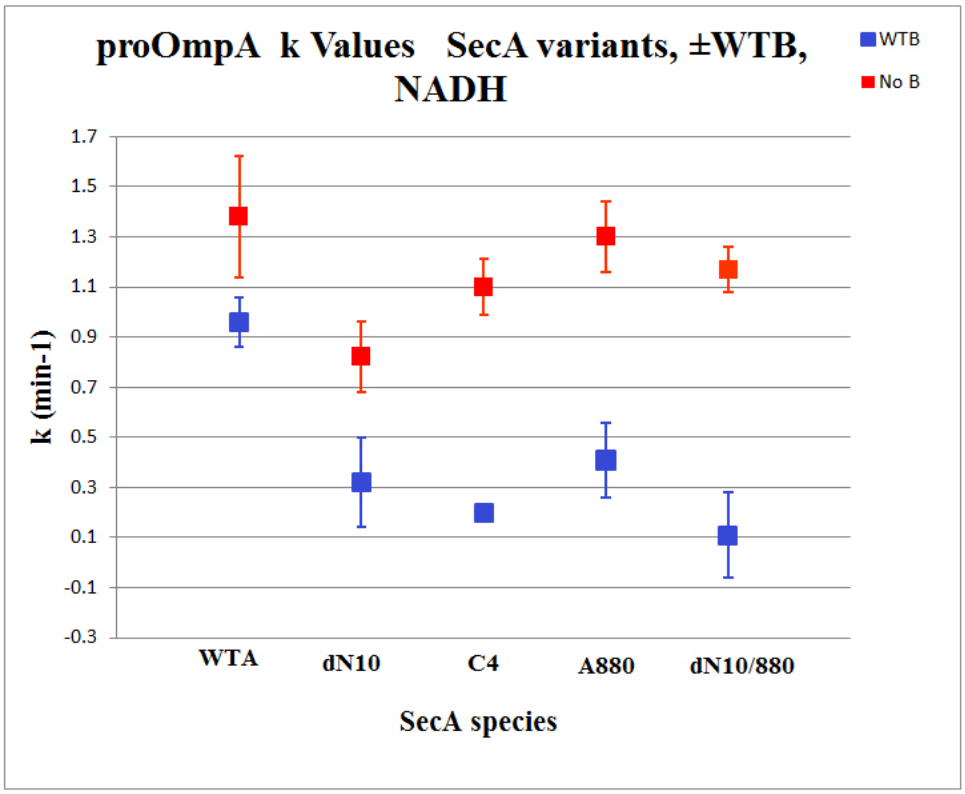
proOmpA k Values SecA variants, ±WTB, NADH
WTB
No B
k (min-1)
1.7
1.5
1.3
1.1
0.9
0.7
0.5
0.3
0.1
-0.1
-0.3
WTA
dN10
C4
A880
dN10/880
SecA species

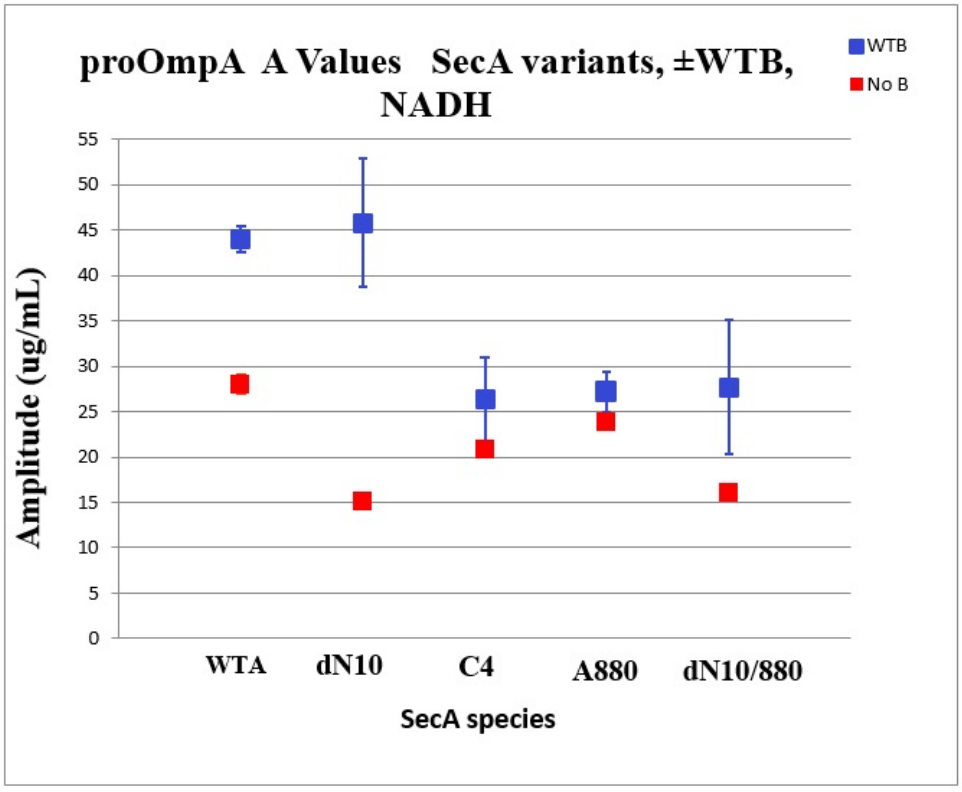
proOmpA A Values SecA variants, ±WTB, NADH
WTB
No B
Amplitude (ug/mL)
55
50
45
40
35
30
25
20
15
10
5
0
WTA
dN10
C4
A880
dN10/880
SecA species

**Figure 34.** Effect of addition of SecB on the rate constant and extent of translocation Red symbols are in the absence of wild-type SecB, blue symbols are in the presence of wild-type SecB. The error bars represent the error in the global fit of the data. SecAWT±SecB, *n* = 3; SecAdN10-SecB, n=2; SecA880±SecB, n=2; SecAdN10/880-SecB, *n* = 2. SecAdN10+SecB, SecAC4±SecB and SecAdN10/880+SecB were done only once.

**Pairwise comparison of the altered species within SecA:SecB defective complexes**

Defects in either SecA or SecB can result in the inability to bind at a given site within a complex. In the previous section, we examined the defective SecA variants that lack interactions within the complex with wild-type SecB. To examine whether the observations are the direct result of lack of the interaction or a result of defects in other functions of either SecA or SecB, three pairs of SecA and SecB that lack the contacts were used and the results compared (Figure 35). Each of the variants was tested in the presence of the wild-type species of the binding partner. All assays, discussed here, were carried out in the absence of NADH; therefore, we cannot compare these results with those in the previous section.

The first pair was examined for the differences in elimination of the interaction at the tail sites of SecB depending on whether the mutational change is in SecB (SecB142) or the N-terminal region of SecA (SecAdN10). The first 10 residues of SecA bind the C-terminal tail of SecB. Therefore the SecB variant, SecB142, which lacks the C-terminal tails, displays the same defect in interaction as does SecAdN10. In this pair, the higher level of the rate constant and the higher level of translocation were observed when the defect was in SecB. The rate constant with SecB142 was 3 fold (0.87 $min^{-1}$) higher and the final level of translocation was 1.9 fold (38.4 μg/ml) higher relative to that seen with SedAdN10 (0.29 $min^{-1}$ and 21 μg/ml). The difference that is observed between the pairs might arise from the fact that whereas SecAdN10 forms A1B4, SecB142 is able to make an A2B4 complex since it has two active side sites.

The second pair was chosen to test the role of side site interaction of SecB with SecA. SecA880 is lacking the zinc containing region of SecA that binds the side sites of

SecB. For a variant of SecB defective in the side site, SecBL75Q was used. Both variants form an A1B4 complex with the wild-type partner. The higher rate constant was observed with the defect in SecB (SecBL75Q, 0.52 $min^{-1}$) as was the case with the first pair. The rate constant in the presence of SecA880 was 23 $min^{-1}$, 44 % of that seen with SecBL75Q. However, the level of translocation with SecBL75Q was 51% lower than with SecA880.

As a third pair, bindless variants were compared: SecAdN10/880 and SecBL75Q/142. No complex was observed between the bindless species and the cognate wild-type binding partners via size exclusion chromatography, although a weak complex was shown by analytical sedimentation velocity centrifugation for the complex with SecBL75Q/142 (data not shown, done by L. L. Randall). Since both SecA and SecB bind precursor independently, the addition of precursor tethers the two proteins as indicated by the elution profile using size exclusion chromatography and by analytical sedimentation velocity centrifugation (data not shown, done by L. L. Randall). A significant difference was not observed between the rate constants of the bindless species. However, when the SecB is the defective partner (SecBL75Q/142), the level of translocation is 3.2 fold higher than the level observed when the defect is in SecA (SecAdN10/880). The higher level of translocation with the SecBL75Q/142 might be the result of the weak interaction observed with the wild-type SecA.

In summary, the greatest effect on rate constant was observed when SecA was the defective species, except with the bindless species in which case the rate constants were equal. The greatest difference among the three pairs was observed when the defective interaction tested was in the tail site.

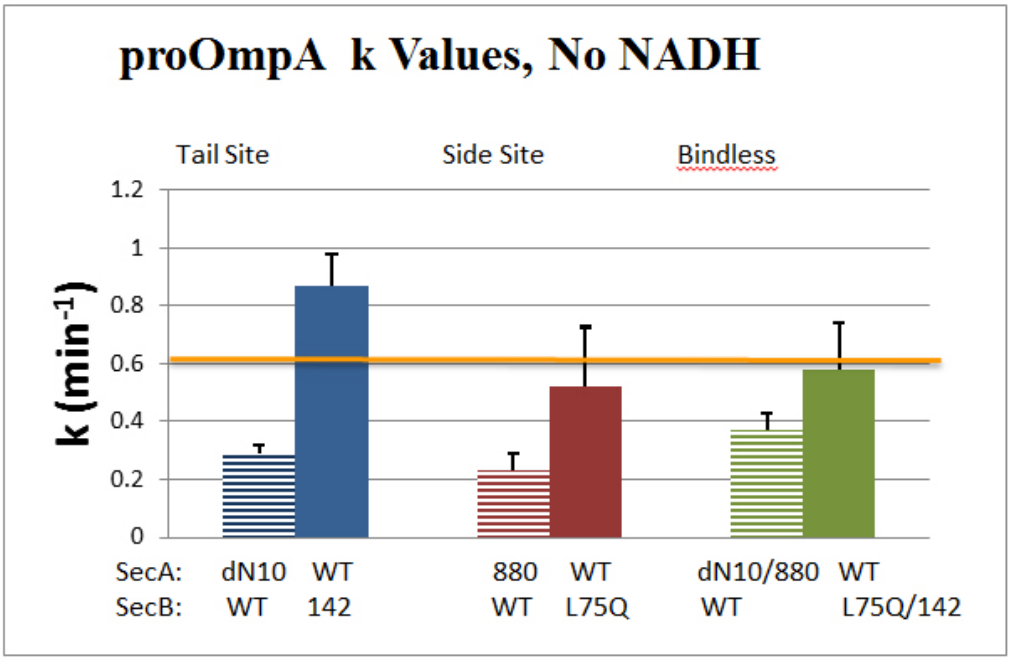


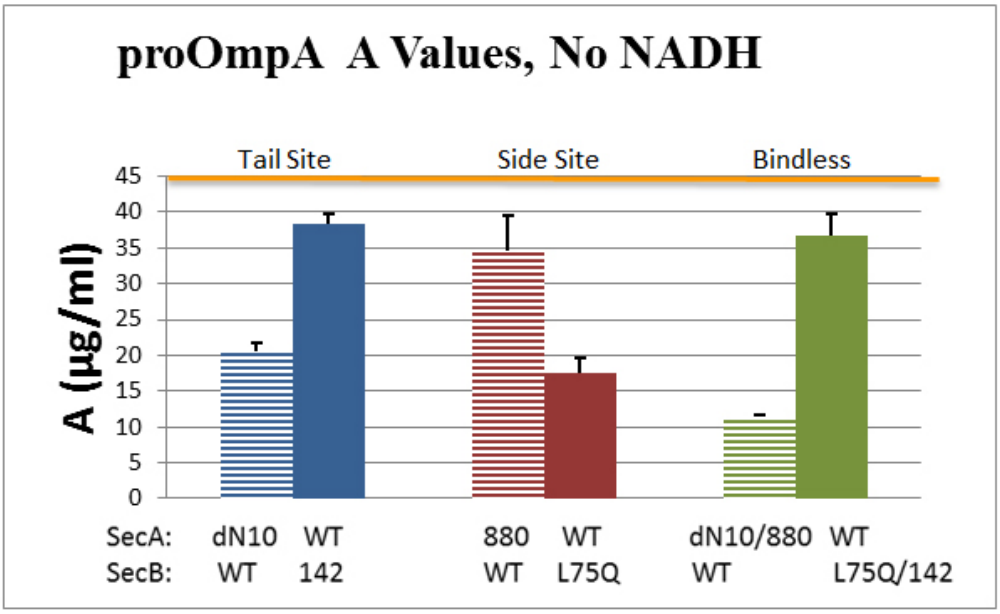


**Figure 35.** Results for the comparison of the activity of the pairs of defective species. All experiments were done once except for SecBL75Q, n=2. The yellow line represent the wild-type SecA:SecB complex (0.61 $min^{-1}$ ± 0.3 and 44 µg/ml ± 5, n=2). The error is the error of the fit.

**Summary for results with species defective in the interactions between SecA and SecB**

All the results taken together indicate an important role for first 10 residues of SecA. In the absence of first 10 residues of SecA, SecAdN10, the addition of wild-type SecB increased the level of translocation to close the wild-type level even though the rate constant was greatly decreased; whereas, translocation is not stimulated by addition of SecB if the defect is in the side sites. The difference is where the defect lies, in the side site versus the tail site.

Here we present several ideas based on our preliminary results. There are two possible explanations for the ability of SecB to correct the defect in level of translocation in the presence of SecAdN10: first, leaving the SecB tails free could restore the activity; second, the defect in SecA might be related to its chaperone function.

First, we will consider the role of the SecB tails. It is possible that leaving the tails free causes an increase in the level of translocation. The C-terminal tails of SecB interact with the Linker Helix of SecA as well as with the N-terminal region. In a complex between SecAdN10 and SecB, A1B4, the C-terminal tails of two SecB monomers would not have N-terminal cognate binding sites on SecA. Therefore two SecB tails might be available to bind the linker helices of a second protomer of SecA resulting in an A2B4 complex (for details see Figure 32 in the text). However, this is not the case. It has been shown that only one protomer of SecAdN10 binds SecB (A1B4) by size exclusion chromatography (Randall et al., 2005). Therefore two of the SecB tails might remain free and result in a high level of translocation.

Support for this idea is found in studies which we report here. In a complex between SecB142 and wild-type SecA, the rate constant (0.87 $min^{-1}$) is higher than that of a complex with wild-type SecB (0.61 $min^{-1}$) whereas the level of translocation is similar to the level of wild type SecA:SecB. In this complex, there are no tails present and thus no interactions with tails. These results indicate that the tail sites of SecB have a negative effect on translocation when they are in a complex with SecA. In addition, it has been shown previously that SecB142 has higher affinity for SecA than does wild-type SecB (Randall & Henzl, 2010).

Secondly consider the chaperone function of SecA. SecA acts as a chaperone as shown by its ability to bind precursor in the absence of SecB (Cooper et al., 2008). If the N-terminal region of SecA had a role to keep precursor competent, the absence of first 10 residues would cause a decrease in the level of translocation; therefore, addition of SecB, a chaperone, to the system could restore the level of translocation. Our results reported here support this idea.

The absence of first 10 residues also causes a decreased in rate constant which was not corrected by addition of SecB but rather decreased the rate constant. We should remember that deletion of first 10 residues might cause two defects in the function. The low rate constant might arise from a role of the first 10 residues of SecA to bind lipids. In the chapter 3, we demonstrated that these residues of SecA are immersed into the lipid bilayer. Lack of this interaction with lipids might cause a change in the rate-limiting step. Therefore, addition of SecB restores the chaperone function of SecA but not the lipid penetration. Thus, it could not restore the rate constant.

**The effect on translocation of SecB variants that have reduced affinity to precursor on translocation**

To achieve transfer from SecB to SecA, it is possible that the affinity of SecB for the precursor could be weakened by interactions of SecB with SecA within the complex. It has been shown that when SecB bound a ligand a conformational change occurred. The distance between the edges of the channel across the dimer interface of the tetramer was changed (Haimann Michaela et al., 2011). A model proposed by L. L. Randall (Suo et al., 2015) suggests that this change at the interface might be reversed as a result of interaction between SecA and SecB. Thereby reducing the affinity of the precursor within the complex for SecB allows precursor to pass to SecA.

The N-terminus of SecA and the Linker Helix might be responsible for the proposed movement of the dimers relative to each other by binding on opposite dimers of SecB tetramer. Two protomers of SecA might be needed to induce a change in conformation so that the relative affinities of SecB and SecA for the precursor favor binding to SecA. It has been also shown that two protomers of SecA are required for a maximal efficiency of coupling between ATP hydrolysis and translocation of polypeptides (Mao et al., 2009). All variants of SecA and SecB studied here except SecA142, make a complex of one protomer of SecA and a tetramer of SecB (A1B4) and have a low translocation rate constant. Therefore, use of SecB species with altered affinity for binding precursor would be expected to increase both the rate constant and/or final level of translocation even in the presence of A1B4 complex.

With the aim of demonstrating whether transfer from SecB to SecA is facilitated by changes in affinity of SecB for precursor or for SecA, we used SecB variants. Two

strategies were used to alter the affinity; mutational changes and chemical modification of cysteine. The SecB variant, SecBF74I, isolated by selection *in vivo* as defective in export (Kimsey et al., 1995). SecBF74I has a point mutation on the side of SecB that weakened the interface of tetramer of SecB. SecBF74I binds SecA normally. However, SecBF74I binds the precursor pGBP 10 times more weakly than does wild-type of SecB shown by isothermal titration calorimetry (unpublished, done by L. Randall) (data not shown). Treatment of SecB with the sulfhydryl reagent dithiobisnitrobenzoic acid (DTNB or Ellman's reagent) results in modification of cysteine 97 (Topping et al., 2001). The SecB species modified by Ellman's reagent showed a six-fold decrease in binding affinity for pGBP assessed by isothermal titration calorimetry (unpublished, done by L. Randall). The proOmpA used in this study is not a suitable precursor to assess affinity directly by calorimetry. We know that proOmpA binds SecB more tightly than does galactose-binding protein (pGBP) by a competition assay using size exclusion chromatography (unpublished data, L. Randall). The affinity of wild-type SecB for pGBP is the range of 80 to 120 nM. The affinity of SecB species modified with Ellman's reagent (E-SecB, E-SecBL75Q and E-SecBL75Q/142) are weakened at least 6 fold (~750 nM) shown by isothermal titration calorimetry (data are not shown, done by L. Randall). We assume the affinity of E-SecB species for proOmpA is also decreased.

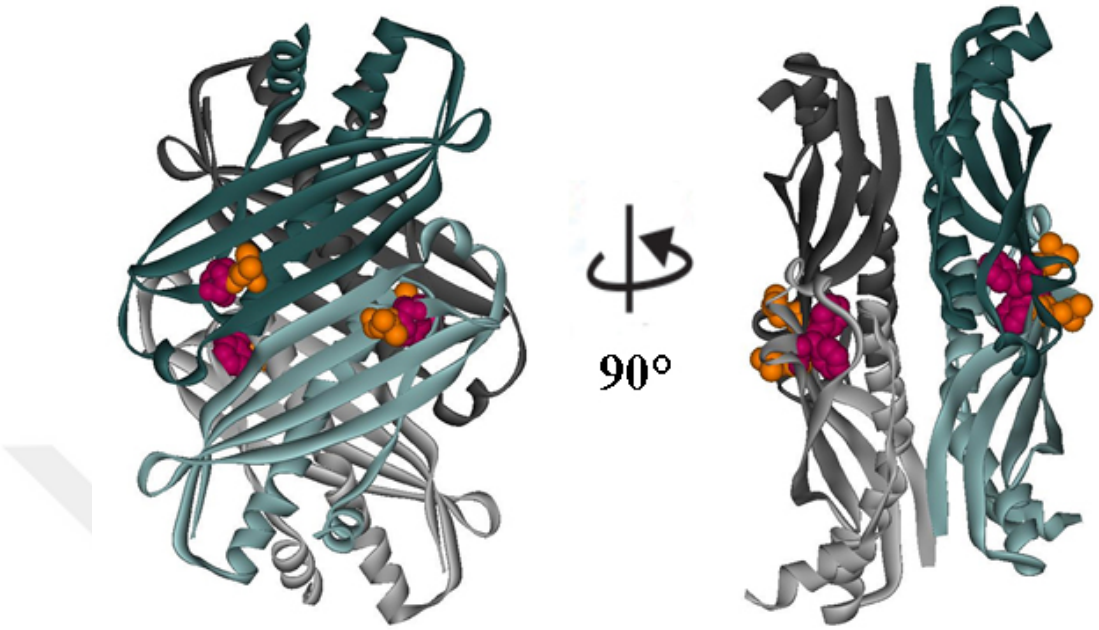


**Figure 36.** Crystal Structure of tetrameric SecB from *Escherichia coli* The two aminoacyl residues of SecB, F74 (magenta) and L75 (orange), are shown on the SecB tetramer. Each dimer of SecB is colored with two shades of gray or green. The monomers within a dimer are colored dark and light tone of the dimer color. The left view shows the flat side of the dimer which serves as the binding site for the C-terminal region of SecA. Rotation of that view 90º around the vertical axis reveals the interface of dimers (right view). SecBF74 points toward the dimer interface. Replacing the phenylalanine residues at F74 with isoleucine weakens the dimer interface.

We tested three SecB species that were modified with Ellman`s reagent: E-SecB142, E-SecBL75Q and E-SecBL75Q/142 (Figue 39). The rate constants of translocation were enhanced for all SecB species that are modified with Ellman's reagent (Figure 37). The highest effect was observed with the bindless SecB. The rate constant was increased 2.9 fold in the presence of E-SecBL75Q/142. The final level of translocation was stimulated with only E-SecBL75Q. The other species showed no increase in the level of translocated precursor. The stimulation of the rate constant by altering the affinity of SecB for precursor indicates that the release of precursor from SecB to SecA might be the rate limiting step of translocation reaction and that the relative affinities of SecA and SecB for precursor must be reversed for the release of precursor. These experiments were done only once and the error bars overlap. We will continue experiment with these variants to determine if the preliminary results are valid since they support the idea that reducing the affinity of SecB to precursor allows transfer to SecA. The results also indicate that SecBL75Q has a defect in chaperone function since the final level of translocation was decreased.

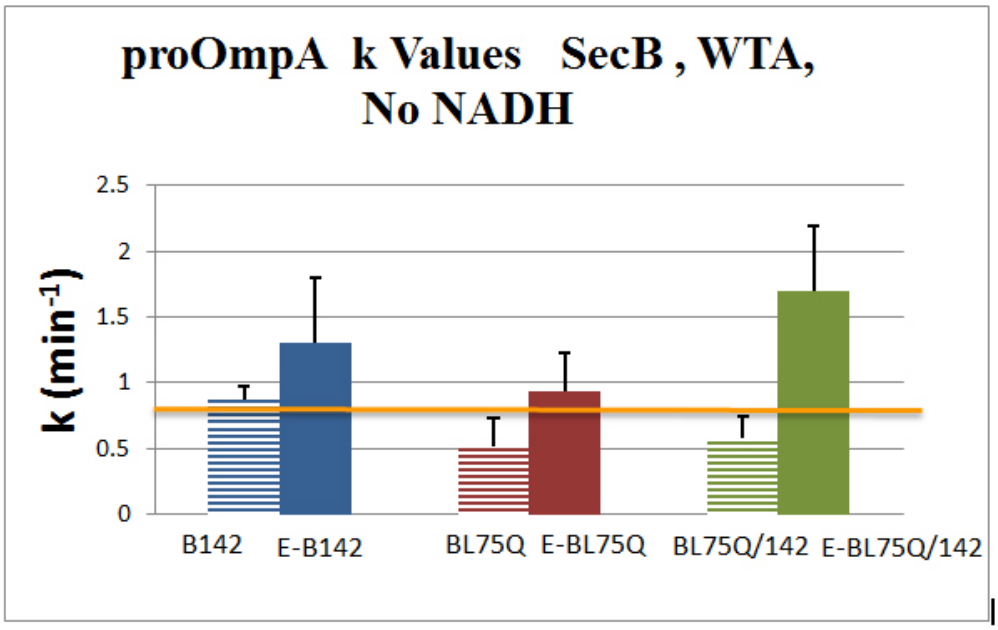


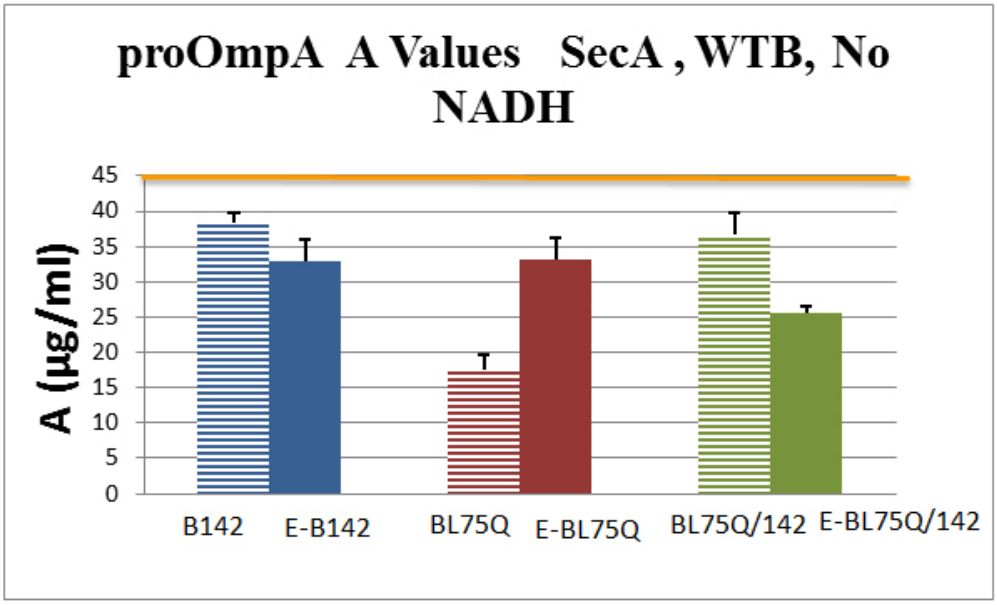


**Figure 37.** Effect of altered affinity of SecB for precursor on the rate constant and extent of translocation. All experiment was done once, except SecBL75Q, n=2. The yellow line represent the wild-type SecA:SecB complex (0.61 $min^{-1}$ ± 0.3and 44 µg/ml ± 5, n=2).

**Effect of proton-motive force in the translocation**

The energy requirement for protein export in *E. coli* is provided by ATP and proton-motive force. While ATP is essential for translocation, precursors can be translocated in the absence of proton-motive force. However the presence of proton-motive force has been shown to stimulate translocation (L. Chen & Tai, 1985; Geller, Movva, & Wickner, 1986; Yamada, Tokuda, & Mizushima, 1989; Yamane, Ichihara, & Mizushima, 1987).

To determine the effect of proton-motive force on the rate constant of the translocation and final level of translocation, we compared translocation assays in the presence (Figure 38, blue square) and absence (Figure 38, red square) of NADH, which results in generation of proton-motive force in IMV. To data we have examined all the SecA species in the absence of SecB except SecAC4. Proton-motive force resulted in a significant increase in the rate constant and the level of translocation for SecAdN10/880. The rate constant increased to near the level of wild-type SecA. Small increase in k was observed for the other species; however, the error in the assays is too large to determine significance.

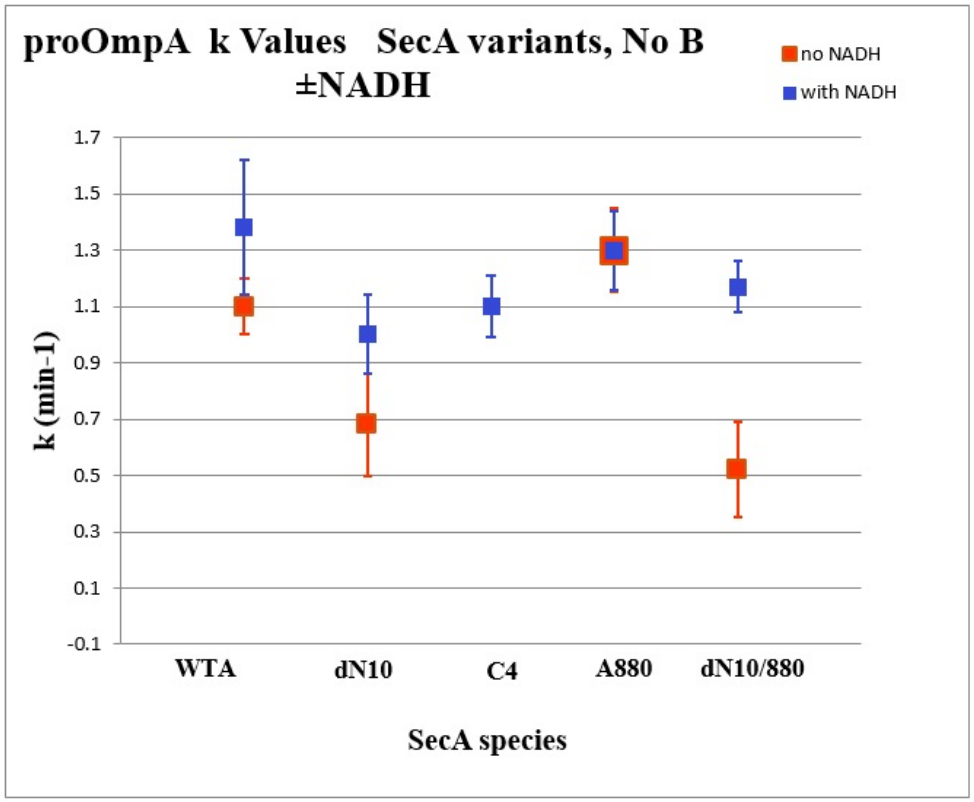
proOmpA k Values SecA variants, No B ±NADH
no NADH
with NADH
k (min-1)
1.7
1.5
1.3
1.1
0.9
0.7
0.5
0.3
0.1
-0.1
WTA
dN10
C4
A880
dN10/880
SecA species

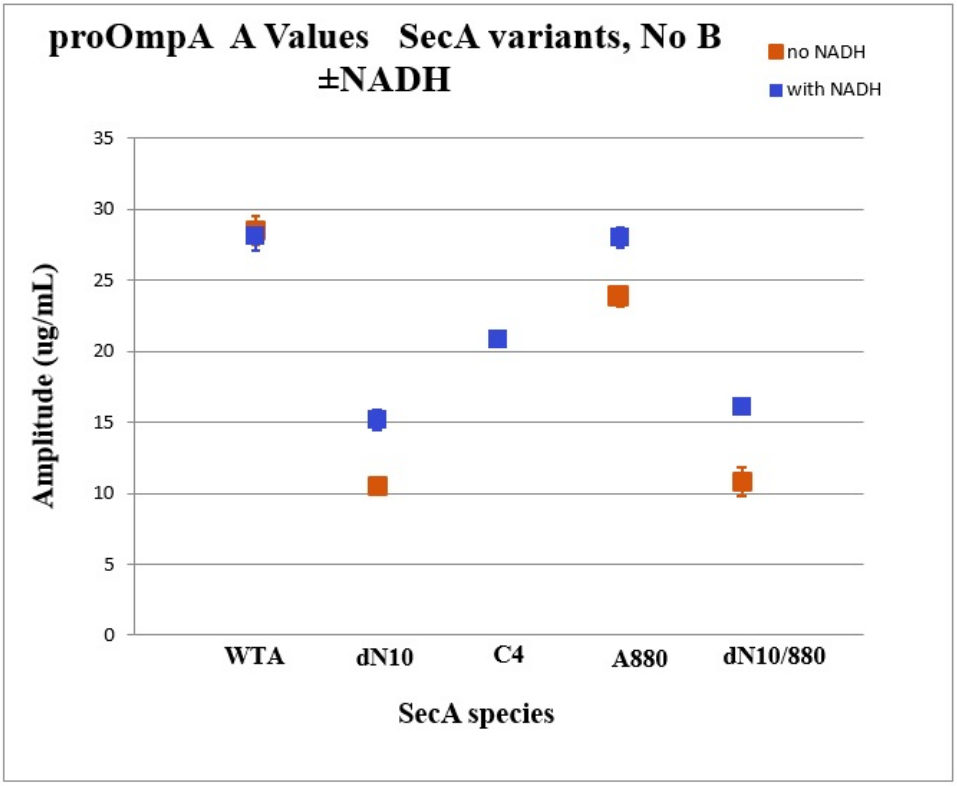
proOmpA A Values SecA variants, No B ±NADH
no NADH
with NADH
Amplitude (ug/mL)
35
30
25
20
15
10
5
0
WTA
dN10
C4
A880
dN10/880
SecA species

**Figure 38.** Effect of proton-motive force in the translocation Additional *in vitro* translocation assays were done in the presence of different combinations of SecA and SecB. However, because the data set is incomplete, we do not yet have a final conclusion. We highlighted the possible outcomes that might be obtained when the further research is done. The available results are promising and will help us in developing experiments further to understand the mechanism of the steps in translocation.

## Materials and Methods

### Purification of Proteins

All variants of SecA and SecB were generated by standard recombinant DNA techniques (QuikChange, Stratagene). Wild-type SecA was purified from HB1745, which is JM109 (New England Biolabs) harboring plasmid pMAN400 (Kawasaki, Matsuyama, Sasaki, Akita, & Mizushima, 1989). SecAN880, a truncated SecA consisting of the first 880 aminoacyl residues, was purified from *E.coli* strain HB1732 (Woodbury et al., 2000b). SecAC4, lacking the zinc-coordinating cysteine residues, was purified from the strain (HB3101) harboring the *secA*-containing plasmid, pT7secA2C4 encoding SecA with the four natural cysteine residues changed to serine, C98S, C885S, C887S, C896S (a generous gift from Donald Oliver). SecAdN10 was purified from HB3414, which is BL21(DE3) harboring plasmid pAL291, a derivative of pMAN400 constructed as described (Asymmetric Binding Between SecA and SecB Two Symmetric Proteins: Implications for Function in Export) SecAdN10/880, which has aminoacyl residues 2 through 11 deleted and is truncated after aminoacyl residue of 880, is purified from a strain (HB3458) harboring plasmid pAL312. Wild-type SecB was purified from HB1042 harboring plasmid pJW25 (Weiss, Ray, & Bassford, 1988b); SecB142 from HB1596, which is CK2212 harboring plasmid pTV6 (Volkert, Baleja, & Kumamoto, 1999); SecBL75Q from HB1579 harboring plasmids as described (Kimsey et al., 1995). SecBL75Q/142 is a strain (HB3505) harboring plasmid pAL329, in which SecB L75Q has a point mutation and is truncated after aminoacyl residue 142. SecBF74I was purified from a strain (HB1563) harboring plasmid as described in (Carol A. Kumamoto, 1995).

All SecA and SecB species were purified as described (PNAS). The protein concentrations were determined spectrophotometrically at 280 nm by using extinction coefficients as follows: 47,600 $M^{-1}$ $cm^{-1}$ for SecB tetramer and 157, 800 $M^{-1}$ $cm^{-1}$ for SecA dimer. All concentrations are expressed as tetrameric SecB and dimeric SecA.

**Modification of cysteine sulfhydryl groups on SecB with Ellman's reagent**

Ellman's reagent, 5, 5'-dithio-bis-(2-nitrobenzoic acid), also known as DTNB, is a water-soluble compound that reacts with free sulfhydryl group yielding a measurable yellow-colored product with molar extinction coefficient of 14.15 $mM^{-1}$ $cm^{-1}$ at 412 nm (ELLMAN, 1959). Cysteine residues at position 97 on SecB were modified by treatment with 5,5'-dithiobis-(2-nitrobenzoic acid) (DTNB or Ellman's reagent, Sigma). DTNB was added at a molar ratio of 2.5 DTNB: 1 cysteine in 0.1 M sodium phosphate pH 8, 1 mM EDTA and incubated at room temperature for 3 hours. The reaction was stopped by addition of 2 mM cysteine and 1M Tris-Cl pH 6.8 for a final concentration of 20 mM. The sample was dialyzed against 20 mM Tris-Cl pH 7.0 before applying it to an anion exchange column (QAE, TosoHass). QAE was used to separate SecB dimer from the mixture. Each fraction was checked by high performance liquid chromatography using a TSK G3000SW size exclusion column (60 cm x 7.5mm, TosoHaas). Fractions containing SecB dimer were pooled, concentrated using a Centricon10 (Amicon), and dialyzed against 10 mM HEPES-KOH pH 7.0, 300 mM KOAc, 1 mM EGTA.

**Inverted membrane vesicles**

Inverted membrane vesicles were prepared from *E.coli* strain, HB4105, which carries a Δ*unc*BC deletion to eliminate the proton-translocating ATPase. This strain

harbors plasmid pB22 encoding *secE* with a His-tag at the N-terminus, *secYC329S, C385S,* and *secG*. Bacterial culture was grown in Luria broth including 0.5 % glucose in the presence of ampicillin to an optical density (OD) of 0.7 at 560 nm. Glucose was removed from media by centrifugation. The cell culture was induced for the synthesis of high levels of the translocation SecYEG by addition of arabinose (0.5% w/v), and grown at 35°C to an OD of 1.5 at 560 nm. Cells were rapidly chilled on ice and harvested by centrifugation in SLC600 rotor (Sorvall) at 14,000 x g for 10 minutes at 4 °C. The cell pellet was suspended in 50 mM triethanolamine, 1mM EDTA, pH 7.5, 1 mM DTT, 0.5 mM PMSF. The cells were disrupted by two passages through a French press (8,000 psi/inch$^2$). The membrane vesicles were pelleted at 362,000 x g for 62 min at 4°C in Ti60 rotor (Beckman Coulter). The pellets were suspended in 50 mM triethanolamine, 1mM EDTA, pH 7.5, 1 mM DTT, 0.5 mM PMSF, and 250 mM sucrose. The suspension was gently layered on top of a sucrose gradient (25-55 % (w/v)). Equilibrium density gradient centrifugation was carried out at 175,000 x g for 14.5 h at 4°C in SW32 Ti rotor (Beckman Coulter). The sample was fractionated and the fractions having a density between 1.14 and 1.19 (32 to 42 % sucrose (w/v)) were collected. The fractions were diluted to < 10% sucrose with 10 mM HEPES, pH 7.6, 0.25 M KCl, 5 mM $MgCl_2$. The membrane vesicles were pelleted by centrifugation (60-Ti rotor, 362,000 x g, 90 min, 4°C). The pellets were resuspended in the same buffer and centrifuged again (60-Ti rotor, 362,000 x g, 63 min, 4°C). The washed vesicles were resuspended in 10 mM HEPES, pH 7.6, 0.25 M KCl, 5 mM $MgCl_2$, and stored at −80°C.

**Preparation of Radiolabeled Proteins**

In this study, two precursor proteins were used: the precursors of outer membrane protein A (OmpA) and periplasmic galactose-binding protein (GBP). The precursors, OmpA and pGBP were produced from plasmids (pAL612 and pAL663, respectively) carrying the *ompA* gene or the *mglB* gene altered to generate polypeptides with only two cysteine residues. For proOmpA, C290 and G244 were substituted by serine and cysteine, respectively, and the native C302 was retained. In pGBP, two cysteines were introduced, L267C and D310C. The proteins were radiolabeled by the addition of a mixture of 14C-L-amino acids (Perkin-Elmer) to cells growing in M9 minimal media, as described (5). Precursor OmpA (proOmpA) was purified as described (5) and pGBP was purified as described (PNAS). Precursors were stored at −80 °C in 10 mM HEPES at pH 7.6 with 1 mM tris(2-carboxyethyl)phosphine (TCEP), with the addition of 0.1 M KOAc and 4 M urea in the case of proOmpA; and 0.3 M KOAc, 1 N GnHCl, and 1 mM EGTA for pGBP.

**Translocation Assay**

Translocation of precursor, proOmpA, labeled with $^{14}C$ amino acid mixture into inverted membrane vesicles or proteoliposomes was carried out at 30 °C under conditions of limiting SecY (Mao et al., 2013). The reaction mixtures were prepared in a glass tube (12 x 75 mm) on ice. The mixture contained 20 mM HEPES-KOH (pH 7.6), 250 mM KOAc, 5 mM $Mg(OAc)_2$, 3.3 mM ATP. Phosphocreatine (7.5 mM) and creatine phosphokinase (37 mg/ml) were also present in the reaction mixture to regenerate ATP. When specified, NADH was added to the reaction mixture to a final concentration of 1.7

mM. Additions of 1 µM SecYEG, 1.2 µM $SecA_2$ and 1.2 µM $SecB_4$ were made to the reaction mixture. The precursor was added last at a final concentration of 1 µM. In the case of pGBP, 1 mM EGTA was added to the system to prevent folding. The reactions were initiated by transferring the glass tubes to a water bath at 30 °C immediately after addition of precursor. The precursors are stored in denaturant and diluted into the translocation assay. The final denaturant concentrations in the reactions were 70 mM Urea for proOmpA.

To assess translocation, 8 µl samples were taken from the reaction mixture at given time points. At zero time point (on ice), an 8 µl sample was taken in duplicate to determine the total radioactivity of the starting material (input). All samples except the inputs were incubated with proteinase K (5 units/ml) after addition of urea (final concentration of 2.7M) and DTT (for a final concentration of 25 mM) for 15 min on ice. In this step, untranslocated precursors are degraded. To stop digestion, tricholoroacetic acid was added to 11% to precipitate protein. The samples were pelleted by centrifugation (16,000 x g, 15 minutes, 4°C, Eppendorf benchtop centrifuge). The precipitate was washed and suspended in gel sample buffer containing DTT and subjected to SDS-polyacrylamide gel electrophoresis. The gels were dried to analyze the amount of translocated precursors.

**Analyses of Translocation Data**

The amount of radioactivity in the protein bands in the gel of the translocated precursor was measured using a Fujifilm FLA 3000 Phosphorimager in the linear range of its response. The full length precursor proteins were observed at the molecular weight

of 35 kDa for proOmpA. When the translocation was stopped, not all precursor proteins had completed the translocation. Thus, the intermediate stages of translocated precursor proteins were observed at the molecular weight ranges of 23.8–30.5 (?) kDa for proOmpA. We do not observed any intermediates for pGBP. The sample of the reaction mixture taken at t = 0 min was used to calculated the percentage of the initial precursors added. Both the full-length and intermediate-length species protected were included in this calculation. From the percentage, we calculate the total amount of precursors translocated either in µg/ml or nM, plotted as a function of time. The equation used for the fit is,

$$y = A(1 - e^{-k(x-x_0)})$$

Where A is the final level of translocation, k is the rate constant, and $x\text{-}x_0$ corrects for the time before the reaction starts.

## Notes

1. Angela Lily constructed all of the SecB and SecA variants used in this study.
2. Chunfeng Mao and Priya Briya purified the inverted membrane vesicles used in this study.
3. Yuying Suo purified and modified all of the SecB used in this study.

## *SUMMARY*

In our laboratory, we investigate the export of proteins across or into the membranes by the general secretory (Sec) pathway in the Gram-negative bacterium, *Escherichia coli*. The Sec pathway only transports unstructured proteins containing a characteristic signal sequence at the N-terminal region. SecB, a cytosolic chaperone, captures unstructured proteins by binding the mature domain of precursor proteins, and keeps them competent during translocation by mediating a kinetic partitioning between precursor folding and its association with SecB (Diamond & Randall, 1997; Hardy & Randall, 1991). SecB with precursor bound binds SecA via specific interactions. SecA, an ATPase, provides energy for protein export by binding and hydrolyzing ATP during translocation. Two protomers of SecA bind precursor-bound SecB for efficient translocation (Mao et al., 2009). SecA not only supplies energy to the system, but also directs the ternary complex of SecA-SecB-precursor to the translocation channel through interactions with both the channel and the membrane lipids. The precursor is released first from SecB to SecA, then from SecA into the channel of SecYEG to cross the membrane. The work described in this thesis represents a significant contribution to our understanding of the interactions of SecA with SecB and with lipids during export.

Understanding interactions studied *in vitro* among proteins involved in export requires knowledge of the cellular concentrations of all components involved in the Sec system. There has been no direct determination of the concentration of SecB *in vivo* in cells that express SecB at the chromosomal level. Therefore, we began our investigation by determination of the cellular concentration of SecB expressed at the chromosomal level. Cells grown in rich media contain SecB at 4 μM tetramer whereas in minimal

media with glycerol as the carbon source the concentration of SecB is ~10 μM. The unexpected result that the level of SecB is lower when cells are grown in rich media might indicate that SecB is down regulated. To make these determinations, we developed a quantitative procedure for immunoblotting. In the course of study, we discovered the importance of the proper sample preparation in the generation of a standard that can be used in quantitative analyses. We showed that the cellular content in the sample that is quantified affects the intensity of the reaction with antisera on immunoblots resulting in incorrect quantification. To overcome the problem, standards must be generated by mixing the purified protein with the amount of cell culture of a strain lacking the protein of interest equal to that in the samples to be quantified. This work is described in Chapter 2 and is in preparation for submission to the Journal of Bacteriology.

Chapter 3 describes the first direct demonstration that the N-terminal region of SecA penetrates to a depth of approximately 6 Å into the hydrocarbon region of the membrane lipids. The technique used was electron paramagnetic resonance (EPR) power saturation. In the standard method used for *in vitro* studies of export in the field, SecYEG is reconstituted into liposomes (referred to as proteoliposomesYEG, PLYEG) and SecA is added to the system externally (PLYEG+A). In our laboratory, a new method was developed in which SecYEG is reconstituted into liposomes in complex with SecA (referred to as (PLYEG•A). Co-assembly of SecYEG and SecA increases the number of active translocons in the proteoliposomes by up to six-fold relative to the usual method. We compared interaction of first 10 residues of SecA with lipids in PLYEG•A, PLYEG+A and liposomes without SecYEG to determine if there is a difference among

the three systems that might be the reason for activation in PLYEG•A. We found that SecA sinks a maximum of 2 Å deeper into lipids in PLYEG+A than it does in PLYEG•A. It is likely that when SecA is co-assembled with SecYEG, it does not penetrate as far into the membrane as when it is added after SecYEG is reconstituted alone into liposomes. This suggests that the interaction differs between PLYEG•A and PLYEG+A.

We also observed that these 10 residues display a helical pattern that has a periodicity close to that of a π helix when they associate with lipids as part of the entire SecA protein. Whereas, a synthetic peptide (A2/11) that is mimic of the first 10 amino acid residues of SecA shows α-helical structure in the presence of *E.coli* lipids as determined by circular dichroism. The peptide is mostly disordered in the absence of lipid (Figure 23).

Work in progress using inverted membrane vesicles as a model system for studies of the Sec secretory system *in vitro* is presented in Chapter 4. The maximum level of translocation is observed when SecB binds two protomers of SecA. The two protomers bind directly across the dimer interface of SecB. Thus, the precursor protein, which wraps around SecB, is trapped between SecA and SecB in the complex, like a sandwich. In solution the affinity of precursor for SecB is higher than for SecA. Thus, to let the precursor pass from SecB to SecA and subsequently to the channel in SecY, the between SecB and the precursor must be decreased. Each of the interactions between SecA and SecB might have a role in release of the precursor. Chapter 4 describes investigations of the effects of alterations in SecA and in SecB on the function of the complexes with the aim of answering questions about the mechanism of release of a precursor protein from

SecB to SecA. The preliminary results indicate that deletion of the first 10 residues of SecA has the greatest impact on translocation as compared with the other defective SecA species. The addition of wild-type SecB to SecAdN10 increased the level of translocation to near the level of wild-type SecA even though the rate constant was greatly decreased. On the other hand, no stimulation was observed by addition of SecB to SecA variants that are defective in interaction at the side site of SecB (SecAC4, SecA880 and SecAdN10/880).

The defects in translocation observed with SecAdN10, a low level and a low rate constant, might arise from defects in the SecA chaperone function and in improper lipid binding, respectively. The results presented here support the idea that there is a defect in chaperone function since addition of the chaperone SecB restores the level of translocation. The addition of SecB had no effect on the low rate constant seen with SecAdN10. This is consistent with the idea that the low rate constant results from a lack of interaction with lipids, which SecB would not affect.

Currently one of the goals for the next several years in the laboratory is the elucidation of the mechanism of transfer of the precursor from SecB to SecA. The data we have presented in Chapter 3 suggests that when SecA binds SecYEG at the membrane the N-terminal region of SecA would insert into the lipid bilayer breaking its contacts with the tails of SecB. Work by others (Breukink et al., 1995) has shown that the C-terminal zinc-containing region of SecA also binds lipids. Therefore, interaction of SecA with the membrane would break its interaction with SecB on the side site. Disruption of these interactions between SecB and the protomer of SecA bound to SecYEG would

release SecB and its associated protomer (A1B4) (See Figure 39). Transfer of the precursor from SecB to the protomer of SecA that remains associated with SecYEG could occur during this step.

The model presented in Suo et al. (Suo et al., 2015) proposes that changes in conformation of SecB, which result from binding interactions between SecB and SecA, cause a decrease in affinity of the SecB for precursor, allowing transfer to SecA. The preliminary data in Chapter 4 support this proposal since assays of two SecB species that have decreased affinity for precursor (E-SecBL75Q and E-SecBL75Q/142) stimulate the rate constant of translocation. The data presented here contribute to the existing body of knowledge, and must be considered when proposing a model to account for the dynamic interactions among SecA, SecB, precursors and the membrane that are involved in protein export.

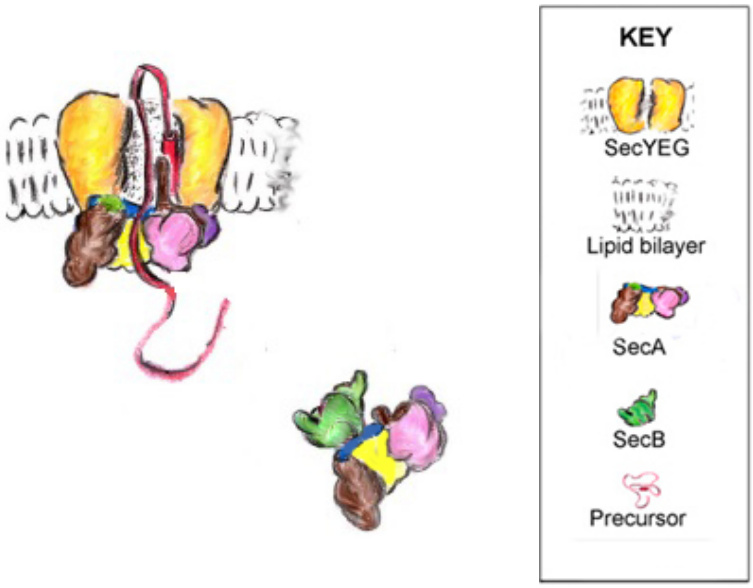


**Figure 39.** Representative schematic cartoons for the release of precursor.

## *LITERATURE CITED*


Akimaru, J., Matsuyama, S., Tokuda, H., & Mizushima, S. (1991). Reconstitution of a protein translocation system containing purified SecY, SecE, and SecA from Escherichia coli. *Proc. Natl. Acad. Sci. U S A, 88*(15), 6545-6549.

Akita, M., Sasaki, S., Matsuyama, S., & Mizushima, S. (1990). SecA interacts with secretory proteins by recognizing the positive charge at the amino terminus of the signal peptide in Escherichia coli. *J. Biol. Chem., 265*(14), 8164-8169.

Akita, M., Shinkai, A., Matsuyama, S., & Mizushima, S. (1991). SecA, an essential component of the secretory machinery of Escherichia coli, exists as homodimer. *Biochem. Biophys. Res. Commun., 174*(1), 211-216.

Altenbach, C., Flitsch, S. L., Khorana, H. G., & Hubbell, W. L. (1989). Structural studies on transmembrane proteins. 2. Spin labeling of bacteriorhodopsin mutants at unique cysteines. *Biochemistry, 28*(19), 7806-7812.

Altenbach, C., Froncisz, W., Hemker, R., McHaourab, H., & Hubbell, W. L. (2005). Accessibility of Nitroxide Side Chains: Absolute Heisenberg Exchange Rates from Power Saturation EPR. *Biophysical Journal, 89*(3), 2103-2112. doi: 10.1529/biophysj.105.059063

Baars, L., Ytterberg, A. J., Drew, D., Wagner, S., Thilo, C., van Wijk, K. J., & de Gier, J.-W. (2006). Defining the Role of the Escherichia coli Chaperone SecB Using Comparative Proteomics. *Journal of Biological Chemistry, 281*(15), 10024-10034. doi: 10.1074/jbc.M509929200

Becker, T., Bhushan, S., Jarasch, A., Armache, J.-P., Funes, S., Jossinet, F., . . . Beckmann, R. (2009). Structure of Monomeric Yeast and Mammalian Sec61 Complexes Interacting with the Translating Ribosome. *Science, 326*(5958), 1369-1373. doi: 10.1126/science.1178535

Berliner, L. J., Grunwald, J., Hankovszky, H. O., & Hideg, K. (1982). A novel reversible thiol-specific spin label: Papain active site labeling and inhibition. *Analytical Biochemistry, 119*(2), 450-455. doi: http://dx.doi.org/10.1016/0003-2697(82)90612-1

Bonardi, F., Halza, E., Walko, M., Du Plessis, F., Nouwen, N., Feringa, B. L., & Driessen, A. J. M. (2011). Probing the SecYEG translocation pore size with preproteins conjugated with sizable rigid spherical molecules. *Proceedings of the National Academy of Sciences of the United States of America, 108*(19), 7775-7780. doi: 10.1073/pnas.1101705108

Breukink, E., Demel, R. A., De Korte-Kool, G., & De Kruijff, B. (1992). SecA insertion into phospholipids is stimulated by negatively charged lipids and inhibited by ATP: a monolayer study. *Biochemistry, 31*(4), 1119-1124. doi: 10.1021/bi00119a021

Breukink, E., Keller, R. C. A., & Kruijff, B. d. (1993). Nucleotide and negatively charged lipid-dependent vesicle aggregation caused by SecA: Evidence that SecA contains two lipid-binding sites. *FEBS Letters, 331*(1–2), 19-24. doi: http://dx.doi.org/10.1016/0014-5793(93)80289-7

Breukink, E., Nouwen, N., van Raalte, A., Mizushima, S., Tommassen, J., & de Kruijff, B. (1995). The C terminus of SecA is involved in both lipid binding and SecB binding. *J. Biol. Chem., 270*(14), 7902-7907.

Breyton, C., Haase, W., Rapoport, T. A., Kuhlbrandt, W., & Collinson, I. (2002). Three-dimensional structure of the bacterial protein-translocation complex SecYEG. *Nature, 418*(6898), 662-665.

Burkinshaw, B. J., & Strynadka, N. C. J. (2014). Assembly and structure of the T3SS. *Biochimica et Biophysica Acta (BBA) - Molecular Cell Research, 1843*(8), 1649-1663. doi: http://dx.doi.org/10.1016/j.bbamcr.2014.01.035

Cabelli, R. J., Dolan, K. M., Qian, L. P., & Oliver, D. B. (1991). Characterization of membrane-associated and soluble states of SecA protein from wild-type and SecA51(TS) mutant strains of *Escherichia coli*. *Journal of Biological Chemistry, 266*(36), 24420-24427.

Chen, L., & Tai, P. C. (1985). ATP is essential for protein translocation into Escherichia coli membrane vesicles. *Proceedings of the National Academy of Sciences of the United States of America, 82*(13), 4384-4388.

Chen, X., Brown, T., & Tai, P. C. (1998). Identification and characterization of protease-resistant SecA fragments: secA has two membrane-integral forms. *J Bacteriol, 180*(3), 527-537.

Chen, X., Xu, H., & Tai, P. C. (1996). A significant fraction of functional SecA is permanently embedded in the membrane. SecA cycling on and off the membrane is not essential during protein translocation. *Journal of Biological Chemistry, 271*(47), 29698-29706.

Chun, S. Y., & Randall, L. L. (1994). In vivo studies of the role of SecA during protein export in Escherichia coli. *Journal of Bacteriology, 176*(14), 4197-4203.

Collier, D. N., Bankaitis, V. A., Weiss, J. B., & Bassford, P. J., Jr. (1988). The antifolding activity of SecB promotes the export of the E. coli maltose-binding protein. *Cell, 53*(2), 273-283.

Collier, D. N., Strobel, S. M., & Bassford, P. J. (1990). SecB-independent export of Escherichia coli ribose-binding protein (RBP): some comparisons with export of maltose-binding protein (MBP) and studies with RBP-MBP hybrid proteins. *J Bacteriol, 172*(12), 6875-6884.

Cooper, D. B., Smith, V. F., Crane, J. M., Roth, H. C., Lilly, A. A., & Randall, L. L. (2008). SecA, the motor of the secretion machine, binds diverse partners on one interactive surface. *J Mol Biol, 382*(1), 74-87.

Costa, T. R. D., Felisberto-Rodrigues, C., Meir, A., Prevost, M. S., Redzej, A., Trokter, M., & Waksman, G. (2015). Secretion systems in Gram-negative bacteria: structural and mechanistic insights. *Nat Rev Micro, 13*(6), 343-359. doi: 10.1038/nrmicro3456

Crane, J. M., Lilly, A. A., & Randall, L. L. (2010). Characterization of Interactions Between Proteins Using Site-Directed Spin Labeling and Electron Paramagnetic Resonance Spectroscopy. In A. Economou (Ed.), *Protein Secretion - Methods and Protocals* (Vol. 619, pp. 173-190): Humana Press.

Crane, J. M., Mao, C., Lilly, A. A., Smith, V. F., Suo, Y., Hubbell, W. L., & Randall, L. L. (2005). Mapping of the docking of SecA onto the chaperone SecB by site-directed spin labeling: insight into the mechanism of ligand transfer during protein export. *J Mol Biol, 353*(2), 295-307.

Crane, J. M., Suo, Y., Lilly, A. A., Mao, C., Hubbell, W. L., & Randall, L. L. (2006). Sites of interaction of a precursor polypeptide on the export chaperone SecB mapped by site-directed spin labeling. *J Mol Biol, 363*(1), 63-74.

Cunningham, K., Lill, R., Crooke, E., Rice, M., Moore, K., Wickner, W., & Oliver, D. (1989). SecA protein, a peripheral protein of the Escherichia coli plasma membrane, is essential for the functional binding and translocation of proOmpA. *EMBO J, 8*(3), 955-959.

Dalbey, R. E., Kuhn, A., Zhu, L., & Kiefer, D. (2014). The membrane insertase YidC. *Biochimica et Biophysica Acta (BBA) - Molecular Cell Research, 1843*(8), 1489-1496. doi: http://dx.doi.org/10.1016/j.bbamcr.2013.12.022

Das, S., Grady, L. M., Michtavy, J., Zhou, Y., Cohan, F. M., Hingorani, M. M., & Oliver, D. B. (2012). The variable subdomain of Escherichia coli SecA functions to regulate SecA ATPase activity and ADP release. *J Bacteriol, 194*(9), 2205-2213. doi: 10.1128/JB.00039-12

de Vrije, T., de Swart, R. L., Dowhan, W., Tommassen, J., & de Kruijff, B. (1988). Phosphatidylglycerol is involved in protein translocation across Escherichia coli inner membranes. *Nature, 334*(6178), 173-175.

Dekker, C., de Kruijff, B., & Gros, P. (2003). Crystal structure of SecB from Escherichia coli. *J. Struct. Biol., 144*(3), 313-319.

Diamond, D. L., & Randall, L. L. (1997). Kinetic partitioning. Poising SecB to favor association with a rapidly folding ligand. *J. Biol. Chem., 272*(46), 28994-28998.

Douville, K., Price, A., Eichler, J., Economou, A., & Wickner, W. (1995). SecYEG and SecA are the stoichiometric components of preprotein translocase. *Journal of Biological Chemistry, 270*(34), 20106-20111.

Economou, A., & Wickner, W. (1994). SecA promotes preprotein translocation by undergoing ATP-driven cycles of membrane insertion and deinsertion. *Cell, 78*(5), 835-843.

ELLMAN, L. G. (1959). Tissue sulfhydryl groups. *Arch Biochem Biophys, 82*(1), 70-77.

Fajer, P. G. (2000). Electron spin resonance spectroscopy labeling in peptide and protein analysis. In R. A. Meyers (Ed.), *Encyclopedia of Analytical Chemistry* (pp. 5725-5761). London: John Wiley & Sons Ltd.

Farahbakhsh, Z. T., Altenbach, C., & Hubbell, W. L. (1992). SPIN LABELED CYSTEINES AS SENSORS FOR PROTEIN-LIPID INTERACTION AND CONFORMATION IN RHODOPSIN. *Photochemistry and Photobiology, 56*(6), 1019-1033. doi: 10.1111/j.1751-1097.1992.tb09725.x

Fekkes, P., de Wit, J. G., Boorsma, A., Friesen, R. H., & Driessen, A. J. (1999). Zinc stabilizes the SecB binding site of SecA. *Biochemistry, 38*(16), 5111-5116.

Fekkes, P., van der Does, C., & Driessen, A. J. (1997). The molecular chaperone SecB is released from the carboxy-terminus of SecA during initiation of precursor protein translocation. *EMBO J., 16*(20), 6105-6113.

Filloux, A., Hachani, A., & Bleves, S. (2008). The bacterial type VI secretion machine: yet another player for protein transport across membranes. *Microbiology, 154*(6), 1570-1583. doi: doi:10.1099/mic.0.2008/016840-0

Fronzes, R., Christie, P. J., & Waksman, G. (2009). The structural biology of type IV secretion systems. *Nat Rev Microbiol, 7*(10). doi: 10.1038/nrmicro2218

Gannon, P. M., Li, P., & Kumamoto, C. A. (1989). The mature portion of Escherichia coli maltose-binding protein (MBP) determines the dependence of MBP on SecB for export. *Journal of Bacteriology, 171*(2), 813-818.

Geller, B. L., Movva, N. R., & Wickner, W. (1986). Both ATP and the electrochemical potential are required for optimal assembly of pro-OmpA into Escherichia coli inner membrane vesicles. *Proceedings of the National Academy of Sciences of the United States of America, 83*(12), 4219-4222.

Haimann Michaela, M., Akdogan, Y., Philipp, R., Varadarajan, R., Hinderberger, D., & Trommer Wolfgang, E. (2011). Conformational changes of the chaperone SecB upon binding to a model substrate – bovine pancreatic trypsin inhibitor (BPTI) *Biological Chemistry* (Vol. 392, pp. 849).

Hardy, S. J., & Randall, L. L. (1991). A kinetic partitioning model of selective binding of nonnative proteins by the bacterial chaperone SecB. *Science, 251*(4992), 439-443.

Hartl, F. U., Lecker, S., Schiebel, E., Hendrick, J. P., & Wickner, W. (1990). The binding cascade of SecB to SecA to SecY/E mediates preprotein targeting to the E. coli plasma membrane. *Cell, 63*(2), 269-279.

Hartmann, E., Sommer, T., Prehn, S., Gorlich, D., Jentsch, S., & Rapoport, T. A. (1994). Evolutionary conservation of components of the protein translocation complex. *Nature, 367*(6464), 654-657.

Henderson, I. R., Navarro-Garcia, F., Desvaux, M., Fernandez, R. C., & Ala'Aldeen, D. (2004). Type V Protein Secretion Pathway: the Autotransporter Story. *Microbiol Mol Biol Rev, 68*(4), 692-744. doi: 10.1128/mmbr.68.4.692-744.2004

Hendrick, J. P., & Wickner, W. (1991). SecA protein needs both acidic phospholipids and SecY/E protein for functional high-affinity binding to the Escherichia coli plasma membrane. *J Biol Chem, 266*(36), 24596-24600.

Hermanson, G. T. (2008). Chapter 2 - The Chemistry of Reactive Groups *Bioconjugate Techniques (Second Edition)* (pp. 169-212). New York: Academic Press.

Jilaveanu, L. B., Zito, C. R., & Oliver, D. (2005). Dimeric SecA is essential for protein translocation. *Proc. Natl. Acad. Sci. U. S. A., 102*(21), 7511-7516.

Karamanou, S., Gouridis, G., Papanikou, E., Sianidis, G., Gelis, I., Keramisanou, D., . . . Economou, A. (2007). Preprotein-controlled catalysis in the helicase motor of SecA. *EMBO J, 26*(12), 2904-2914.

Karamanou, S., Vrontou, E., Sianidis, G., Baud, C., Roos, T., Kuhn, A., . . . Economou, A. (1999). A molecular switch in SecA protein couples ATP hydrolysis to protein translocation. *Molecular Microbiology, 34*(5), 1133-1145.

Kawasaki, H., Matsuyama, S., Sasaki, S., Akita, M., & Mizushima, S. (1989). SecA protein is directly involved in protein secretion in Escherichia coli. *FEBS Lett., 242*(2), 431-434.

Keramisanou, D., Biris, N., Gelis, I., Sianidis, G., Karamanou, S., Economou, A., & Kalodimos, C. G. (2006). Disorder-order folding transitions underlie catalysis in the helicase motor of SecA. *Nat Struct Mol Biol, 13*(7), 594-602. doi: 10.1038/nsmb1108

Khisty, V. J., Munske, G. R., & Randall, L. L. (1995). Mapping of the binding frame for the chaperone SecB within a natural ligand, galactose-binding protein. *J Biol Chem, 270*(43), 25920-25927.

Kim, J., Lee, Y., Kim, C., & Park, C. (1992). Involvement of SecB, a chaperone, in the export of ribose-binding protein. *Journal of Bacteriology, 174*(16), 5219-5227.

Kim, K. H., Aulakh, S., & Paetzel, M. (2012). The bacterial outer membrane β-barrel assembly machinery. *Protein Sci, 21*(6), 751-768. doi: 10.1002/pro.2069

Kimsey, H. H., Dagarag, M. D., & Kumamoto, C. A. (1995). Diverse effects of mutation on the activity of the Escherichia coli export chaperone SecB. *J. Biol. Chem., 270*(39), 22831-22835.

Korotkov, K. V., Sandkvist, M., & Hol, W. G. J. (2012). The type II secretion system: biogenesis, molecular architecture and mechanism. *Nat Rev Micro, 10*(5), 336-351. doi: http://www.nature.com/nrmicro/journal/v10/n5/suppinfo/nrmicro2762_S1.html

Kuhn, A., & Wickner, W. (1985). Conserved residues of the leader peptide are essential for cleavage by leader peptidase. *Journal of Biological Chemistry, 260*(29), 15914-15918.

Kumamoto, C. A., & Beckwith, J. (1983). Mutations in a new gene, secB, cause defective protein localization in Escherichia coli. *J Bacteriol, 154*(1), 253-260.

Kumamoto, C. A., & Beckwith, J. (1985). Evidence for specificity at an early step in protein export in Escherichia coli. *J. Bacteriol., 163*(1), 267-274.

Kumamoto, C. A., & Nault, A. K. (1989). Characterization of the Escherichia coli protein-export gene secB. *Gene, 75*(1), 167-175.

Kusukawa, N., Yura, T., Ueguchi, C., Akiyama, Y., & Ito, K. (1989). Effects of mutations in heat-shock genes groES and groEL on protein export in Escherichia coli. *EMBO J., 8*(11), 3517-3521.

Kyrychenko, A., & Ladokhin, A. S. (2013). Molecular Dynamics Simulations of Depth Distribution of Spin-Labeled Phospholipids within Lipid Bilayer. *The Journal of Physical Chemistry B, 117*(19), 5875-5885. doi: 10.1021/jp4026706

Lecker, S., Lill, R., Ziegelhoffer, T., Georgopoulos, C., Bassford, P. J., Jr., Kumamoto, C. A., & Wickner, W. (1989). Three pure chaperone proteins of Escherichia coli--SecB, trigger factor and GroEL--form soluble complexes with precursor proteins in vitro. *EMBO J, 8*(9), 2703-2709.

Li, W., Schulman, S., Boyd, D., Erlandson, K., Beckwith, J., & Rapoport, T. A. (2007). The plug domain of the SecY protein stabilizes the closed state of the translocation channel and maintains a membrane seal. *Mol Cell, 26*(4), 511-521. doi: 10.1016/j.molcel.2007.05.002

Lill, R., Cunningham, K., Brundage, L. A., Ito, K., Oliver, D., & Wickner, W. (1989). SecA protein hydrolyzes ATP and is an essential component of the protein translocation ATPase of Escherichia coli. *EMBO J, 8*(3), 961-966.

Lill, R., Dowhan, W., & Wickner, W. (1990). The ATPase activity of SecA is regulated by acidic phospholipids, SecY, and the leader and mature domains of precursor proteins. *Cell, 60*(2), 271-280.

Lilly, A. A., Crane, J. M., & Randall, L. L. (2009). Export chaperone SecB uses one surface of interaction for diverse unfolded polypeptide ligands. *Protein Sci, 18*(9), 1860-1868. doi: 10.1002/pro.197

Mao, C., Cheadle, C. E., Hardy, S. J. S., Lilly, A. A., Suo, Y., Gari, R. R. S., . . . Randall, L. L. (2013). Stoichiometry of SecYEG in the active translocase of escherichia coli varies with precursor species. *Proceedings of the National Academy of Sciences of the United States of America, 110*(29), 11815-11820.

Mao, C., Hardy, S. J. S., & Randall, L. L. (2009). Maximal efficiency of coupling between ATP hydrolysis and translocation of polypeptides mediated by SecB requires two protomers of SecA. *Journal of Bacteriology, 191*(3), 978-984.

Matsumoto, G., Yoshihisa, T., & Ito, K. (1997). SecY and SecA interact to allow SecA insertion and protein translocation across the Escherichia coli plasma membrane. *EMBO Journal, 16*(21), 6384-6393.

Miller, A., Wang, L., & Kendall, D. A. (2002). SecB modulates the nucleotide-bound state of SecA and stimulates ATPase activity. *Biochemistry, 41*(16), 5325-5332.

Milo R, P. R. (2016). *Cell biology by the numbers*. New York, NY: Garland Science.

Morita, K., Tokuda, H., & Nishiyama, K. (2012). Multiple SecA molecules drive protein translocation across a single translocon with SecG inversion. *Journal of Biological Chemistry, 287*(1), 455-464. doi: 10.1074/jbc.M111.301754

Murén, E. M., Suciu, D., Topping, T. B., Kumamoto, C. A., & Randall, L. L. (1999). Mutational alterations in the homotetrameric chaperone SecB that implicate the structure as dimer of dimers. *J. Biol. Chem., 274*(27), 19397-19402.

Nishiyama, K., Mizushima, S., & Tokuda, H. (1992). The carboxyl-terminal region of SecE interacts with SecY and is functional in the reconstitution of protein translocation activity in Escherichia coli. *J Biol Chem, 267*(10), 7170-7176.

Nishiyama, K., Suzuki, T., & Tokuda, H. (1996). Inversion of the membrane topology of SecG coupled with SecA-dependent preprotein translocation. *Cell, 85*(1), 71-81.

Oliver, D. B., & Beckwith, J. (1981). E. coli mutant pleiotropically defective in the export of secreted proteins. *Cell, 25*(3), 765-772.

Oliver, D. B., & Beckwith, J. (1982). Regulation of a membrane component required for protein secretion in Escherichia coli. *Cell, 30*(1), 311-319.

Palmer, T., & Berks, B. C. (2012). The twin-arginine translocation (Tat) protein export pathway. *Nat Rev Micro, 10*(7), 483-496.

Papanikolau, Y., Papadovasilaki, M., Ravelli, R. B., McCarthy, A. A., Cusack, S., Economou, A., & Petratos, K. (2007). Structure of dimeric SecA, the Escherichia coli preprotein translocase motor. *J Mol Biol, 366*(5), 1545-1557. doi: 10.1016/j.jmb.2006.12.049

Park, E., Menetret, J. F., Gumbart, J. C., Ludtke, S. J., Li, W., Whynot, A., . . . Akey, C. W. (2014). Structure of the SecY channel during initiation of protein translocation. *Nature, 506*(7486), 102-106. doi: 10.1038/nature12720

Park, S., Liu, G., Topping, T. B., Cover, W. H., & Randall, L. L. (1988). Modulation of folding pathways of exported proteins by the leader sequence. *Science, 239*(4843), 1033-1035.

Patel, C. N., Smith, V. F., & Randall, L. L. (2006). Characterization of three areas of interactions stabilizing complexes between SecA and SecB, two proteins involved in protein export. *Protein Sci, 15*(6), 1379-1386. doi: 10.1110/ps.062141006

Peach, M. L., Hazelbauer, G. L., & Lybrand, T. P. (2002). Modeling the transmembrane domain of bacterial chemoreceptors. *Protein Sci., 11*(4), 912-923.

Powers, E. L., & Randall, L. L. (1995). Export of periplasmic galactose-binding protein in *Escherichia coli* depends on the chaperone SecB. *Journal of Bacteriology, 177*(7), 1906-1907.

Rajapandi, T., & Oliver, D. (1994). Carboxy-terminal region of Escherichia coli SecA ATPase is important to promote its protein translocation activity in vivo. *Biochem Biophys Res Commun, 200*(3), 1477-1483. doi: 10.1006/bbrc.1994.1617

Randall, L. L., Crane, J. M., Lilly, A. A., Liu, G., Mao, C., Patel, C. N., & Hardy, S. J. (2005). Asymmetric binding between SecA and SecB two symmetric proteins: implications for function in export. *J Mol Biol, 348*(2), 479-489. doi: 10.1016/j.jmb.2005.02.036

Randall, L. L., Crane, J. M., Liu, G., & Hardy, S. J. (2004). Sites of interaction between SecA and the chaperone SecB, two proteins involved in export. *Protein Sci, 13*(4), 1124-1133. doi: 10.1110/ps.03410104

Randall, L. L., & Hardy, S. J. (1995). High selectivity with low specificity: how SecB has solved the paradox of chaperone binding. *Trends Biochem Sci, 20*(2), 65-69.

Randall, L. L., & Hardy, S. J. S. (1986). Correlation of competence for export with lack of tertiary structure of the mature species: a study in vivo of maltose-binding protein in E. coli. *Cell, 46*(6), 921-928.

Randall, L. L., & Henzl, M. T. (2010). Direct identification of the site of binding on the chaperone SecB for the amino terminus of the translocon motor SecA. *Protein Science, 19*(6), 1173-1179.

Randall, L. L., Topping, T. B., & Hardy, S. J. S. (1990). No specific recognition of leader peptide by SecB, a chaperone involved in protein export. *Science, 248*(4957), 860-863.

Randall, L. L., Topping, T. B., Suciu, D., & Hardy, S. J. (1998). Calorimetric analyses of the interaction between SecB and its ligands. *Protein Sci, 7*(5), 1195-1200. doi: 10.1002/pro.5560070514

Saraogi, I., & Shan, S.-o. (2014). Co-translational protein targeting to the bacterial membrane. *Biochimica et Biophysica Acta (BBA) - Molecular Cell Research, 1843*(8), 1433-1441. doi: http://dx.doi.org/10.1016/j.bbamcr.2013.10.013

Schatz, P. J., Bieker, K. L., Ottemann, K. M., Silhavy, T. J., & Beckwith, J. (1991). One of three transmembrane stretches is sufficient for the functioning of the SecE protein, a membrane component of the E. coli secretion machinery. *EMBO J, 10*(7), 1749-1757.

Seoh, H. K., & Tai, P. C. (1997). Carbon source-dependent synthesis of SecB, a cytosolic chaperone involved in protein translocation across Escherichia coli membranes. *J. Bacteriol., 179*(4), 1077-1081.

Seoh, H. K., & Tai, P. C. (1999). Catabolic repression of secB expression is positively controlled by cyclic AMP (cAMP) receptor protein-cAMP complexes at the transcriptional level. *J. Bacteriol., 181*(6), 1892-1899.

Smith, V. F., Hardy, S. J., & Randall, L. L. (1997). Determination of the binding frame of the chaperone SecB within the physiological ligand oligopeptide-binding protein. *Protein Sci, 6*(8), 1746-1755. doi: 10.1002/pro.5560060815

Sreerama, N., & Woody, R. W. (2000). Estimation of Protein Secondary Structure from Circular Dichroism Spectra: Comparison of CONTIN, SELCON, and CDSSTR Methods with an Expanded Reference Set. *Analytical Biochemistry, 287*(2), 252-260. doi: http://dx.doi.org/10.1006/abio.2000.4880

Sugai, R., Takemae, K., Tokuda, H., & Nishiyama, K. (2007). Topology inversion of SecG is essential for cytosolic SecA-dependent stimulation of protein translocation. *J Biol Chem, 282*(40), 29540-29548. doi: 10.1074/jbc.M704716200

Suo, Y., Hardy, S. J. S., & Randall, L. L. (2011). Orientation of SecA and SecB in complex, derived from disulfide cross-linking. *Journal of Bacteriology, 193*(1), 190-196. doi: 10.1128/jb.00975-10

Suo, Y., Hardy, S. J. S., & Randall, L. L. (2015). The Basis of Asymmetry in the SecA:SecB Complex. *Journal of Molecular Biology, 427*(4), 887-900. doi: http://dx.doi.org/10.1016/j.jmb.2014.12.008

Teschke, C. M., Kim, J., Song, T., Park, S., Park, C., & Randall, L. L. (1991). Mutations that affect the folding of ribose-binding protein selected as suppressors of a defect in export in Escherichia coli. *J. Biol. Chem., 266*(18), 11789-11796.

Thanassi, D. G., & Hultgren, S. J. (2000). Multiple pathways allow protein secretion across the bacterial outer membrane. *Curr. Opin. Cell. Biol., 12*(4), 420-430.

Thom, J. R., & Randall, L. L. (1988). Role of the leader peptide of maltose-binding protein in two steps of the export process. *Journal of Bacteriology, 170*(12), 5654-5661.

Thomas, S., Holland, I. B., & Schmitt, L. (2014). The Type 1 secretion pathway — The hemolysin system and beyond. *Biochimica et Biophysica Acta (BBA) - Molecular Cell Research, 1843*(8), 1629-1641. doi: http://dx.doi.org/10.1016/j.bbamcr.2013.09.017

Topping, T. B., & Randall, L. L. (1994). Determination of the binding frame within a physiological ligand for the chaperone SecB. *Protein Sci, 3*(5), 730-736. doi: 10.1002/pro.5560030502

Topping, T. B., Woodbury, R. L., Diamond, D. L., Hardy, S. J., & Randall, L. L. (2001). Direct demonstration that homotetrameric chaperone SecB undergoes a dynamic dimer-tetramer equilibrium. *J Biol Chem, 276*(10), 7437-7441. doi: 10.1074/jbc.M009584200

Ulbrandt, N. D., London, E., & Oliver, D. B. (1992). Deep penetration of a portion of Escherichia coli SecA protein into model membranes is promoted by anionic phospholipids and by partial unfolding. *J Biol Chem, 267*(21), 15184-15192.

Van den Berg, B., Clemons, W. M., Jr., Collinson, I., Modis, Y., Hartmann, E., Harrison, S. C., & Rapoport, T. A. (2004). X-ray structure of a protein-conducting channel. *Nature, 427*(6969), 36-44. doi: 10.1038/nature02218

van den Brink-van der Laan, E., Antoinette Killian, J., & de Kruijff, B. (2004). Nonbilayer lipids affect peripheral and integral membrane proteins via changes in the lateral pressure profile. *Biochimica et Biophysica Acta (BBA) - Biomembranes, 1666*(1–2), 275-288. doi: http://dx.doi.org/10.1016/j.bbamem.2004.06.010

van der Does, C., Swaving, J., van Klompenburg, W., & Driessen, A. J. M. (2000). Non-bilayer Lipids Stimulate the Activity of the Reconstituted Bacterial Protein Translocase. *Journal of Biological Chemistry, 275*(4), 2472-2478. doi: 10.1074/jbc.275.4.2472

Volkert, T. L., Baleja, J. D., & Kumamoto, C. A. (1999). A highly mobile C-terminal tail of the Escherichia coli protein export chaperone SecB. *Biochem. Biophys. Res. Commun., 264*(3), 949-954.

von Heijne, G. (1983). Patterns of amino acids near signal-sequence cleavage sites. *Eur J Biochem, 133*(1), 17-21.

Watanabe, M., & Blobel, G. (1989). Cytosolic factor purified from Escherichia coli is necessary and sufficient for the export of a preprotein and is a homotetramer of SecB. *Proc Natl Acad Sci U S A, 86*(8), 2728-2732.

Weaver, T. M. (2000). The pi-helix translates structure into function. *Protein Science : A Publication of the Protein Society, 9*(1), 201-206.

Weiss, J. B., Ray, P. H., & Bassford, P. J., Jr. (1988a). Purified secB protein of Escherichia coli retards folding and promotes membrane translocation of the maltose-binding protein in vitro. *Proc Natl Acad Sci U S A, 85*(23), 8978-8982.

Weiss, J. B., Ray, P. H., & Bassford, P. J., Jr. (1988b). Purified secB protein of Escherichia coli retards folding and promotes membrane translocation of the maltose-binding protein in vitro. *Proc. Natl. Acad. Sci. U S A, 85*(23), 8978-8982.

Whitmore, L., & Wallace, B. A. (2008). Protein secondary structure analyses from circular dichroism spectroscopy: Methods and reference databases. *Biopolymers, 89*(5), 392-400. doi: 10.1002/bip.20853

Woodbury, R. L., Hardy, S. J., & Randall, L. L. (2002). Complex behavior in solution of homodimeric SecA. *Protein Sci, 11*(4), 875-882. doi: 10.1110/ps.4090102

Woodbury, R. L., Topping, T. B., Diamond, D. L., Suciu, D., Kumamoto, C. A., Hardy, S. J., & Randall, L. L. (2000a). Complexes between protein export chaperone SecB and SecA. Evidence for separate sites on SecA providing binding energy and regulatory interactions. *J. Biol. Chem., 275*(31), 24191-24198.

Woodbury, R. L., Topping, T. B., Diamond, D. L., Suciu, D., Kumamoto, C. A., Hardy, S. J., & Randall, L. L. (2000b). Complexes between protein export chaperone SecB and SecA. Evidence for separate sites on SecA providing binding energy and regulatory interactions. *J. Biol. Chem., 275*(31), 24191-24198.

Xu, Z., Knafels, J. D., & Yoshino, K. (2000). Crystal structure of the bacterial protein export chaperone secB. *Nat Struct Biol, 7*(12), 1172-1177. doi: 10.1038/82040

Yamada, H., Tokuda, H., & Mizushima, S. (1989). Proton motive force-dependent and -independent protein translocation revealed by an efficient in vitro assay system of Escherichia coli. *Journal of Biological Chemistry, 264*(3), 1723-1728.

Yamane, K., Ichihara, S., & Mizushima, S. (1987). In vitro translocation of protein across Escherichia coli membrane vesicles requires both the proton motive force and ATP. *Journal of Biological Chemistry, 262*(5), 2358-2362.

Zavoisky, E. K. (1945). Paramagnetic Relaxation of Liquid Solutions for Perpendicular

Fields. *Zhur. Eksperiment. i Theoret. Fiz, Vol.15*, 344–350.

Zimmer, J., Li, W., & Rapoport, T. A. (2006). A novel dimer interface and conformational changes revealed by an X-ray structure of B. subtilis SecA. *J Mol Biol, 364*(3), 259-265. doi: 10.1016/j.jmb.2006.08.044

Zimmer, J., Nam, Y., & Rapoport, T. A. (2008). Structure of a complex of the ATPase SecA and the protein-translocation channel. *Nature, 455*(7215), 936-943.

## *VITA*

Bahar Tuba Findik was born on February 26, 1984, in Sakarya, Turkey. She received her Bachelor's degree in Biochemistry from Ege University in 2007. She received her M.S degree in Biotechnology from the Anadolu University in 2010. While during her M.S, Bahar received a full scholarship for her doctoral studies abroad from The Turkish Ministry of National Education. She started her graduate studies at the University of Missouri under the supervision of Dr. L. L. Randall in 2011. Bahar completed her Doctorate of Philosophy in Biochemistry from the University of Missouri, Columbia in August, 2016.